UNIVERSIDADE FEDERAL DO RIO GRANDE DO SUL
INSTITUTO DE CIÊNCIAS BÁSICAS DA SAÚDE
PROGRAMA DE PÓS-GRADUAÇÃO EM NEUROCIÊNCIAS

SIMULAÇÃO DA PREFERÊNCIA DO ODOR MATERNAL: DA NEUROETOLOGIA À BIOFÍSICA

ENVER MIGUEL ORURO PUMA

Porto Alegre
2020

UNIVERSIDADE FEDERAL DO RIO GRANDE DO SUL
INSTITUTO DE CIÊNCIAS BÁSICAS DA SAÚDE
PROGRAMA DE PÓS-GRADUAÇÃO EM NEUROCIÊNCIAS

SIMULAÇÃO DA PREFERÊNCIA DO ODOR MATERNAL: DA NEUROETOLOGIA À BIOFÍSICA

ENVER MIGUEL ORURO PUMA

Tese apresentada ao Programa de Pós-Graduação em Neurociências do Instituto de Ciências Básicas da Saúde da Universidade Federal do Rio Grande do Sul como requisito parcial para a obtenção do título de doutor em Neurociências.

Orientador: Prof. Dr. Marco Aurélio Pires Idiart
Coorientadora: Prof. Dra. Maria Elisa Calcagnotto

Porto Alegre
2020

SUMÁRIO

Sumário ---- 3
Agradecimentos ---- 4
Resumo ---- 5
Abstract ---- 6
Lista de abreviaturas ---- 7
Lista de Figuras ---- 8

Capítulo 1 ---- 9

Introdução, motivação e objetivos ---- 9
1.1. Estrutura da tese ---- 9
1.2. Uma visão introdutória da motivação da pesquisa ---- 9
1.3. Visão geral e propósito da tese ---- 10
1.4. Visão da integração de níveis para o estudo da preferência ao odor maternal ---- 10
1.5. Hipóteses exploradas na tese ---- 11
1.6. Objetivos da tese ---- 12

Capítulo 2 ---- 14

Fenômeno de estudo, estratégia de abordagem e visão geral dos métodos usados ---- 14
2.1. O aprendizado de preferência do odor maternal ---- 14
2.2. Estratégia de abordagem ---- 17
2.2.1. Perspectiva da neuroetologia computacional ---- 17
2.2.2. Circuitos neurais para o aprendizado de preferência do odor materno ---- 18
2.2.3. Princípio Unificado do Reforço ---- 20
2.2.4. Modelagem e simulação do circuito olfatório ---- 21
2.3. Visão geral dos métodos usados ---- 23
2.3.1. Modelando o circuito olfatório em desenvolvimento ---- 23
2.3.2. Níveis de Modelagem ---- 23
2.3.3. Modelagem baseado em agentes: estratégia para simular o fenômeno ---- 23
2.3.4. Registro eletrofisiológico de neurônios do córtex piriforme anterior em desenvolvimento 24

Capítulo 3 ---- 25

3.1. Artigo 1 ---- 25

Capítulo 4 ---- 40

4.1 Artigo 2 ---- 40

Capítulo 5 ---- 53

Discussão geral e conclusão ---- 53
5.1 Principais contribuições do trabalho ---- 53
5.1.1 Abordagem integrativa da neuroetologia e neurociencia computacional no estúdio de fenômenos comportamentais ---- 53
5.1.2 O aprendizado da preferência do odor maternal e o aprendizado precoce de preferência olfatória para um odor artificial ---- 56
5.1.3 O papel das caraterísticas maturacionais dos neurônios piramidais do CPa no aprendizado da preferência do odor maternal e implicâncias para o aprendizado precoce de preferência olfatória para um odor artificial ---- 57
5.1.4 O papel das caraterísticas maturacionais das entradas GABAérgicas no CPa no aprendizado de preferência do odor maternal ---- 58
5.2 Conclusões ---- 59
5.3 Futuras perspectivas da neuroetologia computacional ---- 60
Referências ---- 61
ANEXO ---- 66
Pôsteres apresentados em eventos acadêmicos ---- 66
Pôster SNF 2017 ---- 67
Cartas de aceitação dos artigos e convite para submeter figura capa de jornal ---- 68

AGRADECIMENTOS

Meus agradecimentos:

Ao professor Marco Idiart pela orientação e suporte durante o doutorado.

A professora Maria Elisa Calcagnotto pela coorientação e suporte durante o doutorado.

Ao professor Aldo Lucion pela valiosa colaboração nos artigos e apoio nos seminários.

A professora Aline Villavicencio pelos importantes comentários feitos para o primer artigo.

A Grace Pardo pela coautoria nos artigos e discussões incansáveis e muito emocionantes

A Izabela Espíndula pela colaboração nos pôsteres

A Cátia Nunes Corrêa pela ajuda com o Português na escrita da Tese.

Ao professor Yuefan Deng da *Stony Brook University* (*Departament of Applied Mathematics and Statistics*) pela orientação em supercomputação

Ao professor Paul Bourgine da UNESCO UniTwin CS-DC (*Complex System Digital Campus*) pelo apoio nosso seminário de complexidade.

Ao professor Tadeu Mello e Souza pelos valiosos comentários feitos na Tese.

Ao FONDECyT do *Consejo Nacional de Ciencia, Tecnología e Innovación Tecnológica* CONCyTEC do Peru pelo financiamento da passagens e estadia para o treino em supercomputação nos Estados Unidos.

Novamente ao professor Marco e professora Maria Elisa pela compreensão e ajuda em todo momento da minha formação de doutorado na Universidade Federal do Rio Grande do Sul.

Aos professores Antônio Roque da Silva Filho, Lisiane Bizarro Arraujo e Tadeu Mello e Souza pelas discussões durante a defesa da tese.

A Coordenação de Aperfeiçoamento de Pessoal de Nível Superior, CAPES, pelo financiamento da minha bolsa de doutorado.

RESUMO

A tese é composta por dois trabalhos complementares. No primeiro trabalho, estudamos o aprendizado do odor materno em ratos neonatos, com foco no final do período sensível para o aprendizado precoce de preferência de odor. No segundo trabalho, estudamos as características das correntes GABAérgicas dos interneurônios do córtex piriforme anterior (CPa) e seu papel no aprendizado precoce de preferência de odor. Para ambos os estudos, foram usados dados eletrofisiológicos experimentais e modelos computacionais foram desenhados usando modelagem baseada em agentes. Os resultados são descritos como o número acumulado de *spikes* e número de neurônios ativos, antes e depois do condicionamento. No primeiro artigo, mostramos que as mudanças nas propriedades intrínsecas das células piramidais no CPa reduzem a disponibilidade de células piramidais que respondem *à* exposição do odor materno. No segundo artigo, experimentos computacionais mostraram que a entrada GABAérgica no CPa melhora a habilidade do circuito olfatório para o aprendizado do odor materno. A discussão geral apresenta uma integração dos níveis da neuroetologia à biofísica como uma perspectiva de trabalho.

Palavras-chave: Neurociência computacional, relação mãe-filhote, córtex olfatório, abordagem biocomportamental.

ABSTRACT

The thesis consists of two complementary studies. In the first study, we investigated the maternal odor learning in neonatal rats, focusing on the end of the sensitive period for early odor preference learning. In the second study, we examined the characteristics of the GABAergic currents of the interneurons of the anterior piriform cortex (aPC) and their role in early odor preference learning. For both studies, experimental electrophysiological data were used, and computational models were designed using agent-based modeling. The results are described as the cumulative number of spikes and the number of active neurons, before and after conditioning. In the first article, we showed that changes in the intrinsic properties of aPC pyramidal cells reduced the availability of the responsive pyramidal cells during maternal odor exposure. In the second article, computational experiments showed that GABAergic entry into the aPC improves the olfactory circuit's ability to learn maternal odor. The general discussion presents an integration of the levels from neuroethology to biophysics as a work perspective.

Keywords: Computational neuroscience, maternal-infant relationship, Olfactory cortex, Biobehavioral approach.

LISTAS DE ABREVIATURAS

BO	Bulbo olfatório
CP	Córtex Piriforme
CPa	Córtex Piriforme Anterior
LC	Locus Coeruleus
NA	Noradrenalina
OSN	Neurônios sensoriais olfatórios
PG	Neurônios periglomerulares
Mi	Neurônios mitrais
Gr	Neurônios granulares
Ff	Interneurônios de conexões pró-ação
Pyr	Neurônios piramidais
Fb	Interneurônios de conexões de retroalimentação
US	Estímulo reforçador
UR	Resposta incondicionada
CR	Resposta condicionada
S	Estímulo ambiental
CS	Estímulo condicionado
DPN	Dia pós-natal
MBA	Modelagem baseada em agentes
EGABA	Potencial de reversão das as respostas inibitórias mediadas por GABA
GABA	Ácido gama-aminobutírico
sIPSC	Correntes inibitórias pós-sinápticas espontâneas
LTP	Potenciação de longa duração

LISTA DE FIGURAS

Figura 1 ---------- 16
Figura 2 ---------- 18
Figura 3 ---------- 19
Figura 4 ---------- 21
Figura 5 ---------- 22
Figura 6 ---------- 70
Figura 7 ---------- 71
Figura 8 ---------- 72

Capítulo 1

Introdução, motivação e objetivos

1.1. Estrutura da tese

Essa tese está estruturada em cinco capítulos e um anexo. O conteúdo de cada capítulo será descrito a seguir. O **Capítulo 1** estabelece a motivação para desenvolver a pesquisa, o propósito, as hipóteses e objetivos da tese. No **Capítulo 2,** o fenômeno de estudo e a estratégia de abordagem são detalhadas. São descritas a perspectiva da neuroetologia computacional, os circuitos neurais do aprendizado de preferência ao odor maternal, o princípio unificado do reforço, modelagem e simulação do circuito olfatório e uma visão geral dos métodos usados. No **Capítulo 3**, a primeira publicação referente à hipótese 1 é apresentada com uma breve introdução. No **Capítulo 4**, a segunda publicação referente à hipótese 2 é apresentada com uma breve introdução. Finalmente, o trabalho encerra-se no **Capítulo 5**, no qual são apresentadas uma discussão geral e uma conclusão com base nos dois artigos. Na parte do **Anexo**, a lista de pôsteres apresentados em vários eventos acadêmicos antes da publicação dos dois artigos é incluída.

1.2. Uma visão introdutória da motivação da pesquisa

A pesquisa do sistema nervoso nas últimas décadas forneceu uma quantidade imensa de dados e hipóteses que, devido à sua natureza como método experimental, são obtidos através do isolamento dos componentes de um sistema reduzido de variáveis. Nesse contexto, é necessário integrar dados e microteorias em micromodelos. Essa atividade de integração existe na neurociência, apresentada em trabalhos de revisão como hipóteses de grandes sistemas. Com os avanços da computação, é possível construir modelos que envolvam micro-teorias em grandes sistemas computacionais. No entanto, a neurociência e o estudo do comportamento na psicologia provêm de diferentes tradições e são categorizados em diferentes níveis de análise. Tentar integrar culturas científicas independentes da neurociência e do comportamento é um problema atual.

1.3. Visão geral e propósito da tese

A presente tese procura contribuir na área da neurociência com a perspectiva de uma abordagem integrada da neuroetologia à biofísica, com o objetivo de estudar circuitos neurais de fenômenos comportamentais, usando como exemplo ilustrativo o fenômeno de aprendizado de preferência ao odor materno em filhotes de rato. Um único fenômeno comportamental ou cognitivo pode ser tratado usando estratégias diferentes. No entanto, cada uma dessas estratégias se concentra em diferentes níveis do fenômeno. Acreditamos que é necessária uma estratégia para integrar níveis da neuroetologia à biofísica ou da biofísica à neuroetologia. Uma integração desses níveis seria necessária para estudar qualquer comportamento. Contudo, há uma dificuldade. Cada uma desses níveis tem as suas próprias teorias e existem muitos níveis entre neuroetologia e biofísica. Então, como os níveis podem ser integradas da neuroetologia à biofísica? E por que a integração deve estar nessa direção?

O significado último dessa abordagem integrativa é contribuir para entender como as mudanças ambientais poderiam levar a alterações no nível neural. Desse modo, essa tese propõe responder a duas perguntas: primeiro, como podemos integrar as mudanças ambientais às mudanças no nível neural e como podemos organizar esses níveis; e segundo, uma vez organizados os níveis, como podemos estudar com esse esquema um fenômeno comportamental específico, como o aprendizado de preferência pelo odor maternal em filhotes de rato? Portanto, o objetivo desta tese foi tentar integrar computacionalmente o nível neuroetológico à biofísica.

1.4. Visão da integração de níveis para o estudo da preferência ao odor maternal

A preferência pelo odor maternal, na prática, é um teste no qual o filhote de rato ou camundongo é colocado em uma caixa-teste para escolher entre dois odores. Através da mensuração do tempo gasto na área do odor do ninho ou o odor da mãe, em relação ao da área neutra, é inferida uma preferência por um desses odores (Moriceau and Sullivan, 2005; Morrison et al., 2013). Esse aprendizado é nosso fenômeno comportamental básico. Portanto, é importante explorar o que se sabe sobre ele, como estudá-lo, quais estruturas neurais podem ser ativadas por esses estímulos, quais neurotransmissores estão envolvidos e o que é conhecido experimentalmente.

Na neurociência computacional, existem modelos do bulbo olfatório (BO) e o córtex piriforme anterior (CPa) nos quais a modulação da noradrenalina (NA) é empregada no estudo da percepção e aprendizado olfatório em ratos adultos (DE ALMEIDA et al, 2013; DE ALMEIDA et al., 2015; LI et al., 2015). Portanto, nesse trabalho, usamos as equações do modelo de DE ALMEIDA et al. (2013, 2015), e, com base na arquitetura neural também proposta por eles, implementamos um modelo baseado em agentes com características de ratos neonatos. No modelo computacional desenvolvido, mostramos que no aprendizado olfatório em neonatos a projeção noradrenérgica do *locus coeruleus* (LC) funciona como um estímulo incondicionado, semelhante ao relatado em modelos experimentais de condicionamento clássico em ratos neonatos. Integramos o circuito, simulamos o ambiente como interação mãe-filhote e treinamos o circuito com uma série de diferentes estratégias computacionais. Os resultados foram apresentados em vários eventos acadêmicos (**Anexo**). Com o sistema integrado e os novos dados experimentais, em nosso primeiro artigo trabalhamos em uma nova teoria para o final do período sensível de aprendizado precoce de preferência do odor. Finalmente, no último manuscrito focalizamos a biofísica das correntes GABAérgicas e sua importância durante o aprendizado de odor materno.

Em resumo, testamos nossas hipóteses em um modelo de neuroetologia computacional. Nosso modelo de neuroetologia computacional considera os níveis neurais, plasticidade-microcircuito, comportamento animal e o ambiente. O modelo resultante deste trabalho permitiu a integração de dados experimentais desenvolvidos na Universidade Federal do Rio Grande do Sul (UFRGS), fazendo convergir as linhas de pesquisa de eletrofisiologia, relação mãe-filhote e neurociência computacional.

1.5. Hipóteses exploradas na tese

Na presente tese, foram exploradas as seguintes hipóteses:

1. **O período sensível para o aprendizado do apego se deve à maturação dos neurônios piramidais do córtex piriforme anterior**. O filhote de rato ou camundongo pode aprender odores artificiais pareados com estimulação táctil que simula o contato materno (por exemplo, lambidas da mãe). Esse pareamento induz preferência pelo odor somente se for realizado dentro do período correspondente aos primeiros dez dias de vida pós-natal do filhote, considerado período sensível. Após esse período, o pareamento dos mesmos

estímulos deixa de induzir uma preferência pelo odor (veja o **Capítulo 2**). Presume-se que o filhote aprenderia o cheiro da mãe dessa maneira, e manteria essa habilidade nos primeiros dez dias pós-natais, a fim de garantir sua sobrevivência em uma fase em que ele está completamente dependente dos cuidados dela. Esse fenômeno nos levou a pensar em outras duas hipóteses específicas que podem apoiar o final do período sensível do aprendizado de apego. **Primeiro**, o filhote aprende a associar o cheiro da sua mãe dentro do ninho, e então isso serviria como base para aprender outros cheiros fora do ninho, mas isso não ocorreria após o período sensível. **Segundo**, aprender o odor materno dentro do ninho aumenta a conectividade do circuito olfatório envolvido, e essa conectividade está disponível quando o filhote é exposto a um experimento de condicionamento para induzir a preferência por um odor artificial. Mas esse condicionamento não resulta em preferência após o período sensível, pois o número de neurônios que são responsivos ao odor materno é reduzido. Essa redução na responsividade ao odor materno ocorreria devido à caraterística de maturação dos neurônios piramidais e não à perda da habilidade de aprendizado. Os resultados do teste dessa hipótese foram publicados no artigo 1 (veja **Capítulo 3**).

2. **As caraterísticas de maduração das entradas GABAérgicas no córtex piriforme anterior contribuem em dar suporte ao aprendizado do odor materno durante o período sensível.** Na literatura considera-se que o papel do GABA, durante o período sensível, possui um efeito inibitório nas células piramidais do córtex piriforme anterior, impedindo o aprendizado da preferência olfatória (veja **Capítulo 2**). No entanto, a exemplo de outros córtices em desenvolvimento, também é possível que o GABA possa ter um efeito excitatório e, se houver, poderia contribuir no suporte do aprendizado do odor materno. Os resultados da exploração dessa hipótese estão descritos no artigo 2 (veja **Capítulo 4**).

1.6. Objetivos da tese

Objetivo geral:

Simular computacionalmente a interação ambiente-organismo-comportamento em modelo neuroetológico de aprendizado de preferência olfatória no início do desenvolvimento pós-natal de ratos.

Objetivos específicos:

1. Criar um modelo computacional do circuito olfatório do filhote de rato durante o período sensível para o aprendizado do odor maternal, usando dados eletrofisiológicos de neurônios piramidais do córtex piriforme anterior, obtidos de filhotes com idade dentro do período sensível.
2. Simular o aprendizado da preferência ao odor maternal, durante o período sensível, no circuito olfatório artificial.
3. Simular o papel dos interneurônios GABAérgicos no córtex piriforme anterior no aprendizado da preferência ao odor maternal durante o período sensível.

Capítulo 2

Fenômeno de estudo, estratégia de abordagem e visão geral dos métodos usados

2.1. O aprendizado de preferência do odor maternal

O aprendizado de preferência olfatória é um fenômeno comportamental observado em roedores no início da vida pós-natal, descrito principalmente em ratos e camundongos. Logo após o nascimento, os filhotes de roedores são capazes de formar memórias de odor associados tanto a estímulos prazerosos, como leite, calor e estimulação táctil (MORICEAU;SULLIVAN, 2005; ROTH *et al.*, 2013; GHOSH *et al.*, 2015) quanto aversivos (RAINEKi *et al.*, 2009; UPTON; SULLIVAN, 2010; ROTH *et al.*, 2013; MEYER; ALBERTS, 2016). As memórias dos odores são expressas como preferências nas fases posteriores do desenvolvimento desses filhotes (MORICEAU; SULLIVAN, 2006). Igualmente foi demonstrado que outras formas de vínculo social no início do desenvolvimento, como o amontoamento com os irmãos de ninhada, ocorrem por meio de processos associativos de sinais olfativos com estimulação termo-táctil (ALBERTS; BRUNJES, 1978; KOJIMA; ALBERTS, 2009). Mas como ocorre esse aprendizado de preferência olfatória no filhote? O mecanismo para aprender o odor materno dentro do ninho é semelhante ou diferente do aprendizado de um odor artificial fora do ninho? Para aproximar algumas respostas a essas perguntas, consideramos importante separar os contextos etológicos em que o filhote aprende as preferências olfatórias dentro do ninho, interagindo com mãe, e fora do ninho em um ambiente controlado.

O aprendizado de preferência olfatória, tanto do odor da mãe quanto de um odor artificial, pode ser rapidamente induzido em um período do desenvolvimento pós-natal, durante o qual o filhote depende completamente dos cuidados da mãe para sobreviver (<DPN 10, dia pós-natal). Após esse período, os mesmos estímulos pareados (odor e estimulação táctil) perdem a habilidade de induzir a mesma preferência (**Figura 1A**). Foi sugerido, então, que esse tipo de aprendizado precoce em filhotes de rato ou camundongo ocorre durante um período sensível (SULLIVAN,

2003). Embora o aprendizado de preferência pelo odor materno e de um odor artificial estejam restritos ao mesmo período sensível, aparentemente, por mecanismos associativos semelhantes, ambos ocorrem em contextos e tempos diferentes. O filhote dentro do ninho está exposto ao cheiro da mãe desde o nascimento (DPN 0) (**Figura 1A, barra amarela**), e os experimentos de condicionamento de odor artificial e estimulação táctil, que simula as lambidas da mãe, são realizados principalmente a partir do DPN 5 (**Figura 1A, barra azul**). Foi proposto que esses dois tipos de aprendizado de preferência têm como suporte um único circuito neural (MORICEAU; SULLIVAN, 2004). Na segunda parte da tese, descrevemos detalhes desse circuito. Propomos que o aprendizado de preferência pelo odor materno modela o circuito neural em desenvolvimento, e esse circuito suporta o aprendizado posterior de preferência olfatória induzida fora do ninho dentro da janela temporal do período sensível. A seguir discutimos a proposta.

Como indicado acima, tanto a preferência pelo odor materno (**Figura 1B**) quanto a pelo odor artificial (**Figura 1C**) são induzidas por processos associativos, especificamente por condicionamento clássico (SULLIVAN, 2003). O processo de condicionamento clássico baseia-se na associação de dois tipos estímulos, um estimulo incondicionado (EI, para o qual a resposta do organismo é reflexa, por exemplo o jato de ar nos olhos de uma pessoa provoca que ela feche os olhos) e um estímulo neutro (EN, para o qual a resposta do organismo é diferente de sua resposta para o EI). A exposição repetitiva aos estímulos pareados EI-EN faz com que o EN, uma vez apresentado sozinho, seja capaz de induzir uma resposta semelhante à induzida pelo EI. Portanto, após o pareamento, o estímulo inicialmente neutro tornou-se condicionado (EC). No paradigma de condicionamento clássico para induzir preferência por um odor artificial, o EI é a estimulação táctil no dorso do filhote (pinceladas vigorosas) e o EN é o odor artificial (Moriceau and Sullivan, 2005; Morrison et al., 2013).

Usando modelos de condicionamento, associando estimulação táctil a um odor, e usando o teste de preferência olfatória, o grupo liderado pela Dra. Regina Sullivan propôs que o BO, modulado por uma alta inervação noradrenérgica originada no LC, é a estrutura necessária e suficiente para o aprendizado da memória de preferência a odores em filhotes durante o período sensível (SULLIVAN; WILSON, 2003; ROTH *et al*, 2006). Por outro lado, usando o mesmo modelo de comportamento, o grupo

liderado pela Dra Qi Yuan sugeriu que o aprendizado do odor é modulado por projeções de LC no CPa, que também seria uma estrutura necessária e suficiente para a representação do odor (MORRISON *et al*, 2013).

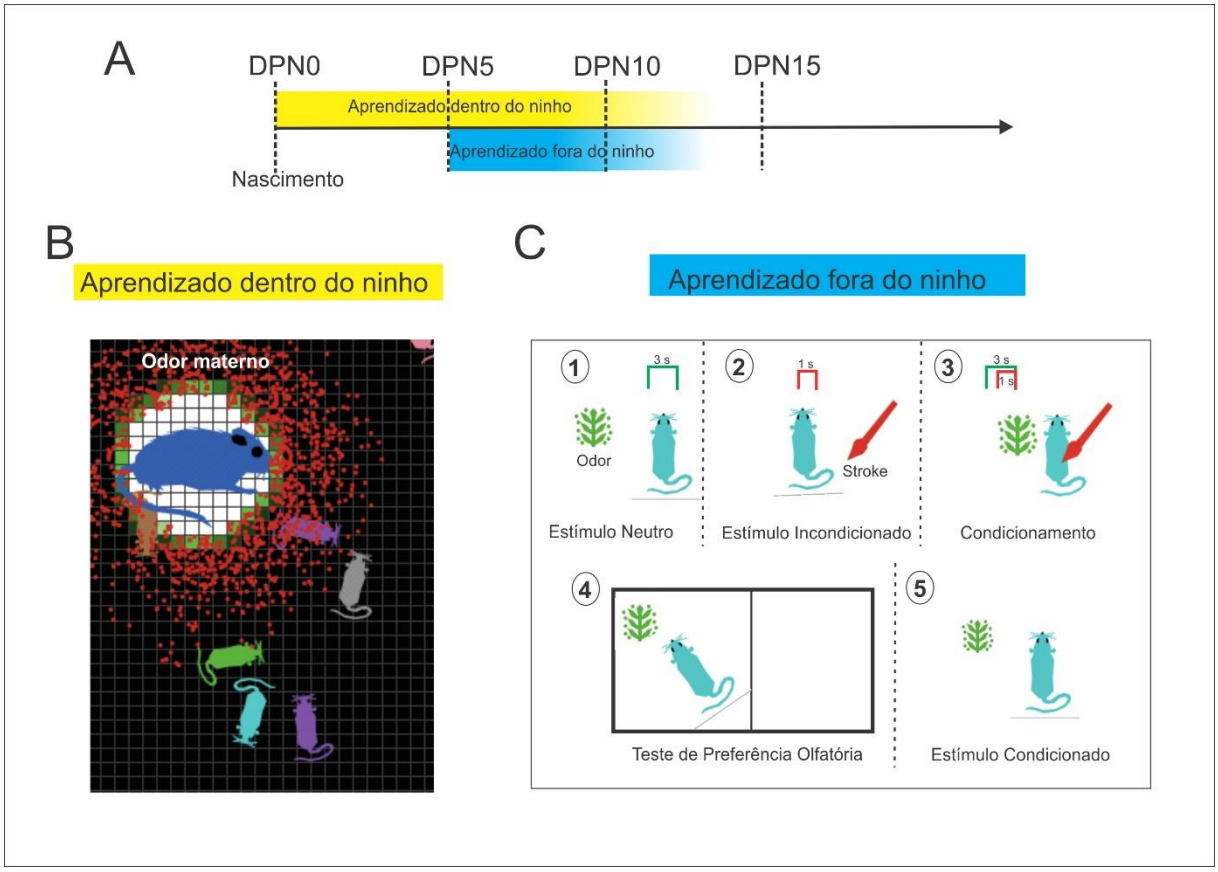

Figura 1. **Simulação do ambiente etológico no qual o filhote de rato ou camundongo aprende a preferência pelo odor materno.** A simulação foi realizada usando o software NetLogo, usando a metodologia baseada em agentes. **A)** Linha temporal do desenvolvimento pós-natal do filhote de rato durante o qual os fenômenos de aprendizado de preferência para o odor maternal ou para um odor artificial são observados. Após nascimento, o filhote, dentro do ninho está exposto ao aprendizado do odor maternal mediante processos associativo do odor da mãe e os estímulos sensoriais que ela provê no cuidado materno (calor, lambidas, leite). Esse aprendizado ocorre dentro de uma janela temporal chamado de período sensível (linha amarela). A resultante desse aprendizado é a formação de uma preferência para o odor materno ou ninho materno, medido mediante comportamentos de aproximação para esses odores. Outro fenômeno observado em filhotes neonato é também a habilidade para formar preferências para odores artificiais quando pareados com estímulos táctеis que simulam as lambidas da mãe. Esse fenômeno tem sido observado em filhotes entre idades de DPN 5 e DPN 8. O pareamento do odor artificial e os estímulos táctеis não induzem preferência pelos odores condicionados depois do DPN 10 (linha azul). **B)** Simulação da representação do aprendizado do odor materno dentro do ninho usando o NetLogo. O odor da mãe (bolinhas vermelhas ao redor da mãe (rata azul grande) atrai os filhotes que se encontram perto da mãe. Quando os filhotes se aproximam da mãe, a mãe lambe ele, provê de calor e alimento. Esses estímulos podem servir de reforço para o aprendizado do odor materno. **C)** Representação das fases do condicionamento fora do ninho para o aprendizado de preferência de um odor artificial em filhotes DPN 5-DPN 10. Um odor inicialmente neutro (**1**) pareado repetidas vezes com um estímulo táctil (**2-3**) (estimulação vigorosa no dorso do filhote com um pincel suave) induze uma preferência no filhote, o qual é

medido em um labirinto de duas escolhas (**4**) e o odor artificial inicialmente neutro torna-se condicionado (**5**). Fonte elaborada pelo autor a partir do fenômeno descrito na seção 2.1.

Nosso projeto inicial foi criar um modelo computacional para diferenciar as duas propostas de suporte do aprendizado de preferência olfatória no nível neural durante o período sensível. Finalmente, o resultado do nosso modelo conseguiu integrar as duas propostas no mesmo modelo, tanto o incremento da frequência de disparo das células mitrais no BO como o efeito da taxa de disparo nos terminais axônicos nas conexões do trato olfatório lateral (LOT). No artigo 1, incluído no **Capítulo 2,** pode-se apreciar os esforços dessa integração.

2.2. Estratégia de abordagem

Para testar nossa hipótese, usamos um modelo de neuroetologia computacional no qual consideramos os seguintes níveis de integração: neural, plasticidade-microcircuito, comportamento animal e ambiente. Para representar os níveis neurais e o comportamento, a modelagem foi desenvolvida de acordo com as principais variáveis obtidas na revisão da literatura (SULLIVAN *et al*., 2000; MORRISON *et al.*, 2013). Para a confiabilidade da modelagem, consideramos variáveis experimentais dependentes e independentes análogas as utilizadas pelos autores que descreveram o fenômeno e o circuito neural (Sullivan e Yuan); garantindo, assim, a consistência das saídas do sistema de simulação com os dados de laboratório. Para representar a plasticidade dentro do circuito olfatório, usamos o modelo de Jensen, Idiart e Lisman (JENSEN; IDIART; LISMAN, 1996). Além disso, para o nosso projeto usamos o princípio unificado do reforço (DONAHOE *et al*, 1993; BURGOS, 2010), descrito mais adiante, como um esquema teórico e para o desenho das contingências. Este referencial teórico também foi essencial para organizar os registros de saída da simulação e apresentação dos estímulos em um paradigma de condicionamento respondente. Em vista disso, usamos essas estratégias para o caso especifico do circuito BO e CPa no aprendizado ao odor materno. A seguir descrevemos cada uma das estratégias mencionadas.

2.2.1. Perspectiva da neuroetologia computacional

A neuroetologia computacional estuda as bases neurais dos padrões de comportamento animal expostos em condições naturais (**Figura 2A**), propondo

modelos computacionais para avaliar teorias na área através de uma abordagem evolutiva e comparativa do comportamento animal.

Nessa tese, nossa perspectiva para a neuroetologia computacional enfoca o nível após a ocorrência de mudanças ambientais, especificamente o comportamento da mãe, que é o ambiente natural para um filhote de rato e que pode ser representado através das entradas e saídas do ninho. Isso implica que o filhote seja exposto a estímulos intermitentes, como odor da mãe e o contato maternal (**Figura 5B**). Esse é considerado nosso esquema de trabalho.

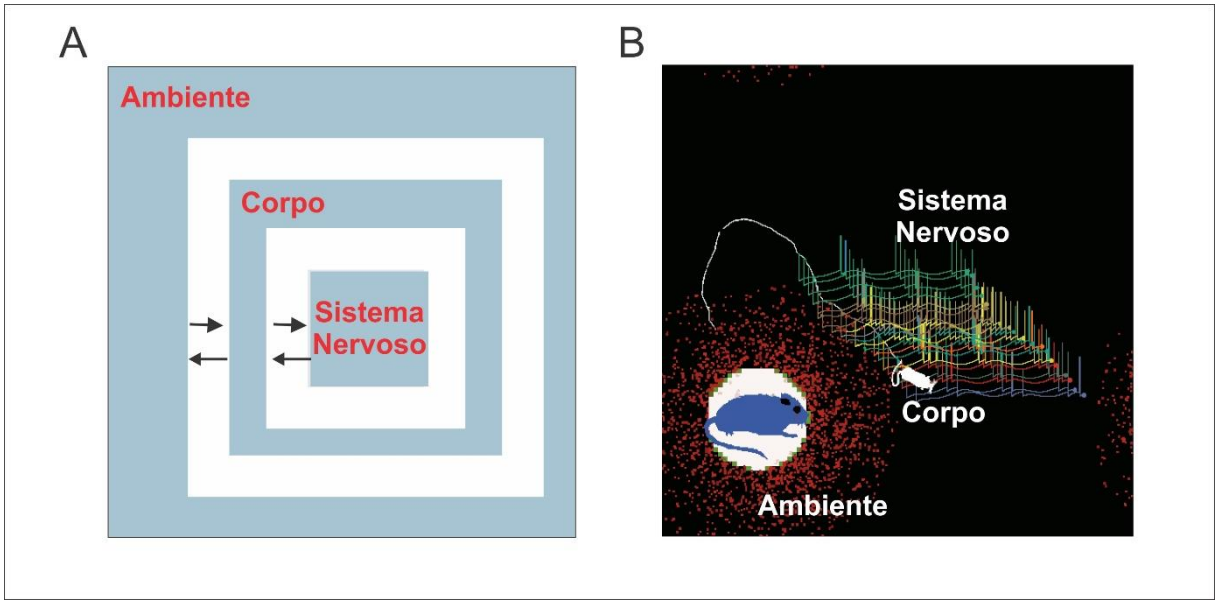

Figura 2. **Perspectiva da neuroetologia computacional para a modelagem da base neural do comportamento animal**. **A**) Esquema representando como o comportamento animal surge da interação entre a dinâmica neural com o periférico e o ambiente ecológico (Adaptado de http://www.scholarpedia.org/article/Computational_neuroethology). **B**) Representação do ambiente etológico dentro do ninho, no qual o comportamento do filhote de aproximação a mãe surge da interação da dinâmica neural com seu entorno que é a mãe.

2.2.2. Circuitos neurais para o aprendizado de preferência do odor materno

O aprendizado precoce para a preferência ao odor é uma forma rápida de condicionamento clássico que provou ser um modelo útil para identificar circuitos celulares e mecanismos moleculares de aprendizado. Ratos e camundongos recém-nascidos podem ser condicionados a novos odores, mediante a utilização de estímulos que imitam os estímulos recebidos durante o cuidado materno. Uma

variedade de estímulos foi empregada como estímulo incondicionado (EI) na indução de respostas condicionadas a novos odores (estímulo condicionado, EC) em recém-nascidos, incluindo o ambiente do ninho, apresentação de leite, estimulação táctil, o odor materno, choque elétrico leve na pata, e estimulação cerebral intracraniana (YUAN *et al.*, 2014). Uma variedade de trabalhos sugere a existência de um período sensível para o desenvolvimento das preferências iniciais ao odor. Ensaios de 10 min de pareamento de choque elétrico e odor aplicado no DPN 6, induziram a preferência pelo odor e isso pode permanecer apenas 24 horas (YUAN *et al*., 2014) (**Figura 3A**).

Sullivan e seus colegas (SULLIVAN *et al*, 2000) demonstraram a natureza associativa do comportamento de preferência precoce pelo odor. Seus trabalhos sugerem que os eventos simultâneos da entrada do odor e a liberação de noradrenalina dos terminais do LC no bulbo olfatório são suficientes para estabelecer o aprendizado de preferência olfatória (SULLIVAN *et al.*, 2000) (**Figura 3B**). Além disso, Yuan e seus colegas também demostraram que o córtex piriforme anterior é importante para esse aprendizado (MORRISON *et al*, 2013) (**Figura 3C**).

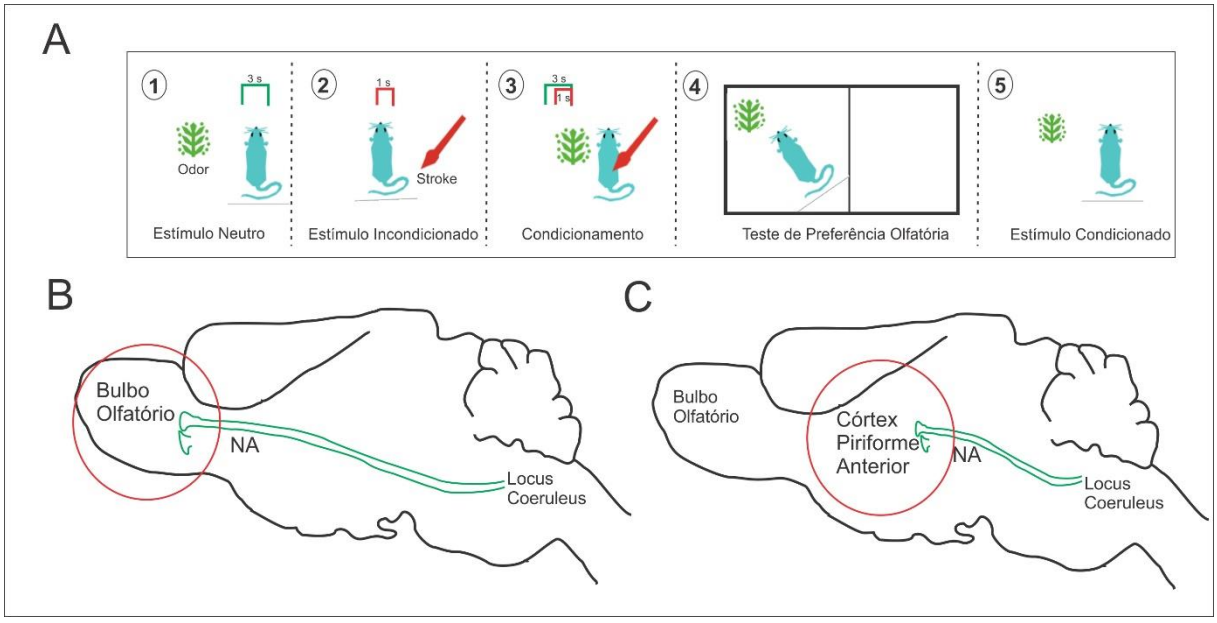

Figura 3. **Hipótese de circuitos neurais que suportam o aprendizado de preferência olfatória**. **A**) Representação do condicionamento de um odor artificial inicialmente neutro (1) com um estímulo táctil (estimulação vigorosa no dorso do filhote usando um pincel suave) que induz incremento na atividade locomotora do filhote (2) quando pareados (3) em tempos específicos, o odor apresentado durante 3 segundos e a estimulação táctil no último segundo, resulta em uma preferência pelo odor artificial quando testado contra um odor neutro (4), tornando-se assim o odor neutro inicial em um odor condicionado (5). **B**) A noradrenalina liberada do *locus coeruleus* no bulbo olfatório (proposta do grupo da Regina Sullivan em SULLIVAN *et al*, 2000) e também no córtex piriforme anterior (proposta do grupo da Qi Yuan em YUAN *et al*., 2014) (**C**) é necessária e suficiente para a aquisição do aprendizado de preferência olfatória durante o período sensível.

2.2.3. Princípio Unificado do Reforço

O princípio unificado do reforço (DONAHOE *et al*, 1993) foi proposto com base na análise experimental do comportamento. Essa proposta foi importante para a classificação das entradas e saídas do nosso modelo computacional de condicionamento de redes neurais artificiais. Existem estratégias para a avaliação do aprendizado com base no paradigma do princípio unificado do reforço. Para tanto, usamos as mesmas estratégias para examinar o aprendizado de preferência olfatória. Donahoe e colegas indicaram dois conjuntos de condições que são necessárias para que o reforço selecione o comportamento: (a) curtos intervalos de tempo entre o evento ambiental, comportamental e reforço e (b) um estímulo de reforço que evoca mudanças no comportamento ou discrepância (**Figura 4).** Na **Figura 4,** a conectividade neural é mostrada de maneira simplificada a partir de estímulos comportamentais, onde qualquer R (resposta operante) contíguo temporariamente entre o aparecimento de S (estímulo ambiental) e UR (resposta incondicionada) ativa vias neurais que conectam S a R. Desse ponto de vista, as sensibilidades dos organismos a relações definidas em intervalos de tempo mais longos são devidas ao efeito cumulativo das relações momento a momento entre reforços, comportamentos e eventos ambientais (DONAHOE *et al*, 1993).

O princípio unificado do reforço estabelece que, sempre que houver uma discrepância comportamental, todos os estímulos anteriores a essa discrepância adquirirão controle sobre todas as respostas que ocorrem imediatamente antes e simultaneamente a ela (DONAHOE *et al*, 1993). Esse paradigma foi proposto a partir da análise experimental do comportamento como uma estrutura conceitual complementar com os resultados da análise experimental das neurociências, que forneceu uma variedade de modelos computacionais dos fenômenos do condicionamento respondente. Atualmente existem mais de 16 modelos desenvolvidos (BURGOS, 2010).

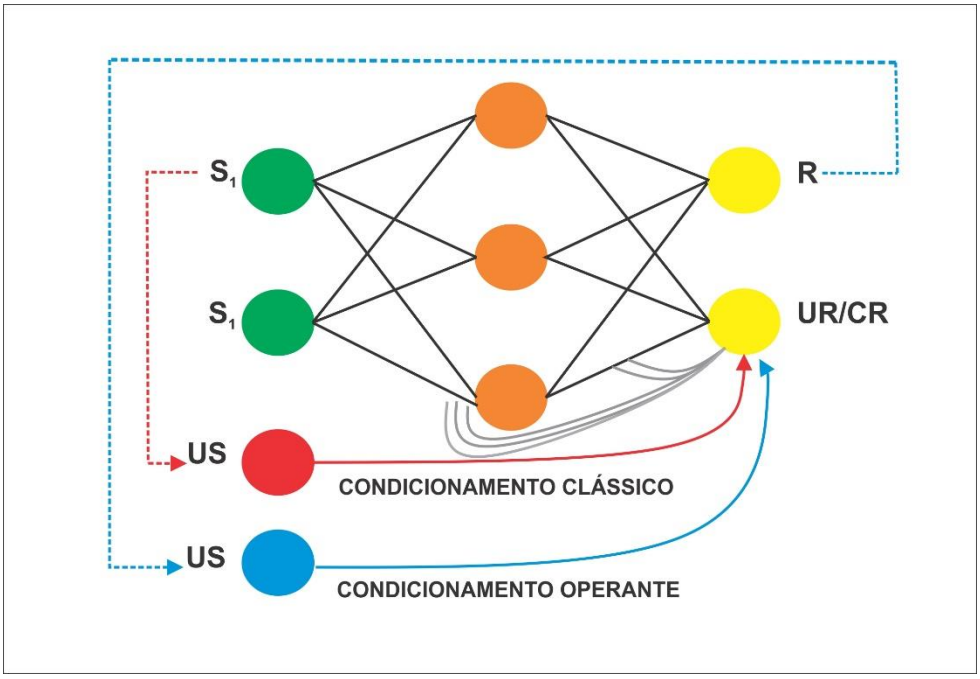

Figura 4. **Princípio Unificado do Reforço.** O componente seleção-resposta de uma rede de seleção com três unidades de entrada, três unidades internas e duas unidades de saída. As unidades de entrada podem ser ativadas tanto por estímulos ambientais (S1 e S2) quanto por um estímulo reforçador (US). A ativação das unidades de saída simula a ocorrência da resposta operante (R) e da resposta incondicionada (UR), ou, quando a unidade UR é ativada por um estímulo diferente do US, a resposta condicionada (CR). A ativação das unidades UR/CR também pode engajar o sistema de reforço difuso que modifica a conectividade de pesos entre todas as unidades coativadas. A figura ilustra a contingência clássica (linhas pontilhadas em vermelho), em que a ocorrência do US é dependente de uma ativação prévia de uma unidade de entrada (S1). Também na figura se ilustra uma contingência operante (linhas pontilhadas em azul), em que a ativação da unidade US é dependente da ativação prévia da unidade de saída (R) pela representação de S1. Gráfico adaptado de DONAHOE *et al.*, 1993).

2.2.4. Modelagem e simulação do circuito olfatório

O modelo canônico consiste em duas redes diferentes que representam o BO e o CPa. O BO é composto pelos neurônios sensoriais olfativos (OSN), neurônios periglomerulares (PG), neurônios mitrais (Mi) e neurônios granulares (Gr). O CPa é constituído por interneurônios de conexões pró-ação ou *feedforward* (Ff), neurônios piramidais (Pyr) e os interneurônios de conexões de retroalimentação ou *feedback* (Fb) (DE ALMEIDA *et al.*, 2015) (**Figura 5**).

No intuito de conferir importância dos dados experimentais e preservar propriedades deduzidas desses dados na simulação, simplificamos essa arquitetura, especificamente no nível das conexões do BO. Nosso modelo considerou apenas

células Mt como um componente do BO. Nos pôsteres (em Anexo), usamos o modelo canônico.

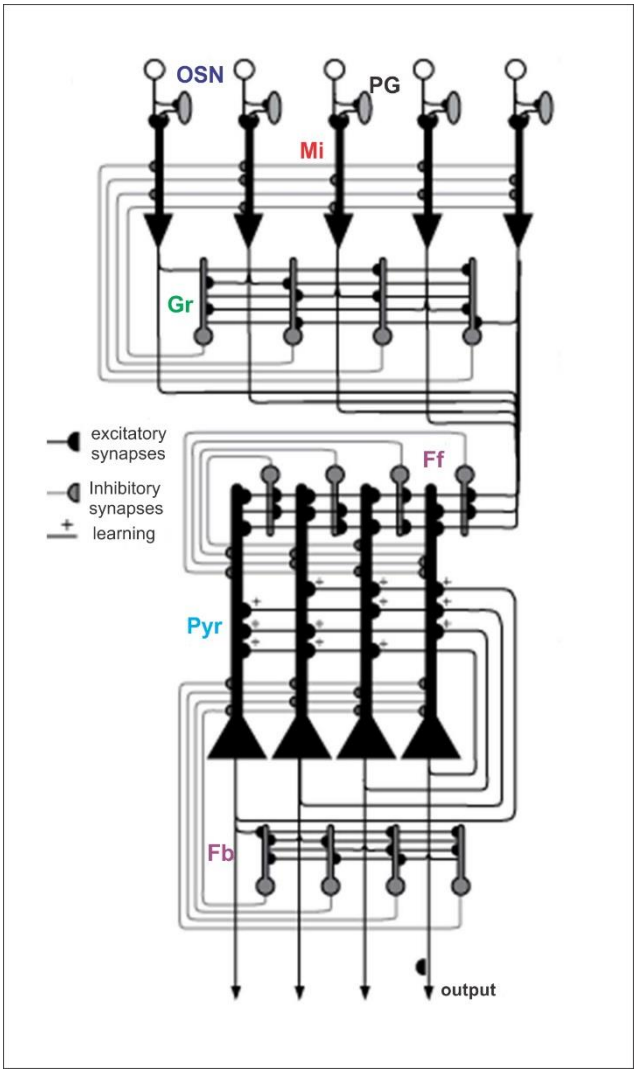

Figura 5. **Arquitetura neural do circuito olfatório**. O ponto de entrada no circuito é o grupo de neurônios sensoriais olfatórios (OSN), os quais projetam seus terminais axônicos para o bulbo olfatório (BO) dentro de estruturas chamados de glomérulos, onde estabelecem conexões sinápticas excitatórias com os dendritos principais dos neurônios Mitrais (Mi) e os interneurônios periglomerulares (PG) que rodeiam esses glomérulos. Os neurônios PG estabelecem conexões inibitórias com os dendritos apicais das células Mi. As células Mi também recebem entradas inibitórias das células granulares (Gr) nos seus dendritos laterais. Os axônios das células Mi saem do BO, formando o trato olfatório lateral (LOT) e se projetam para regiões centrais. O córtex piriforme anterior (CPa) é uma das regiões centrais que recebem esses inputs, formando conexões excitatórias com os dendritos apicais das células piramidais (Pyr) e os interneurônios de conexões pró-ação (f*eedforward*) (Ff) na camada superficial do CPa. Os interneurônios Ff também estabelecem conexões inibitórias com os dendritos apicais das células Pyr. Em outras camadas do CPa, as células Pyr recebem entradas excitatórias de outras células Pyr, sendo chamada esta conexão de recorrente; além disso, também recebe entradas inibitórias de outro grupo de interneurônios que formam conexões de retroalimentação (*feedback*) (Fb). Os axônios das células Pyr se projetam para fora do CPa. Tomado de DE ALMEIDA *et al.*, 2015.

2.3. Visão geral dos métodos usados

2.3.1. Modelando o circuito olfatório em desenvolvimento

Para modelar o circuito olfatório em desenvolvimento, além de revisar a literatura sobre os circuitos neurais envolvidos, foi necessário investigar as características das conexões e da plasticidade sináptica nas células piramidais do CPa. Trabalhos prévios foram muito úteis na determinação desses parâmetros (FRANKS; ISAACSON, 2005; POO; ISAACSON, 2007). Além disso, era necessário ter dados correspondentes às características de maturação dos neurônios. Com a colaboração de Grace Pardo, do PPG Fisiologia UFRGS, obtivemos esses dados através dos experimentos realizados como parte de sua tese de doutorado.

2.3.2. Níveis de Modelagem

As seguintes propriedades e seus respectivos níveis foram consideradas na modelagem:

- Nível 1: Potenciais dos neurônios, potenciais pós-sinápticos excitatórios e inibitórios
- Nível 2: Integração sináptica, plasticidade, microcircuito do BO e do CPa
- Nível 3: Integração do Sistema Neural, Comportamento e Ambiente

O aprendizado foi avaliado nos níveis 2 e 3. As entradas e saídas dos sistemas foram definidas com base nas descrições do fenômeno de aprendizado precoce da preferência olfatória e no princípio unificado do reforço, sendo que esses foram diferentes para cada nível.

2.3.3. Modelagem baseado em agentes: estratégia para simular o fenômeno

A modelagem baseada em agentes (MBA) é uma classe de modelos computacionais utilizada para simular as ações e interações de entidades autônomas individuais chamadas agentes. Cada um desses agentes pode avaliar sua situação e tomar decisões com base em um conjunto de regras introduzidas no modelo. Uma caraterística importante da MBA é a interação repetitiva que existe entre eles, podendo ser simulada com o uso de computadores e softwares que permitem explorar a dinâmica do sistema. Com a MBA, fenômenos têm sido explorados em física, química,

biologia, ecologia e no comportamento animal e humano. Existem diversos ambientes de programação de MBA, os mais conhecidos são Repast, Mason, Breve, Netlogo. Igualmente existem ambientes de MBA implementados em linguagens como MATLAB, Python e C.

NetLogo é um ambiente de programação para MBA e sistemas complexos. É usado por dezenas de milhares de estudantes, professores e pesquisadores em todo o mundo. O programa está disponível gratuitamente. O NetLogo foi projetado e criado por Uri Wilensky, diretor do Centro de Aprendizagem Conectada e Modelagem Computacional da Northwestern University. O Netlogo está sujeito a melhorias aproximadamente a cada 6 meses, e existem outros projetos para aumentar o potencial da plataforma como vínculos com outras linguagens de programação como MATLAB, Mathematica, R, Python, além da construção da extensão RNetlogo para aproveitar a computação paralela em R (WILENSKY, 1999; THIELE; GRIMM, 2010; THIELE *et al*, 2012). Usamos o Netlogo para o nosso trabalho.

2.3.4. Registro eletrofisiológico de neurônios do córtex piriforme anterior em desenvolvimento

Os dados eletrofisiológicos foram fornecidos por Grace Pardo, obtidos como parte da sua tese de doutorado no laboratório da professora Maria Elisa Calcagnotto, Departamento de Bioquímica, UFRGS. Para obter dados sobre as propriedades intrínsecas das células especificadas, foi usada a técnica de fixação de um fragmento da membrana plasmática (*patch-clamp)* no modo de fixação de corrente (*current-clamp)*. As células piramidais na camada 2/3 foram registradas em fatias de CPa, obtidas de filhotes de rato no DPN 5,6,7 e 8 e DPN 14,15,16 e 17. A descrição detalhada da técnica pode ser encontrada no artigo 1 (**Capítulo 3**).

Para obter dados sobre as correntes pós-sinápticas GABAérgicas, foi utilizada a técnica de *patch-clamp no modo de fixação de voltagem* (*voltage-clamp*), na qual também se registraram as células piramidais da camada 2/3 em fatias de CPa, extraídas de cérebros de filhotes de rato nos DPN 5,6,7 e 8. A descrição detalhada pode ser encontrada no artigo 2 (**Capítulo 3**).

Capítulo 3

3.1. Artigo 1

O artigo intitulado "*Maturation of pyramidal cells in anterior piriform cortex may be sufficient to explain the end of early olfactory learning in rats*", propõe a uma nova explicação para o fim do período sensível do aprendizado olfatório em ratos neonatos para o qual integra dados experimentais e modelagem computacional. Esse trabalho foi produzido de maneira colaborativa com a Grace Pardo, quem realizou o trabalho experimental no laboratório da professora Maria Elisa Calcagnotto e do professor Aldo Bolten Lucion como parte de sua tese de doutorado. O artigo fui publicado na Revista Learning and Memory 2020 (27:20–32) e também foi capa da edição 01-2020. O artigo pode ser citado como:

Oruro, E.M., Pardo, G.V.E., Lucion, A.B., Calcagnotto, M.E., Idiart, M.A.P., 2020. Maturation of pyramidal cells in anterior piriform cortex may be sufficient to explain the end of early olfactory learning in rats. Learn. Mem. 27:20–32. https://doi.org/10.1101/lm.050724.119

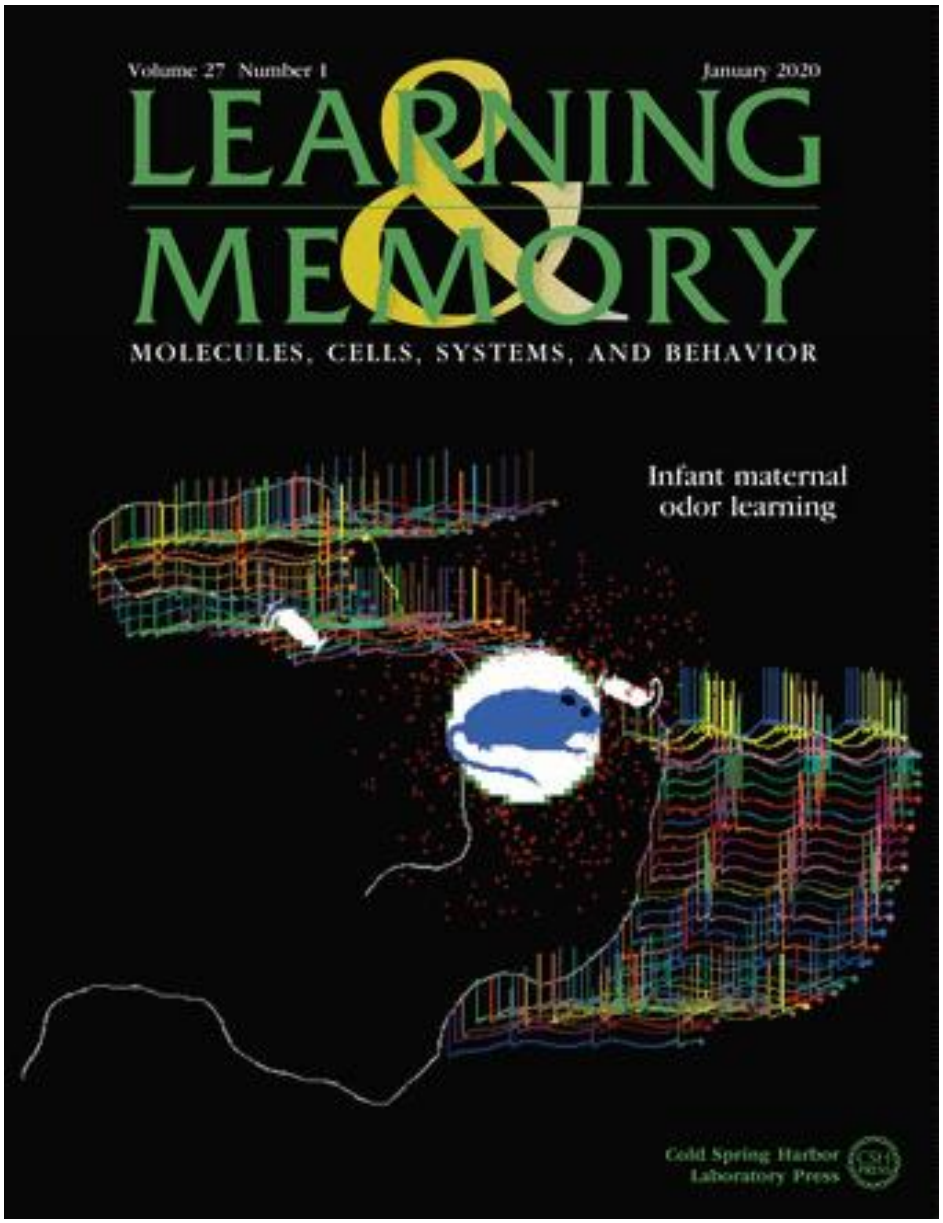

Figura na capa da revista Learning & Memory volume 27, número 1 de janeiro de 2020, **preparada pelos autores**.

Legenda da figura tirada de http://learnmem.cshlp.org/content/27/1.cover-expansion.

The image illustrates a representation of the conditioned behavioral response of the infant rat to the maternal odor. A group of pyramidal neurons in the anterior olfactory cortex (aPC) respond preferentially when the pup is close to the mother`s odor. Using a combined electrophysiological and computational approach, Oruro et al. (*LearnMem* **27:** 20–32) report that more neurons are sensitive to maternal odor in pups younger than 10 postnatal days (P) than in older pups due to the maturation of intrinsic properties of the neurons itself. Early odor preference learning is induced in rat pups <P10 by pairing an artificial odor with tactile stimuli that mimics maternal care. After P10, the pairing of the same stimuli becomes ineffective for conditioning. Based on these results, the authors proposed that odor conditioning in <P10 pups recruits a group of pyramidal cells in the aPC that are also activated by the maternal odor. As this neural circuit promotes approximation to the maternal odor, we assume their coincidental activation also promotes behavioral preference for the conditioned odor. However, this overlap occurs only for younger pups. For older pups, the odor conditioning results in less activation of the aPC pyramidal cells, overlap in the circuit is no longer possible, and the conditioning is no longer effective.

Research

Maturation of pyramidal cells in anterior piriform cortex may be sufficient to explain the end of early olfactory learning in rats

Enver Miguel Oruro,[1,2,3,6] Grace V.E. Pardo,[2,4,5,6] Aldo B. Lucion,[4] Maria Elisa Calcagnotto,[2,3] and Marco A. P. Idiart[1,3]

[1]*Neurocomputational and Language Processing Laboratory, Institute of Physics, Universidade Federal do Rio Grande do Sul, Porto Alegre, RS, 91501-970 Brazil;* [2]*Neurophysiology and Neurochemistry of Neuronal Excitability and Synaptic Plasticity Laboratory, Department of Biochemistry, Institute of Basic Health Sciences, Universidade Federal do Rio Grande do Sul, Porto Alegre, RS, 90035-003 Brazil;* [3]*Neuroscience Graduate Program, Universidade Federal do Rio Grande do Sul, Porto Alegre, RS, 90050-170 Brazil;* [4]*Department of Physiology, Institute of Basic Health Sciences, Universidade Federal do Rio Grande do Sul, Porto Alegre, RS, 90050-170 Brazil;* [5]*Centre for Interdisciplinary Science and Society Studies, Universidad de Ciencias y Humanidades, Los Olivos, Lima, 15314 Peru*

Studies have shown that neonate rodents exhibit high ability to learn a preference for novel odors associated with thermotactile stimuli that mimics maternal care. Artificial odors paired with vigorous strokes in rat pups younger than 10 postnatal days (P), but not older, rapidly induce an orientation-approximation behavior toward the conditioned odor in a two-choice preference test. The olfactory bulb (OB) and the anterior olfactory cortex (aPC), both modulated by norepinephrine (NE), have been identified as part of a neural circuit supporting this transitory olfactory learning. One possible explanation at the neuronal level for why the odor-stroke pairing induces consistent orientation-approximation behavior in <P10 pups, but not in >P10, is the coincident activation of prior existent neurons in the aPC mediating this behavior. Specifically, odor-stroke conditioning in <P10 pups may activate more mother/nest odor's responsive aPC neurons than in >P10 pups, promoting orientation-approximation behavior in the former but not in the latter. In order to test this hypothesis, we performed in vitro patch-clamp recordings of the aPC pyramidal neurons from rat pups from two age groups (P5–P8 and P14–P17) and built computational models for the OB-aPC neural circuit based on this physiological data. We conditioned the P5–P8 OB-aPC artificial circuit to an odor associated with NE activation (representing the process of maternal odor learning during mother–infant interactions inside the nest) and then evaluated the response of the OB-aPC circuit to the presentation of the conditioned odor. The results show that the number of responsive aPC neurons to the presentation of the conditioned odor in the P14–P17 OB-aPC circuit was lower than in the P5–P8 circuit, suggesting that at P14–P17, the reduced number of responsive neurons to the conditioned (maternal) odor might not be coincident with the responsive neurons for a second conditioned odor.

At an early stage of postnatal development, infant rats show a high ability to learn artificial odors associated with tactile stimuli that mimic maternal care. Younger pups (P5–P8) conditioned by pairing a novel scent with vigorous strokes on their backs (using a soft brush) show a consistent orientation-approximation behavior toward the conditioned odor (Moriceau and Sullivan 2005; Morrison et al. 2013; Roth et al. 2013; Ghosh et al. 2015). Interestingly, in older pups (P14–P17) the odor-stroke conditioning protocol did not induce the same behavior (Moriceau and Sullivan 2005; Morrison et al. 2013; Roth et al. 2013; Ghosh et al. 2015). Why does the odor-stroke pairing lose its ability to induce preference to the conditioned odor? Possible answers to this question were offered based on the underlying neural mechanisms of the behavioral phenomena.

It has been proposed that the relevant neural circuit includes the OB and the aPC, both modulated by the NE released from the locus coeruleus (LC). The pairing of odor with activation of β-adrenoceptors in the OB (Sullivan et al. 1992) or in the aPC (Morrison et al. 2013; Ghosh et al. 2015, 2017) induces behavioral olfactory preference in younger infant rodents (rat and mice), while the blocking of these receptors or the lesioning of the LC before pairing (Sullivan et al. 1994) prevents it.

In the LC-OB circuit, it has been suggested that developmental changes in the LC might be in part responsible for the failure of the odor-stroke conditioning in inducing olfactory preference learning in older infant rats. For neonates, LC presents a large response to somatosensory stimuli (noxious and nonnoxious) (Kimura and Nakamura 1985), which no longer occurs in >P10 pups (Rangel and Leon 1995). This functional maturational change in the LC–NE system appears to be dependent on the emergence of the LC autoinhibitory function due to the increase of the NE inhibitory autoreceptor α2 and to the decrease of the autoexcitatory function mediated by NE α1 autoreceptors. Indeed, the pharmacological blockage of the α2 autoreceptors and the activation of the

[6]**These authors contributed equally to this work.**
Corresponding author: envermiguel@gmail.com
Article is online at http://www.learnmem.org/cgi/doi/10.1101/lm.050724.119.

α1 autoreceptors in older pups, during odor presentation, reinstates the odor preference learning (Moriceau and Sullivan 2004).

Another possible explanation focuses on the OB-aPC circuit, specifically at the level of sensory synapses. Sensory information from OB is projected to the aPC by the lateral olfactory tract (LOT), formed by the axons of the mitral and tufted cells. LOT terminals end at the superficial layer of aPC (L1a), forming sensory synapses on the apical dendrites of the pyramidal cells with somas positioned at deep layers (L2 and L3). The L2 and L3 layers and the second portion of the superficial layer (L1b) receive inputs from associative regions, including autoassociative projections (Bekkers and Suzuki 2013). At an early stage of development, high synaptic plasticity at the LOT–L1a aPC synapses is observed, which declines around the first month of postnatal life (Poo and Isaacson 2007) possibly due to down-regulation of NMDA receptors (Franks and Isaacson 2005). Furthermore, it has been found that LOT–L1a plasticity is modulated by β-adrenoceptors induced an increase of L-type calcium channel (LTCC) currents, and that may not be true for older pups (Ghosh et al. 2017).

One hypothesis is that younger rat pups (<P10) learn the mother's odor by associative processes inside the nest (Moriceau and Sullivan 2005). The neural circuit that supports the conditioned learning of artificial odors in experimental conditions (Moriceau and Sullivan 2005) must be the same involved in natural learning in the nest. According to this view, the initially neutral maternal odor (CS) activates a specific group of pyramidal neurons in the aPC, while the maternal care (UCS) elicits a larger response in the pyramidal neurons via the LC–NE system. The repeated natural "pairing" of maternal odor with maternal care (through providing warmth, feeding, touching, licking) causes these neurons to become responsive to the conditioned maternal odor alone and promotes the behavioral approximation. Thus, the response of the neural circuit to the mother's odor in the 1-wk-old pup is completely different from the response to the same stimuli in the newborn rat. Based on this assumption, we offer here an alternative answer for the behavioral olfactory learning phenomena in infant rat pups based on the intrinsic developmental characteristics of the aPC pyramidal cells of younger (<P10) and older pups (>P10).

We hypothesize that odor-stroke conditioning in P5–P8 pups recruits a group of aPC pyramidal cells that are also activated by the maternal odor. As this neural circuit promotes approximation to the maternal odor, we assume their coincidental activation also promotes behavioral preference for the conditioned odor. However, this occurs only for younger pups (<P10). For >P10 pups, the odor-stroke conditioning results in less activation of the aPC pyramidal cells and, therefore, limited chances of recruitment of cells that are also responsive to maternal odor.

To test this hypothesis, we perform a patch-clamp electrophysiological experiment to characterize the intrinsic passive and active properties of the aPC pyramidal cells in two periods of postnatal development (P5–P8 and P14–P18). Then, using the parameters obtained from the experimental data, we implement a computational model of the OB-aPC circuit for the two age periods with a pyramidal cell model that represents the intrinsic properties of real pyramidal cells. Finally, we simulate the process of maternal odor learning inside the nest in the computational OB-aPC model and test the responsiveness of the circuits to the conditioned maternal odor. After conditioning, we expect a lower activation to the presentation of the conditioned maternal odor for P14–P17 aPC pyramidal cells than for P5–P8 aPC.

Results

Patch-clamp electrophysiological data of L2/3 aPC pyramidal cells

Whole-cell patch-clamp recordings were performed from 21 L2/3 pyramidal cells from P5–P8 and P14–P17 age rat pups. As for other sensorial cortices in development, both the passive and active electrophysiological properties of aPC L2/3 pyramidal cell were significantly changed with age (Table 1). In addition, we examined the spike frequency evoked by depolarizing current pulses 500 msec long. The minimum current required for spike train induction (Rheobase) increased significantly with development. At P5–P8, a +40 pA step current-induced spikes in all cells tested ($n = 9$), but at P14–P17, +90 pA or more was needed ($n = 12$). The input–output relationship was examined by plotting the spike frequency versus the amplitude of the injected current (Fig. 1). Pyramidal cells from P5–P8 increased rapidly their spiking frequency reaching their maximum spiking frequency at lower current steps (+60 pA–+120 pA), and after that, the spiking frequency of the cells remained relatively steady despite the increase in the intensities of current injection. On the other hand, cells from P14–P17 reach their maximum spiking frequency at higher current steps (+180pA–+200 pA), and this continued to increase proportionally to the injected current.

Computational model of aPC pyramidal cells

The computational models of P5–P8 and P14–P17 aPC pyramidal cells were calibrated by optimizing their parameters to reproduce

Table 1. Passive and active electrophysiological properties of L2/3 aPC pyramidal neurons

	P5–P8 ($n = 9$ cells)		P14–P17 ($n = 12$ cells)			
Parameters	Mean ± SEM	SD	Mean ± SEM	SD	$t_{(19)}$	P
Passive membrane properties						
V_{rest} (mV)	−39.22 ± 1.89	5.66	−54.35 ± 0.66	2.27	8.45	<0.0001****
R_{in} (MΩ)	438.6 ± 33.15	99.44	177.1 ± 14.44	50.02	7.91	<0.0001****
τ_m (ms)	42.78 ± 4.17	12.53	30.33 ± 1.69	5.88	3.04	0.007**
C_m (pF)	98.21 ± 7.16	21.48	178.1 ± 10.83	37.51	5.70	<0.0001****
Active membrane properties						
AP threshold, (mV)	−36.63 ± 1.35	4.04	−45.96 ± 1.80	6.24	3.90	0.001**
AP amplitude (mV)	76.90 ± 3.38	10.13	85.43 ± 4.53	15.69	1.42	0.17
AP half-amplitude width (ms)	4.32 ± 0.33	0.98	2.97 ± 0.09	0.34	4.46	0.0003***
Max. frequency (Hz)	11 ± 2.36	7.07	21.50 ± 2.53	8.79	2.94	0.0085**
Rheobase (pA)	48.89 ± 6.76	20.28	95.00 ± 11.04	38.26	3.27	0.004**
AP threshold -V_{rest} (mV)	3.92 ± 2.95	8.86	8.77 ± 2.38	8.23	1.29	0.21

Intrinsic properties were measures through whole-cell current clamp of L2/3 aPC pyramidal cells at P5–P8 and P14–P17. Values are mean ± SEM or SD. Asterisks represent statistically significant unpaired Student's *t*-test comparisons. **$P < 0.01$; ***$P < 0.001$; ****$P < 0.0001$.

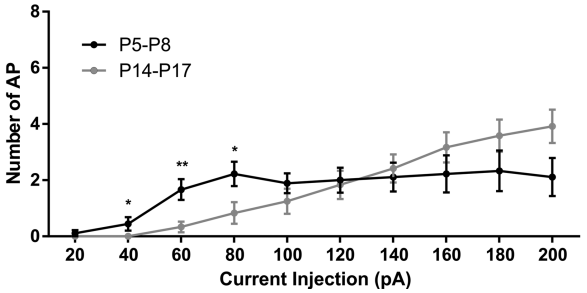

Figure 1. Number of AP-current injected curves of aPC L2/3 pyramidal cells in P5–P8 and P14–P17age rat pups. A relationship between the average number of AP and intensity of injected current (pA) in a 200 msec window recording in brain slices from P5–P8 (black curve, $n=9$ cells) and P14–P17 (gray curve, $n=12$ cells) aged pup rats. Asterisks represent statistically significant unpaired Student's *t*-test comparisons between P5–P8 and P14–P17 at each current intensity. (*) $P<0.05$; (**) $P<0.01$.

the characteristics of the two age groups. In Figure 2 the adjusted, postoptimized, model of aPC pyramidal cells is shown superimposed (blue) to the experimental data (colors) of the spike numbers as a function of current injection for P5-P8 (A, $n=9$ records from nine cells) and P14–P17 (B, $n=12$ records from 12 cells) and for the ISI-current injection relationship obtained from adjusted experimental data (black) for P5–P8 (*C*, $n=7$ records from seven cells) and P14–P17 (D, $n=11$ records from 11 cells). The average injected current that evoked only two spikes was considered for the first ISI adjusted point. For P5–P8 it was 70 pA, and for P14–P17 it was 126 pA, with average ISI values of 56.6 and 107.23 msec, respectively. For the second and third ISI adjusted points, we considered arbitrary representative current injections of 140 and 200 pA, and the ISI average values were obtained from the first two spikes evoked by those currents. For P5–P8, the ISI adjusted point for 140 pA was 31.95 msec, and at 200 pA was 22.17 msec. For P14–P17, the ISI adjusted point at 70 and 140 pA were 62.6 and 37.1 msec, respectively.

We next tested if the distinct pyramidal cells properties of P5–P8 and P14–P17 are still conserved when the adjusted models are included in the OB-aPC circuits. In the OB-aPC circuits, one pyramidal cell receives random excitatory inputs from 20 to 140 mitral cells, and we simulate synaptic change at the Mt–Pyr synapses for 6000 msec. In Figure 3, the change of input dependent weight in pyramidal cells in OB-aPC circuits is shown superimposed for the two age groups in 13 circuits (colors). In P5–P8, the circuit of 20 Mt–Pyr induced an important reduction in the synaptic weight (42.85% from the basal value) (A1, red curve below the dotted line) and circuits with 30–140 Mt–Pyr gain synaptic weight (34%–54% from the basal value) (A1, colors curve above the dotted line). In P14–P17, circuits of 20, 30, and 40 Mt–Pyr induced an important reduction in the synaptic weight (42.85% from the basal value) (A2, color curves below the dotted line), while circuits of 50–180 Mt–Pyr induced a great gain (37%–57% from the basal value).

A plot of individual circuits comparing the weight change in the two ages is shown in Figure 3B. The aPC pyramidal cells receiving inputs from 20 Mt cells present a decrease in synaptic weight, independently of age interval (B1); as the number of Mt inputs increase, we observe a sharp transition after which there is an important increase in synaptic change. For pyramidal cells in the P5–P8 age interval, the transition occurs at approximately 30 Mt inputs, while for P14–P17 at approximately 50 Mt inputs (B1–B9).

A comparative plot of the average of synaptic weight as a function of Mt inputs is shown in Figure 3C. Circuits of 50 Mt–Pyr gain

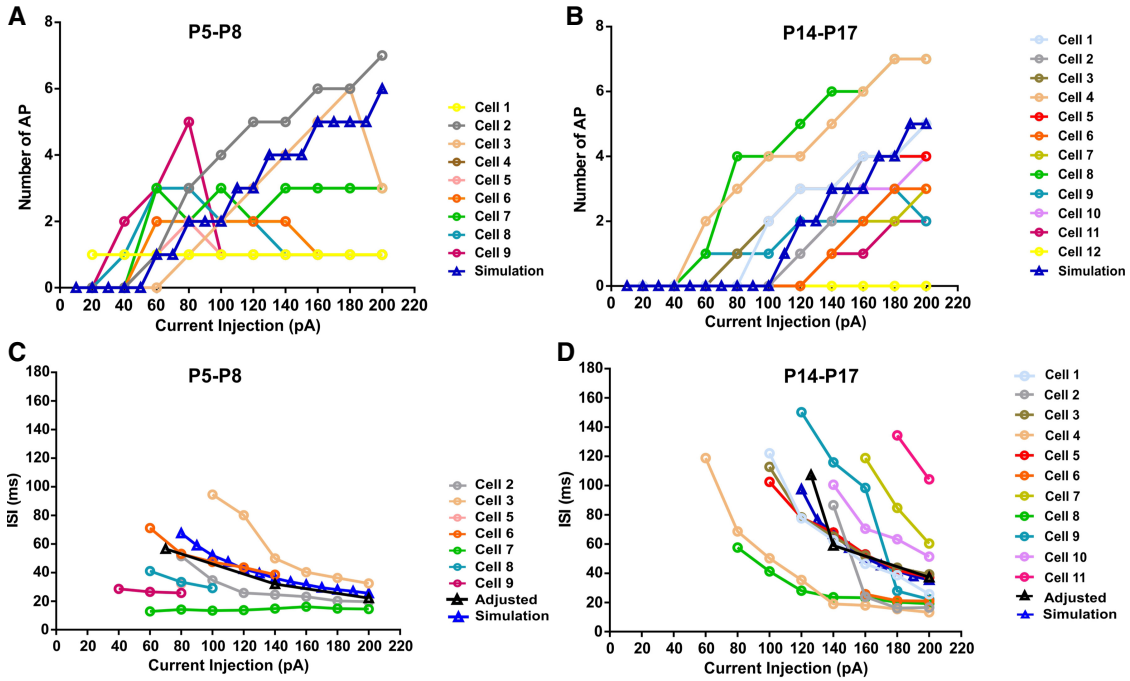

Figure 2. Representative results of current-clamp analysis and simulation of experimental data. Current injection versus the number of AP from individual pyramidal cells in current-clamp recording at (*A*) P5–P8 and at (*B*) P14–P17. Colors represent different pyramidal cells measured in intervals of 20 pA. Note the variability in cell response for different current injections. The blue curve represents the simulated data based on the adjusted curve. (*C*) Current injection versus interspike interval (ISI) from individual pyramidal cells at P5–P8 and at (*D*) P14–P17 in a 200 msec window recording. Each point and color represents the value of each individual pyramidal cell obtained in current-clamp recording from cells with two or more spikes in a given current injection. The black curve (triangle) represents three adjusted points chosen to represent the experimental ISI mean curve for each age group (*C*,*D*).

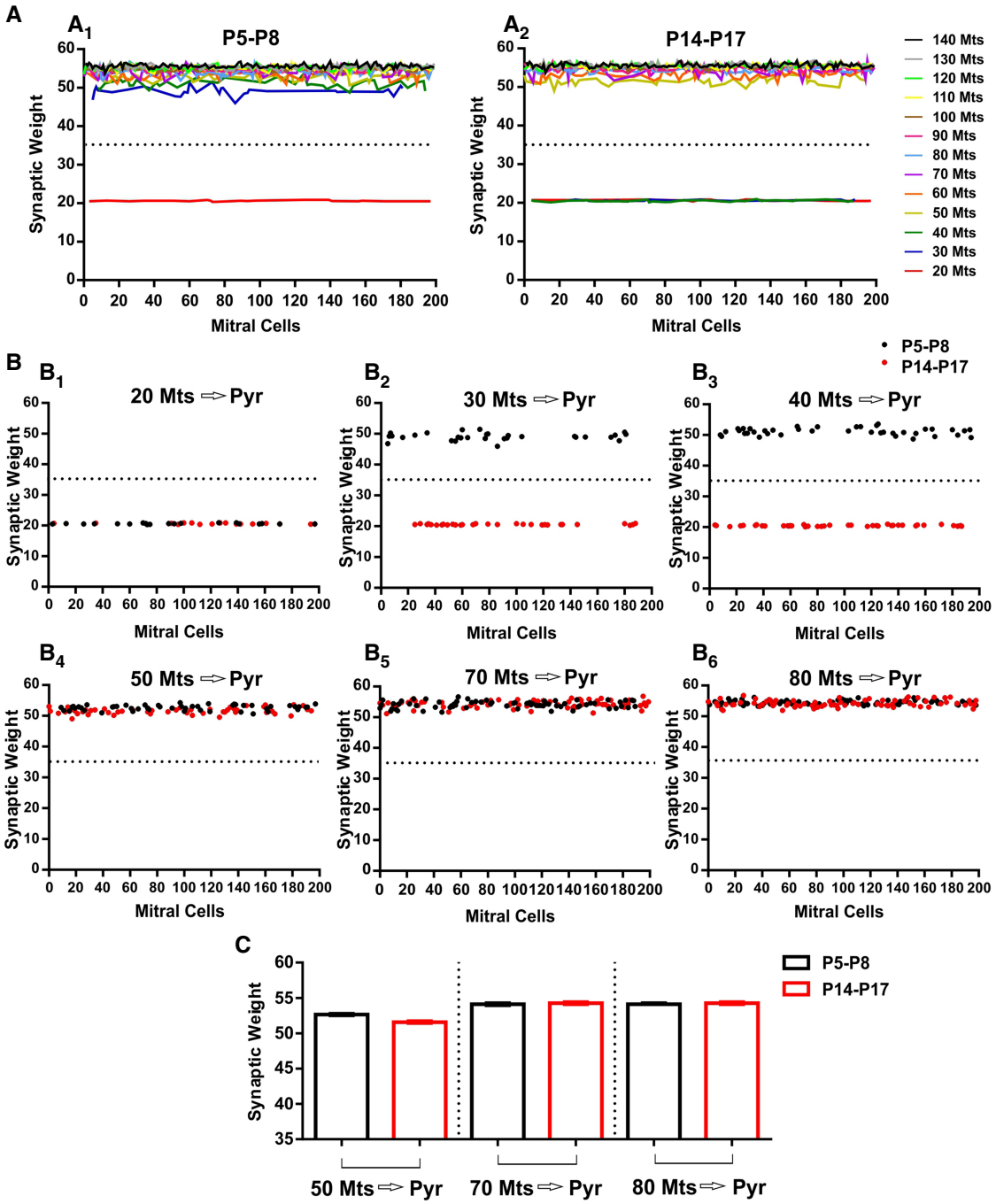

Figure 3. Simulation of plasticity weight change at mitral-pyramidal cells synapses across 6000 msec simulation period for P5–P8 and P14–P17 age group. The circuit formed by 200 mitral cells and 13 pyramidal cells was simulated during 15 respiratory cycles. Each pyramidal cell receives random inputs from 20 to 80 mitral cells firing at respiratory rhythm of 2 Hz (color curves), and their activities induce changes in the synaptic weights of the OB-aPC circuit (*A*). Inputs from 30 to 140 mitral cells (*A*1) or from 50 to 140 mitral cells (*A*2) induce gain in synaptic weight (plotted from synaptic weight before simulation, 35) at P5–P8 and P14–P17, respectively. Note that only inputs from 20 mitral cells induce loss of synaptic weight in pyramidal cells from the P5–P8 group, but inputs from 30 or more induce a great gain of synaptic weight (*B*1), which occurs with 50 or more mitral cells inputs for the P14–P17 age group (*B*1–*B*6). When we look closer at the circuit when the two-age groups gain synaptic weight (*C*), we can note that 50 Mt–Pyr circuits gain more weight in the P5–P8 group than in the P14–P17 group and as the number of mitral cells inputs increase (70 and 80 Mt–Pyr circuits), the gain of synaptic weight become similar for the two ages.

more synaptic weight in P5–P8 (52.66 ± 0.12, $n = 50$) than in P14–P17 (51.58 ± 0.14, $n = 50$) [$t_{(98)} = 5.83$, $P < 0.0001$, unpaired Student's *t*-test]. On the other hand, circuits of 70 Mt–Pyr (P5–P8: 54.12 ± 0.14, $n = 70$ vs. P14–P17: 54.27 ± 0.14, $n = 70$) or 80 Mt–Pyr (P5–P8: 54.18 ± 0.12, $n = 80$ vs. P14–P17: 54.50 ± 0.07, $n = 80$) show a similar gain of synaptic weight ($P > 0.05$, unpaired

Student's *t*-test). These results indicate that in both circuits P5–P8 and P14–P17, the pyramidal cells still conserved their properties to respond to depolarizing inputs and correspondingly gain synaptic plasticity. However, in the continuum development of circuits, what will happen with synaptic modifications induced by Mt depolarizing inputs when the aPC pyramidal cells properties change with the maturation from P5–P8 to P14–P17?

We next tested whether the gain in synaptic plasticity observed in P5–P8 circuits is still conserved when parameters of the pyramidal cells switch from the P5–P8 to the P14–P17. In Figure 4A, we see the change in the resting membrane potential of three pyramidal cells receiving input from 50 random mitral cells (Cell 1, Cell 2, and Cell 3, superimposed orange, green, and blue traces) when their intrinsic electrophysiological properties switch from P5–P8 to P14–P17. After the switch, the Cell 1 reduces in 50% its firing frequency, and after 1700 msec of simulation, it stops (B1). Cell 2 (B2) and Cell 3 (B3) also reduce their firing frequency after the switch but remain active until the end of the simulation.

In Figure 4C, we see the average of synaptic weight change for circuits with 30 Mt–Pyr, 40 Mt–Pyr, and 70 Mt–Pyr cells. Pyramidal cells receiving inputs from 30 Mt cells experienced an increase in synaptic strength with P5–P8 parameters (49.07 ± 0.21, $n = 30$,

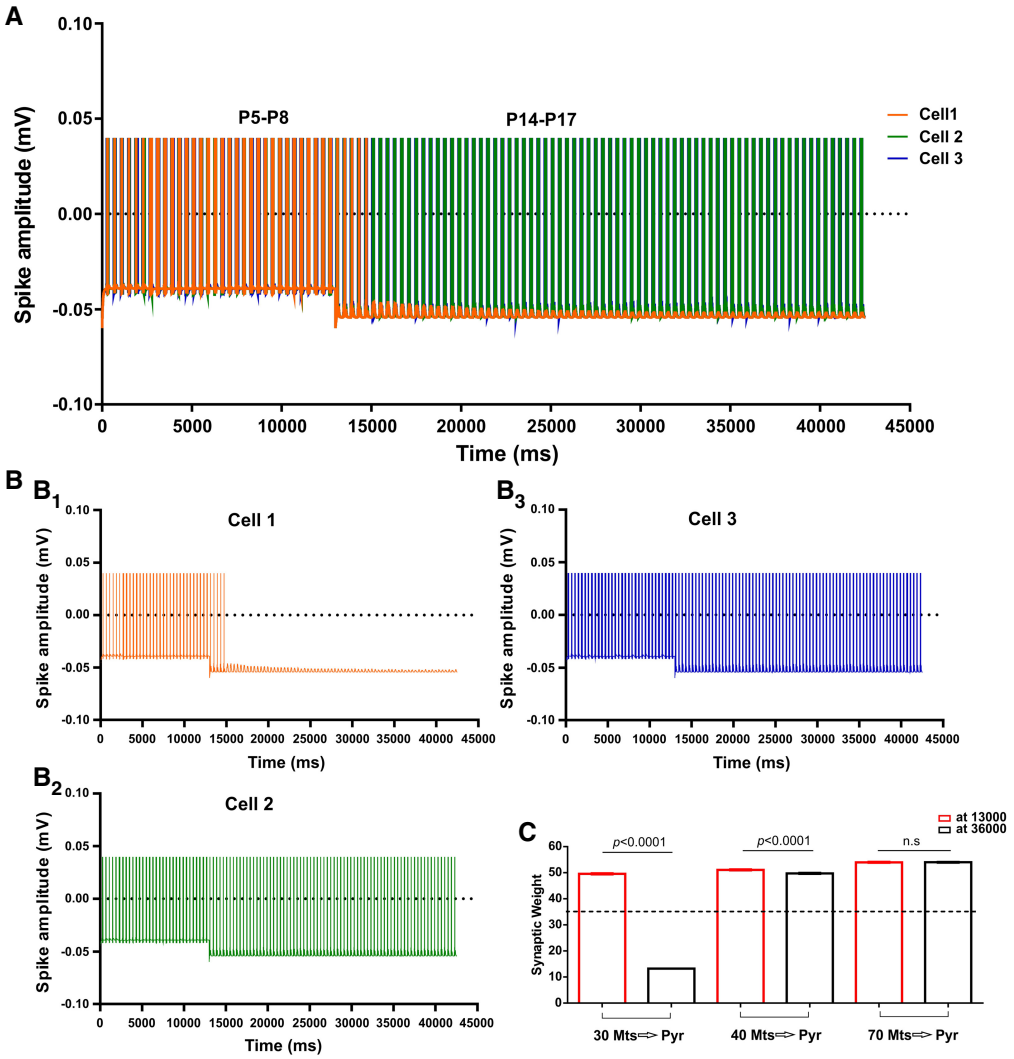

Figure 4. Simulation of the evoked activity in aPC pyramidal cells during the switch in intrinsic properties from P5–P8 to P14–P17. We simulate the Mitral-Pyramidal circuit and the evoked spikes of three random choices of pyramidal cells (color traces) recorded when receiving input from 50 random mitral cells firing at respiratory rhythm of 2 Hz (*A*). Initially, the passive and active membrane properties of these pyramidal cells were set up to represent the profile of the P5–P8 age period and after approximately 10,000 msec of simulation, the passive and active properties membrane properties of pyramidal cells were switched to represent the profile of P14–P17 age period. Note the large hyperpolarization in the resting membrane potential of the three neurons during the change of their membrane potential values, which continues steadily until the end of the simulation. Interestingly, the Cell 1 (orange traces) stops its firing after the switch of membrane properties values, but the Cell 2 (green trace), and Cell 3 (blue trace) continue to firing steadily until the end of the simulation. In the same simulation, we recorded the synaptic changes of those pyramidal cells receiving inputs from 30, 40, and 70 random mitral cells (*C*) and recorded the average of synaptic weight at the end of 13,000 msec (red bar) and 36,000 msec (black bar) of simulation. Pyramidal cells receiving inputs from 30 mitral cells show a synaptic weight gain after 13,000 msec but not after 36,000 msec. On the other hand, the pyramidal cell receiving inputs from 40 and 70 mitral cells show a steady synaptic gain during all simulation periods. Δt: 0.5 msec; Bin: 0.5 msec.

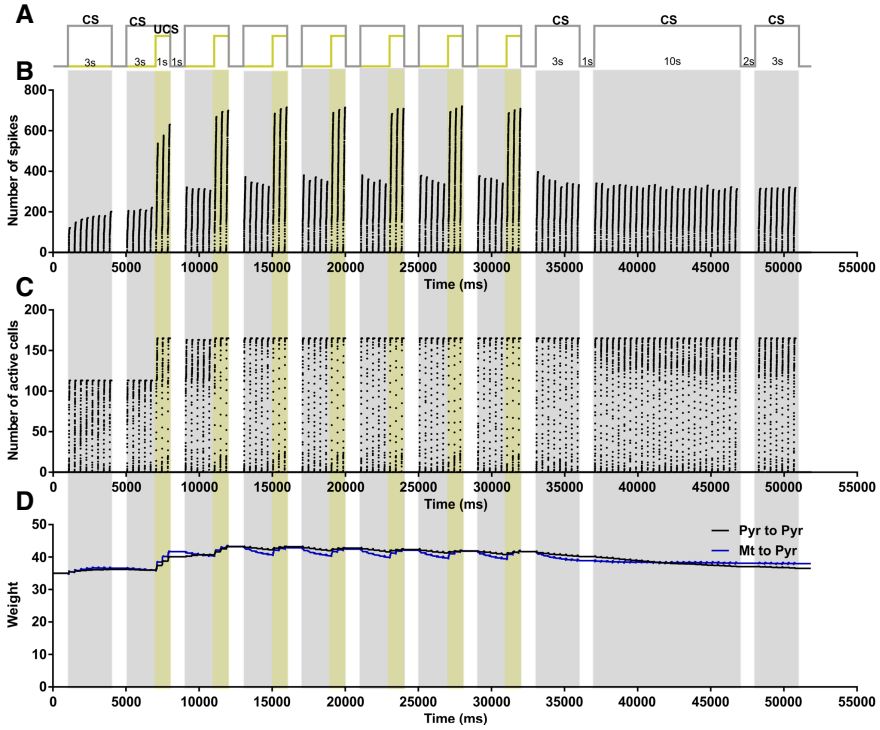

Figure 5. Simulation of the maternal odor preference's learning and exposure to the conditioned maternal odor in P5–P8 aPC pyramidal cells. (*A*) Protocol for classical conditioning of maternal odor preference in the nest. A delayed pairing procedure was used in which the CS (maternal odor) onset preceded the UCS (maternal care, NE action) by 2 sec. CS and UCS overlapped for 1 sec, after which the CS was terminated. The CS–UCS pairing was presented seven times with 1 sec intervals. Learning was tested by the presentation of CS during 3 sec. After the test, CS alone was presented again during 10 sec. After a 2-sec interval learning was tested again by the presentation of CS during 3 sec. During this period, the pyramidal cells of the aPC had properties compatible with the P5–P8 age. (*B*) Number of cumulative aPC pyramidal cell spikes during the CS–UCS pairing and CS presentation, collected at every 100 msec of simulation. (*C*) Number of active aPC pyramidal cells during the CS–UCS pairing and CS presentation, collected at every 100 msec of simulation. (*D*) Synaptic weight gain of Pyr–Pyr (black curve) and Mt–Pyr (blue curve) synapses during CS–UCS pairing and CS presentation. Excitatory mitral inputs fire at the respiratory rhythm (2 Hz). Bin 0.5 msec.

measured at 13,000 msec of simulation, black bar) but suffered a decrease when the parameters changed to the P14–P17 profile (20.57 ± 0.03, measured at 36,000 msec, red bar) [$t_{(58)} = 131.8$, $P < 0.0001$, unpaired Student's *t*-test]. On the other hand, pyramidal cells receiving inputs from 40 Mt cells show an increase in synaptic weight with P5–P8 parameters (51.08 ± 0.17, $n = 40$, measured at 13,000 msec of simulation, black bar). After the switch to the P14–P17 profile the average of synaptic weight (49.75 ± 0.17, $n = 40$, measured at 13,000 msec of simulation, red bar) was above the basal value and slightly smaller than for the P5–P8 profile [$t_{(78)} = 5.55$, $P < 0.0001$, unpaired Student's *t*-test]. On the other hand, pyramidal cells receiving inputs from 70 Mt cells exhibited a gain in synaptic strength independent of the age profile [P5–P8: 54.00 ± 0.16, $n = 70$ vs. P14–P17: 54.01 ± 0.13, $n = 70$; $t_{(138)} = 0.04$, $P = 0.97$, unpaired Student's *t*-test]. These results indicate that circuits that have gained synaptic connections at P5–P8 induced by a given Mt input lost it after the properties of pyramidal cells switched to the P14–P17 profile in response to the same input.

Responses to the presentation of the conditioned odor

First, we submitted the P5–P8 OB-aPC model to a classical conditioning protocol (odor-stroke) to simulate the process of learning the pup preference for the mother's odor. Then we exposed the conditioned OB-aPC model to the conditioned odor (CS) in two conditions: (1) The model has parameters compatible with P5–P8 age (Fig. 5), and (2) the model parameters switch from the P5–P8 to the P14–P17 profile (Fig. 6). In Figure 5, the change in pyramidal cells activity and weight at the Mt–Pyr synapses during conditioning and odor exposure protocol (A) are shown in cumulative dots registered at every 200 msec of simulation. After the conditioning, the number of spikes and the number of active Pyr cells in response to CS increases (B and C) compared to the CS before the conditioning. These changes were maintained steady during the CS presentation (10 msec) (B and C).

Moreover, after conditioning, the synaptic strengths increased at Mt–Pyr (blue curve), Pyr–Pyr synapses (black curve), and this gain was maintained during CS presentation (D). This result indicates that P5–P8 OB-aPC circuits modify their synaptic plasticity, number of active cells, and spikes in response to the conditioned odor because of training. However, in nature, the rodent pups learn the mother`s odor during the first postnatal days (<P10), and this learned odor is tested in >P10 age pups. What will happen at the circuit level with synaptic modifications induced by maternal odor learning when the aPC pyramidal cell properties change with the maturation from P5–P8 to P14–P17?

Next, we repeated the classical conditioning protocol, but this time, after the test of the CS odor, we switched the intrinsic properties of the aPC pyramidal cells to the P14–P17 age profile before submitting the circuit to the CS odor exposure protocol (Fig. 6A). After conditioning, the behavior of the network is similar to Figure 5. But this time, the prolonged exposure to the CS odor results in a gradual reduction in the number of pyramidal spikes (Fig. 6B), the number of active cells (Fig. 6C), and synaptic strength at Mt–Pyr but not at Pyr–Pyr synapses (Fig. 6D).

Figure 7 shows the comparative changes in the number of pyramidal spikes (A) and the number of active pyramidal cells (B) after the conditioning CS test and during CS odor presentation in the switched P14–P17 circuit (red dots) superimposed on the nonswitched P5–P8 circuit (black dots). During CS odor presentation, the pyramidal cells from the switched circuit (P14–P17) showed an important reduction in the number of spikes compared to pyramidal cells from the nonswitched circuit (P5–P8) (A). Similarly, during CS odor presentation, the number of active pyramidal cells was dramatically reduced in the switched circuit (P14–P17) compared to the nonswitched (P5–P8) (B). These results indicate that when the properties of cells mature from P5–P8 to P14–P17, the P5–P8 circuits that have learned the maternal odor lose plasticity at the level of the OB-aPC synapses, as well as the number of active pyramidal cells and spikes in response to the maternal odor. Together these results suggest that the P14–P17 OB-aPC circuits may have a reduced number of pyramidal cells responsive to the maternal odor.

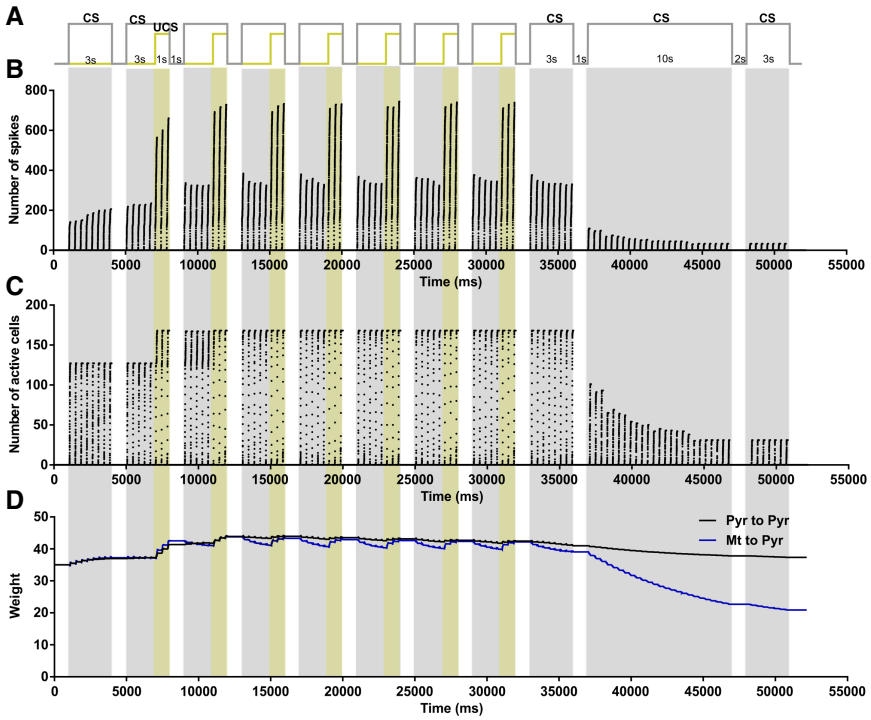

Figure 6. Simulation of maternal odor preference learning in P5–P8 aPC pyramidal cells and exposure to the conditioned maternal odor in P14–P17 aPC pyramidal cells. (*A*) Protocol for classical conditioning of maternal odor preference in the nest. A delayed pairing procedure was used in which the CS (maternal odor) onset preceded the UCS (maternal care, NE action) onset by 2 sec. CS and UCS overlapped for 1 sec, after which the CS was terminated. The CS–UCS pairing was presented seven times with 1s intervals for the network with aPC having parameters compatible with the P5–P8 age. Learning was tested by the presentation of CS during 3 sec. After the test, the network had its parameters shifted to the P14–P17 age and the CS alone was presented again during 10 sec. After 2-sec of interval, learning was tested again by the presentation of CS during 3 sec. (*B*) Number of cumulative aPC pyramidal cell spikes during the CS–UCS pairing and CS presentation, collected at every 100 msec of simulation. (*C*) Number of active aPC pyramidal cells during the CS–UCS pairing and CS presentation, collected at every 100 msec of simulation. (*D*) Synaptic weight gain of Pyr–Pyr (black curve) and Mt–Pyr (blue curve) synapses during CS–UCS pairing and CS presentation. Excitatory mitral inputs fire at the respiratory rhythm (2 Hz). Bin 0.5 msec.

Discussion

Intrinsic membrane properties of aPC pyramidal cells change from P5–P8 to P14–P17, and the number of cells reduces gradually in response to the exposure to the conditioned maternal odor

Younger infant rats (<P10) rapidly learn olfactory preference to a novel odor paired with a vigorous stroke on their back, but the pairing of the same stimuli did not induce this learning in older pups (>P10) (Moriceau and Sullivan 2005). Here we explore whether the odor-stroke conditioning is effective in inducing olfactory preference learning in younger pups because it activates more aPC pyramidal cells responsive to the maternal odor that promotes an orientation-approximation behavior that no longer occurs in older pups. Given that intrinsic membrane properties of pyramidal cells determine the integration of the synaptic inputs and ultimately the action potential generation, we hypothesized that in older pups (P14–P17), there are fewer aPC pyramidal cells responsive to maternal odor than in younger pups (P5–P8) due to their intrinsic maturational properties.

To address this question, we examined the membrane and AP properties of aPC pyramidal cells of rat pups of P5–P8 and P14–P17. We found in aPC slices that L2/3 pyramidal cells in older pups had reduced resting membrane potential, input resistance, and membrane time constant compared to younger pups. Moreover, action potentials (AP) in older pups had a higher hyperpolarizing threshold and more rapid APs than in younger pups. In older pups, higher step amplitudes of depolarizing current were needed to elicit action potentials, and the frequency of their firing increased as the step of current injection amplitude increased. The aPC pyramidal cells of younger pups evoked APs at lower amplitude steps of depolarizing current injection, and after reaching the maximum frequencies of firing, these cells showed a rapid adaptation in their firing frequency. Using characteristics of real cells, we constructed an artificial model of the P5–P8 and P14–P17 OB-aPC circuits and simulated the learning of the maternal odor inside the nest using a classical conditioning paradigm, and after that, we simulated the exposure of the circuits to the conditioned maternal odor. We found that aPC cells from the P5–P8 circuit showed a greater number of active aPC pyramidal cells and spiking responses during the exposure (10 sec) to the maternal odor, while the aPCs from P14–P17 showed a gradual reduction in the number of active aPC pyramidal cells and spiking responses during the exposure to the same stimuli.

Processing of the OB synaptic inputs in the aPC pyramidal cells at P5–P8 and P14–P17

One of the main findings in this study is that the number of aPC pyramidal neurons responsive to the conditioned maternal odor (the neurons that mediate orientation-approximation behavior) decreases with age due to maturational changes in the intrinsic properties of the aPC pyramidal cells. Our proposed explanation is that in older pups (P14–P17) the reduced number of aPC pyramidal neurons responsive to the maternal odor, might be not overlapping with the aPC pyramidal neurons responsive to a second conditioned odor and that this might be more likely to occur when they are younger (P5–P8). We also propose that the different results for odor-stroke conditioning in infant rats at <P10 and >P10 can be explained by the developmental changes in the intrinsic membrane properties of the target aPC pyramidal cells, which have a lower threshold for synaptic inputs from the OB in P5–P8 than in P14–P17. It has been suggested that pyramidal cells with a higher input resistance and prolonged time membrane constant have responses of greater magnitude and prolonged duration for the synaptic input (McCormick and Prince 1987). Therefore, aPC pyramidal cells from younger rats with these intrinsic electric characteristics, would respond better to synaptic inputs with small currents and slow kinetics, while these cells in older pups have more hyperpolarized resting membrane potential, reduced input resistance and faster membrane time constant responding better to prolonged synaptic inputs with higher currents with faster kinetics. Therefore, a novel odor-stroke conditioning in older pups did not induce olfactory preference learning.

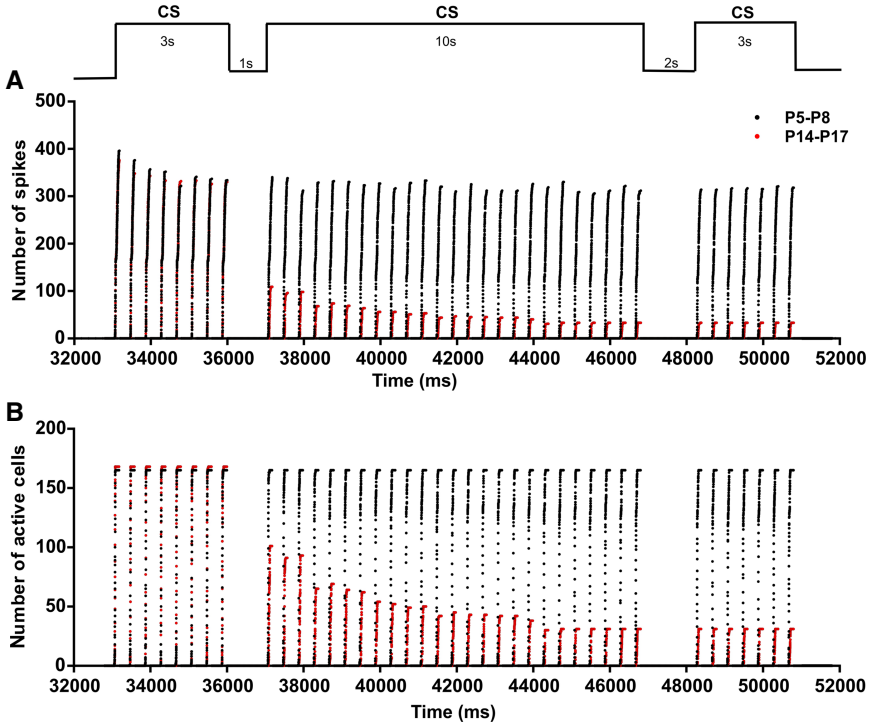

Figure 7. Comparison of the number of spikes and number active cells in P5–P8 and P14–P17 aPC pyramidal cells evoked by conditioned maternal odor. After the conditioning of CS (maternal odor) and UCS (maternal care) in an artificial olfactory circuit with aPC pyramidal cells with passive and active electrophysiological characteristics of P5–P8 rats, the evoked response of pyramidal cells to CS alone was tested in the same age circuit (first CS in *A,B*). In order to compare the evoked pyramidal cells to conditioned maternal odor at P5–P8 and P14–P17, the CS alone was presented again (second CS in *A,B*) 1 sec after the first CS was finished and 2 sec after the second CS was finished (third CS in *A,B*). (*A*) The number of spikes with characteristics of P5–P8 was higher in response to CS alone (black points). On the other hand, the evoked response of pyramidal cells characteristic of P14–P17 was reduced progressively throughout the CS presentation (red points). The same evoked response was observed for the two age group cells during the third CS presentation. (*B*) The reduced spike activity at P14–P17 in response to CS was due to the reduction in the number of active pyramidal cells compared with P5–P8. Excitatory mitral inputs fire at the respiratory rhythm (2 Hz). Bin 0.5 msec.

Maternal odor preference learning is supported by the same circuit that supports early olfactory preference learning for an artificial odor

Our simulation of learning represents the current understanding that rodent pups learn maternal odor through experiences with the mother inside the nest during the first postnatal week. Neonate rats (P1–P4) tested in two-choice tests show organized orientation-approximation behavior toward the maternal odor in relation to nest bedding (Polan and Hofer 1998; Polan et al. 2002), nest bedding in relation to clean bedding (Cornwell-Jones and Sobrian 1977; Szerzenie and Hsiao 1977) and the maternal diet odor in relation to standard diet (Duveau and Godinot 1988). Older pups (in the second and third postnatal weeks) continued to show consistent preferences to the maternal odor (Polan and Hofer 1998; Al Aïn et al. 2016; Perry et al. 2016), to their own nest bedding (Gregory and Pfaff 1971; Cornwell-Jones and Sobrian 1977), and to the maternal diet odor (Duveau and Godinot 1988; Terry and Johanson 1996). All this behavioral evidence suggests that associations formed inside the nest between the maternal/nest odor and a range of maternal care stimuli (warmth, feeding, touching, licking) mediate the olfactory preference learning for the mother/nest's odor (Moriceau and Sullivan 2005). Therefore, at birth, the mother's odor may be a neutral stimulus that elicits little more than an orienting response in pups, and only after a period inside the nest, does the mother's odor becomes effective in eliciting an orientation-approximation behavior in the pup.

It has been proposed that maternal odor learning is the same that supports the conditioned learning of artificial odor outside the nest (paired with stroke and tactile stimuli that mimic maternal licking stimulation) (Sullivan 2001). Thus, in the newborn rat, the neutral maternal odor may elicit the activity of specific groups of pyramidal neurons in the aPC, while maternal care may elicit a great response in the pyramidal neurons via the LC–NA system. The repeated natural "pairing" of maternal odor with maternal care during mother–infant interactions elicits the activity of groups of aPC pyramidal neurons. After a few days, these neurons become responsive only to the conditioned maternal odor and promote behavioral approximation. Therefore, the response of the neural circuit to the mother's odor in the 1 wk pup would be completely different from the response to the same stimuli in the newborn rat.

Future Work

In this work, we show a change in the activity of the aPC pyramidal cells in the OB-aPC circuit for two age periods as a function of the connections of mitral cells with pyramidal cells, where the activity of the mitral cells for both age circuits was the same. To control the number of variables in the experimental model, we made some simplifying assumptions. First of all, some cells types were not included, like the axonal terminal from the olfactory nerve (olfactory sensory neurons), periglomerular cells and granule cells in the OB circuit, the feedforward and feedback interneurons in the aPC circuit (cf. de Almeida 2013, 2016). Additionally, developmental distinctions in the inhibitory synaptic inputs to the aPC pyramidal cells in the two age groups (Pardo et al. 2018) were also not included.

Similarly, we have omitted the NE modulation of the LOT-aPC synapses proposed to mediate the enhanced synaptic excitation and reduced inhibition underlying early odor preference learning in <P10 (Ghosh et al. 2015). The excitatory synaptic plasticity has not been modeled in Mitral-Pyramidal synapses, another developmental difference between these periods (higher at an early postnatal period and progressively declining around the first month (Poo and Isaacson 2007)) as a function of the down-regulation of NMDA receptors at LOT-aPC synapses (Franks and Isaacson 2005). Some of these variables could be relevant to prevent the early odor preference learning in P14–P17 infant rats and are left for future work.

We constructed OB-aPC circuits for P5–P8 and P14–P17 rats, in which we modeled similar spontaneous activity of Mt cells for the two periods. Moreover, during the simulation of conditioning and odor presentation protocols, the Mt cells were modeled to fire at a constant frequency for the two circuits and each pyramidal cell

to receive inputs from 15–45 random Mt cells. Higher inputs from Mt cells to aPC pyramidal cells (>80) may enable P14–P17 infant rats to learn the preference for the novel odor paired with stroke. However, as semilunar cells (SL), whose somas are more superficially located in layer 2 of the piriform cortex (Bekkers and Suzuki 2013), do not have autoassociative connections (Choy et al. 2017), they could be more affected by the reduction in number of aPC pyramidal cells responsive to conditioned maternal odor than the deeper pyramidal cells with autoassociative properties studied here.

Our model does not exclude the other reasons for the odor-stroke conditioning lack of effectiveness in inducing olfactory preference in older pups (i.e., development of the LC–NE system, development of LOT-aPC synaptic plasticity). Instead, our hypothesis adds to these previous findings in explaining the phenomenon. During the maturation of the olfactory system many scenarios may occur. The one we adopt here is due to the maturation of the aPC pyramidal cells, as observed in our experiments, and it is a straightforward and comprehensive hypothesis.

Contributions of the model to the odor-stroke conditioning outcomes in infant rats

The results presented here can help us to understand at a neural level the behavioral outcomes of odor-stroke conditioning in <P10 and >P10 rat pups. In the classical conditioning paradigm adopted for younger rat pups (P5–P8), the unconditioned stimulus is a vigorous stroke on the pup's back, which after repeated pairing with an odor (the conditioned stimulus) induces the behavioral response of approximation toward the conditioned odor. Interestingly, the stroke did not elicit this response before training, only an increase in the motor basal activity of the pups (Sullivan et al. 1986; Sullivan and Wilson 1993). However, how can a novel odor become effective in eliciting an approximation response when it has been paired with a tactile stimulus that did not elicit this response? Our answer for that is to consider that the odor-stroke pairing takes advantage of the circuitry in aPC already developed during the pup`s interactions with the mother in the nest. In other words, the properties of the immature pyramidal cells in aPC allow the odor-stroke conditioning to recruit a circuit that partially overlaps with the circuit supporting the approximation behavior toward the mother`s odor. With the maturation of the pyramidal cells in the aPC after P10 the overlap in the circuits is no longer possible, and the odor-stroke pairing is no longer effective. We think that this is the most straightforward hypothesis given the knowledge of the circuitry, and it is an experimentally testable hypothesis. This approach would also be supported by the unified reinforcement principle proposed by Donahoe et al. (2006), in which the respondent/operant behavior emerges simultaneously inside the nest. From this perspective, the neurons recruited for the conditioned maternal odor in the aPC could be the same activated during the odor-stroke conditioning, and these coincident neurons would be the ones that are reduced in the P14–P17 OB-aPC circuit in the simulation of the maternal odor exposure.

In conclusion, our model suggests two distinct functions for odor processing in the OB-aPC circuit for the associative learning in <P10 and >P10 infant rats based on the development of intrinsic electrophysiological properties of aPC pyramidal cells. For the two developmental OB-aPC circuits, the success for the odor-stroke pairing is dependent on the coincidental activation during conditioning of the aPC pyramidal cells responsive to the maternal odor promoting orientation-approximation behavior (Fig. 8). The change in the intrinsic properties of the aPC pyramidal cells reduces the availability of the maternal odor responsive pyramidal cells during the maternal odor exposure.

Materials and Methods

Experimental procedures

Animals and ethics statement

Electrophysiological data were obtained from Wistar rat pups in two age groups (P5–P8 and P14–P17) from the Centre for Reproduction and Animal Experimentation Laboratory of the Universidade Federal do Rio Grande do Sul (UFRGS). Animals were housed under controlled temperature (21 ± 1°C) and humidity (60%) conditions and were maintained on a 12-h light–dark schedule (lights on at 06:00 h) with free access to water and rodent chow (Nuvilab Cr2). Animal use and all experimental procedures were in concordance with the Guidelines for Animal Care and Use of Laboratory Animals of the National Institute of Health and were approved by the Ethics Committee in Use of Animals (CEUA) of UFRGS (Number 27961/2014).

Patch–clamp current–clamp recording

For electrophysiological studies, slices of aPC were prepared from male and female Wistar rat pups at age P5–P8 and P14–P17 as described previously (Pardo et al. 2018). Whole-cell patch-clamp recordings were made on pyramidal cells located in the L2/3 of aPC under the mode of current-clamp with axon Multiclamp

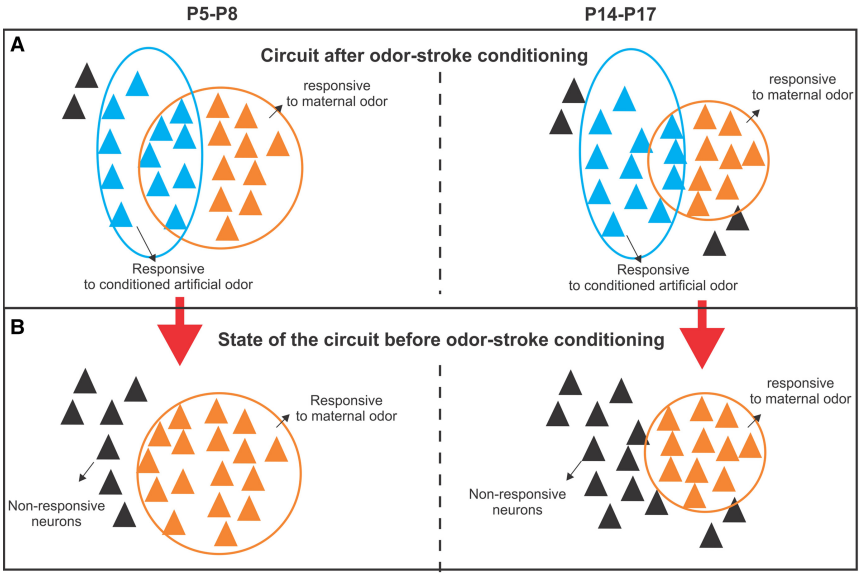

Figure 8. Graphical representations of the hypothesis. Some neurons that are responsive for an artificial odor may be coincident with neurons that are responsive to the maternal odor. This could occur to a lesser extent at P14–P17 than at P5–P8 (*A*). One possibility is that at P14–P17, the number of maternal odor responsive neurons could be reduced before the artificial odor-stroke conditioning in relation to P5–P8 (*B*).

700B amplifier (Molecular Devices). For current-clamp recording (Fig. 1A), the intracellular solution contained (in mM): potassium gluconate (120), KCl (10), $MgCl_2$ (1), $CaCl_2$ (0.025), EGTA (0.2), Na_2-ATP (2), Na_2-GTP (0.2), HEPES (10), titrated to pH 7.2 with KOH, and 290 mOsmol L^{-1}. Whole-cell recording pipettes had a tip resistance of 3–4 MΩ. Data were digitalized at 10 kHz with Digidata 1440-A System (Molecular Devices), filtered at 1 kHz (−3 dB, eight-pole Bessel) and analyzed offline with pClamp 10.6 software (Molecular Devices). The membrane potential was held at −65 mV for all neurons. Cells were excluded if they did not meet the following criteria: a stable resting membrane potential more negative than −55 mV, action potential crossing 0 mV. For measuring intrinsic properties of cells, a series of depolarizing and hyperpolarizing currents, 500 msec long, square-pulse current steps were injected (−180 pA to +300 pA) with intervals of 500 msec, steps of 20 pA.

Data analysis

The membrane resting potential (V_{rest}) was measured within a few minutes after breaking the membrane and defined as the steady-stable membrane potential (in the I = 0 mode). Input resistance (R_{in}) from the steady-stable voltage response to 1 sec of subthreshold current injection of −100 pA was calculated as the ratio of the peak voltage deflection to the current injected. The time constant (τ_m) was defined as the time necessary for the cell to reach 63.2% of its maximal deflection in response to hyperpolarizing current injection (−100 pA). The membrane capacitance (C_m) was calculated using the formula $C_m = \tau_m/R_{in.}$ To measure action potentials (AP) a 1-sec long series of depolarizing steps were applied (range 20–300 pA, at 20 pA increments). Only APs with amplitudes above 10 mV were included in the analysis. Rheobase was defined as the minimal depolarizing current injected to generate at least one AP. The first spike evoked by a current step was used for the measurement of AP properties. The average AP amplitude was defined as the mean of the voltage increase from the AP threshold to the AP peak of the first spike amplitude for all depolarizing current injections. Average of the AP duration was defined as the full width at the half-maximal amplitude for the first spike of all depolarizing current injections. Spike frequency was calculated by quantifying the number of spikes elicited by 1-sec duration of depolarizing current injection. Interspike interval (ISI) was defined as the time between the peak of the first and the second AP. To characterize the pyramidal cell response in a time-window equivalent to the inhalation phase of the respiration cycle, we also quantified the number of spikes and the ISI at the first 200 msec from recordings with a 1-sec duration of depolarizing current injection.

All chemical substances used were obtained from Sigma–Aldrich. For statistical analysis, all data sets were tested for normality using the Kolmogorov–Smirnov test (α = 0.05) in Graph Prism 6. The electrophysiological statistical analysis was performed using a two-tailed unpaired Student's *t*-test after the normality test. Significance was considered when $P < 0.05$. All values in text, figures, and table are given as mean ± SEM.

Computational model

We developed an integrated model of OB and aPC based on the models by de Almeida et al. (2013, 2016) to investigate (a) how the aPC P5–P8 and P14–P17 circuit learn olfactory preference for maternal odor inside the nest and (b) how aPC pyramidal cells in these age groups respond after exposure to the conditioned maternal odor.

The computational model and simulations were developed using NetLogo 6.0.4 Software (Wilensky, U. 1999. NetLogo. http://ccl.northwestern.edu/netlogo/. June 4, 2018). In the framework of NetLogo, each neuron was represented as an individual agent that processes information.

Model architecture and connectivity

The OB network incorporates only the mitral cells (Mt) described in the work of de Almeida et al. (2013, 2016). We considered 100 Mt cells, and these were modeled with their firing dependent on the respiratory rhythm (2 Hz).

The aPC network is comprised only by pyramidal cells (Pyr) (Stokes and Isaacson 2010; Bekkers and Suzuki 2013) and consists of 200 neurons. We added experimental data (results reported in this paper) to the model. Passive (membrane resting potential, input resistance, membrane time constant, membrane capacitance) and active (AP threshold, AP amplitude, AP duration, AP firing frequency) intrinsic properties of aPC pyramidal cells were included from patch-clamp experimental data.

For the connectivity between OB and aPC, we considered that each Pyr cell is randomly connected with ∼15 to 45 Mt cells (Franks and Isaacson 2006). For the associative Pyr–Pyr connectivity, we considered that each Pyr cell is connected randomly with 10% of Pyr cells (Franks et al. 2011). All parameters are presented in Table 2.

Models for the neurons and connections

The Mt and Pyr cells are modeled as leaky integrate-and-fire neurons, in which the change in the membrane voltage is described by the equation (1):

$$\frac{dV(t)}{dt} = \frac{1}{C}(I_e(t) - g_L(V(t) - E_L)), \quad (1)$$

where V (*t*) is the membrane potential, C is the capacitance, g_L is the membrane leaky conductance, E_L is the resting potential, and I_e is the time-dependent external current input. To maintain the adjusted form of the experimental data for ISI and conserve the distribution for aPC pyramidal cells for each age period, I_e was multiplied by an adaptation factor α.

The external input ($I^{ij}{}_e$) to neuron *i* from a given presynaptic neuron *j* at time *t* is a function of the synaptic strength (W_{ij}), the channel conductance g_{ij} (t) at time *t,* and the difference between the equilibrium potential (Nernst) ($E_{N,ij}$) of the specific channel

Table 2. Modeling parameters for P5–P8 and P14–P17

Neurons	P5–P8	P14–P17
Mitral Cells (Mt) ($n = 100$)	$\tau = 20$ msec $\Theta_{min} = -0.0014$; $\Theta_{max} = 0.009$[a] $\Theta_{min} = -0.0014$; $\Theta_{max} = 0.002$[b] $V_{hyper} = -0.01$; $t^{refrac} = 2$ msec	
Pyramidal cells (Pyr) ($n = 200$)	$\Theta_{min} = -0.03922$; $\Theta_{max} = -0.03663$ $V^{hyper} = \Theta_{min}$; $t^{refrac} = 2$ msec $\tau = 42.78$[c] $C_m = 98.21$[c] $R_{inp} = \tau/C_m$[c] $AP_{ampl} = 0.07690$[c] $E_{pahp} = -0.060$ $\tau_{pahp} = 1$ $A_{pahp} = 30$ $Rm_{adapt} = 0.12$ $W_{Mt\ to\ Pyr} = 35$ $g^{max}{}_{Pyr\ to\ Pyr} = 10$ $W_{Pyr\ to\ Pyr} = 35$ $g^{max}{}_{Mt\ to\ Pyr} = 10$ $E_{glu} = 0$ $\tau^{pp} = 12$ msec $\tau^{pnp} = \tau^{npp} = 500$ msec $W_{LTP} = 62.2$ $W_{LTD} = 12.25$	$\Theta_{min} = -0.05435$; $\Theta_{max} = -0.04596$ $V^{hyper} = \Theta_{min}$; $t^{refrac} = 2$ msec $\tau = 30.33$[c] $C_m = 178.1$[c] $R_{inp} = \tau/C_m$[c] $AP_{ampl} = 0.07690$[c] $E_{pahp} = -0.060$ $\tau_{pahp} = 20$ $A_{pahp} = 30$ $Rm_{adapt} = 0.45$ $W_{Mt\ to\ Pyr} = 35$ $g^{max}{}_{Pyr\ to\ Pyr} = 10$ $W_{Pyr\ to\ Pyr} = 35$ $g^{max}{}_{Mt\ to\ Pyr} = 10$ $E_{glu} = 0$ $\tau^{pp} = 12$ msec $\tau^{pnp} = \tau^{npp} = 500$ msec $W_{LTP} = 62.2$ $W_{LTD} = 12.25$

[a]Values without NE modulation.
[b]Values with NE modulation.
[c]Values from electrophysiological data.

type and the membrane potential V_i (t) of the postsynaptic neuron at time *t* and is described by the equation (2):

$$I_e^{ij}(t) = W_{ij} g_{ij}(t)[E_{N,ij} - V_i(t)]. \quad (2)$$

The firing probability of the model neuron at voltage V is described by the equation (3):

$$F_i(V) = \begin{cases} 0 & \text{if } V < \theta^{min} \\ \left(\frac{V - \theta^{min}}{\theta^{max} - \theta^{min}}\right)^{\beta} & \text{if } V \in [\theta^{min}, \theta^{max}], \\ 1 & \text{if } V > \theta^{max} \end{cases} \quad (3)$$

where Θ^{max} represents the saturation value of threshold, Θ^{min} is the minimal value of threshold, and β is a constant defining the nonlinearity of F_i (V). At each spike of the presynaptic neuron *j* the corresponding conductance in the postsynaptic neuron *i* is set to:

$$g_{ij}(t) = g_{ij}^{max}\left(\exp\left(-\frac{t - t_j^{fire}}{\tau_{1,ij}}\right) - \exp\left(-\frac{t - t_j^{fire}}{\tau_{2,ij}}\right)\right), \quad (4)$$

where t_j^{fire} is the last spike time of neuron *j*, g_{ij}^{max} represents the maximum conductance of the corresponding channel, while $\tau_{1,ij}$ and $\tau_{2,ij}$ are its rise and fall. Following an action potential, the voltage of each neuron is reset to the hyperpolarization potential V^{hyper}, where it remains clamped for the refractory period $t^{refract}$.

We also implemented adaptation for the Pyr cells defined as a change in the voltage V_i^{ahc} (*t*) due to a hyperpolarizing current that increases the firing threshold for the recently activated Pyr neurons *i* and it is described by the equation (5):

$$\tau^{ahc}\frac{dV_i^{ahc}}{dt} + V_i^{ahc} = A^{ahc}X_i, \quad (5)$$

where X_i is equal to 1 in the time-step after neuron *i* spikes and 0 otherwise. Therefore, V^{ahc} increases with the constant A^{ahc} and decays with the characteristic time τ^{ahc} (de Almeida et al. 2013, 2016).

In the model, the excitatory output from Mt cells is modulated by the sinusoidal wave of 2 Hz, which mimics the respiratory rhythm (Uchida and Mainen 2003; Kepecs et al. 2007; Verhagen et al. 2007; Wesson et al. 2008; Poo and Isaacson 2009). The duration of each respiratory cycle was based on in vivo experimental works in rodents (Poo and Isaacson 2009; Haddad et al. 2013; Stern et al. 2018) and the beginning of the odor stimulation was programmed to coincide with the beginning of the exhalation phase.

Experimental works have shown that odor-stroke pairing enhances the OB activity in <P10 infant rodents (Sullivan and Wilson 1991a,b, 1995) and that at the same time the level of NE increases (Rangel and Leon 1995). NE release is necessary for the acquisition of olfactory preference in infant rodents, the behavioral orientation-approximation response to the conditioned odor (Sullivan et al. 1991, 2000; Sullivan and Wilson 1991a). The blockage of β-adrenoceptors in the OB (Sullivan et al. 1992) or a lesion of LC, blocking NE release, prevents this learning (Sullivan et al. 1994) and rat pups do not show olfactory preference for the conditioned odor. The presence of NE during odor presentation maintains Mt cells responsiveness to that odor, preventing the habituation they normally exhibit to repeated odor presentations (Wilson and Sullivan 1992). Therefore, we model the circuit so that during the conditioning experiments NE modulates only OB mitral cells.

Model for synaptic plasticity

For synaptic modifications of Mt to Pyr and Pyr to Pyr connections, activity-dependent synaptic plasticity was implemented (Hebbian learning) similar to that used by Jensen et al. (1996). The synaptic strength W_{ij} is increased if both pre- and postsynaptic neurons fire together; otherwise, it is reduced. This change is described by equation (6):

$$\frac{dW_{ij}}{dt} = (W_{LTP} - W_{ij})\frac{i^{post}(t - t_i^{fire})b^{glu}(t - t_j^{fire} - t^{delay})}{\tau^{pp}} + (W_{LTD} - W_{ij})\left(\frac{i^{post}(t - t_i^{fire})}{\tau^{npp}} + \frac{b^{glu}(t - t_j^{fire} - t^{delay})}{\tau^{pnp}}\right) \quad (6)$$

where t^{delay} is the time required for the action potential to travel from the soma to the recurrent collateral connections, i^{post} is the postsynaptic depolarization attributed to the retropropagated action potential of postsynaptic neurons described by equation (7):

$$i^{post}(t) = \frac{t}{\tau^{post}}\exp\left(1 - \frac{t}{\tau^{post}}\right), \quad (7)$$

where the time course of the depolarization at the postsynaptic neuron (τ^{post}) is 2 msec. b^{glu} is the time course of the kinetics of the binding of glutamate on NMDA receptors (de Almeida et al 2013, 2016) described by equation (8).

$$b^{glu}(t) = \exp\left(\frac{-t}{\tau^{NMDAf}}\right)\left(1 - \exp\left(\frac{-t}{\tau^{NMDAr}}\right)\right), \quad (8)$$

where τ^{NMDAf} (7 msec) and τ^{NMDAr} (1 msec) characterize the NMDA receptor kinetics.

During the first postnatal weeks, NMDA receptors are predominant at the LOT-aPC synapses (Mt–Pyr) (Franks and Isaacson 2005), which express a robust NMDA-dependent LTP plasticity but whose strength declines by the first postnatal month. The associative synapses (Pyr to Pyr), on the other hand, are always plastic (Poo and Isaacson 2007). In the simulation, the initial weight value (W) was set to 35, and the maximum weight value (W_{LTP} and the minimum value (W_{LTD} was set to 62.2 and 12.25, respectively. If i^{post} and b^{glu} peak together, then the synaptic weight between the neurons *i* and *j* is driven to W_{LTP} with the characteristic time τ^{pp} (12 msec) otherwise, in the case of unsynchronized firing, it is slowly reduced to W_{LTD} with the time constants $\tau^{pnp} = \tau^{npp} = 500$ msec.

Conditioning

After the model of the OB-aPC circuit was implemented for P5–P8 and P14–P17 age periods, we simulated a classical conditioning protocol. It assumes that by the time the younger pups (<P10) are submitted to the pairing of a novel odor with stroke (a tactile stimulus that mimics maternal licking), they already have learned in the nest the mother's odor. The conditioned maternal odor elicits in the pup an orientation-approximation behavior. At the circuit level, the coincidental activation of the same group of aPC neurons responsive for this behavior toward the mother odor supports the acquisition of a preference for a conditioned novel odor in young pups (<P10) in experimental conditions outside the nest. Conversely, preference learning for a novel artificial odor fails for older pups (>P10) because the stroke-odor pairing recruits less aPC neurons that are sensitive to the maternal odor.

We hypothesized that aPC Pyr cells are less responsive to odor-stroke conditioning after P10 because they become less responsive to the maternal odor with the changes in their intrinsic electric properties. Pyr cells in other sensory cortices of rats become more adult-like around the first postnatal month (Lorenzon and Foehring 1993; Kasper et al. 1994; Maravall et al. 2004; Oswald and Reyes 2008; Valiullina et al. 2016). Moreover, in recent electrophysiological studies, aPC Pyr cells of mice have been found to undergo developmental changes in their intrinsic passive and action potential properties from P8–P11 to P14–P21 (Ghosh et al. 2015). In this paper, we show that from P5–P8 to P14–P17, the resting membrane potential, the input resistance, and the membrane time constant have an important reduction. Moreover, the Pyr cells

APs reduce in threshold and become faster with age but with little change in amplitude.

In our simulation of the classical conditioning protocol, the OB-aPC model initially receives the mother's odor as a neutral stimulus. Before CS–USC pairing, the response of aPC pyramidal cells to the maternal odor was measured in a 3 sec window with 2 sec of interval. In the delayed pairing procedure, the CS onset preceded the UCS onset by 2 sec, CS–USC overlapping for 1 sec, after which the CS was terminated. This pairing was presented seven times with 1-sec intervals. During this procedure, we measured the activity of the pyramidal cells (number of spikes, number of activated cells, and change in the synaptic weight). Two seconds after the last pairing, the CS was presented alone during a 3-sec window.

After the pup has learned the mother`s odor by conditioning (representing pups <P10), exposure to this conditioned odor is expected to elicit orientation-approximation behavior, and at the neural level, it is expected that specific aPC pyramidal cells are highly active. To illustrate this, we exposed the P5–P8 OB-aPC artificial circuit to the CS stimuli for a 10-sec window and measured the activity of the Pyr cells during this period. After a 2 sec interval, we exposed the P5–P8 OB-aPC circuit again during a 3-sec window to the CS and measure the aPC pyramidal cells activity.

In the >P10 pups, exposure to the maternal odor also elicits orientation-approximation behavior (Sullivan et al. 1986; Sullivan and Wilson 1993), but the novel odor repetitively paired with stroke does not induce any of this behavior (Moriceau and Sullivan 2005). We hypothesized that the specific aPC pyramidal cells that were highly active in <P10 pups should have been reduced in >P10 pups. To test this hypothesis, we switched the electrophysiological characteristic of the pyramidal cells from P5–P8 to P14–P17 and exposed the circuit to the CS during a 10 sec time-window and measured the activity of the aPC pyramidal cells. After a 2-sec interval, another 3 sec of CS exposure was measured 2 sec after the first exposure.

Acknowledgments

E.M.O. is supported by Coordenaçao de Aperfeiçoamento de Pessoal de Nível Superior (CAPES, Process number: 1608346). G. V.E.P is supported by a doctoral scholarship from Conselho Nacional de Pesquisa e Desenvolvimento Cientifico e Tecnológico (CNPq, Process number: 141727/2014-4). A.B.L and M.E.C are funded by CNPq (Process number: 465671/2014-4). M.A.I is supported by CNPq (Process number: 423843/2016-8). Other funding that part contributed to the end of this work is provided to G.V.E.P by UCH (Universidad de Ciencias y Humanidades) under research grant "Exploración teórico-experimental neurocomportamental de la formación del apego madre-infante en el desarrollo temprano" (Resolución N° 012-2019-CU-UCH). The authors would like to thank Dr. Aline Villavicencio for her thoughtful and helpful comments on this manuscript.

References

Al Aïn S, Perry RE, Nuñez B, Kayser K, Brehman E, Lacomb M, Wilson DA, Sullivan RM. 2016. Neurobehavioral assessment of maternal odor in developing rat pups: implications for social buffering. *Soc Neurosci* **12:** 32–49. doi:10.1080/17470919.2016.1159605

Bekkers JM, Suzuki N. 2013. Neurons and circuits for odor processing in the piriform cortex. *Trends Neurosci* **36:** 429–438. doi:10.1016/j.tins.2013.04.005

Choy JMC, Suzuki N, Shima Y, Budisantoso T, Nelson SB, Bekkers JM. 2017. Optogenetic mapping of intracortical circuits originating from semilunar cells in the piriform cortex. *Cerebral Cortex* **27:** 589–601. doi:10.1093/cercor/bhv258

Cornwell-Jones C, Sobrian SK. 1977. Development of odor-guided behavior in Wistar and Spraque-Dawley rat pups. *Physiol Behav* **19:** 685–688. doi:10.1016/0031-9384(77)90044-0

de Almeida L, Idiart M, Linster C. 2013. A model of cholinergic modulation in olfactory bulb and piriform cortex. *J Neurophysiol* **109:** 1360–1377. doi:10.1152/jn.00577.2012

de Almeida L, Idiart M, Dean O, Devore S, Smith DM, Linster C. 2016. Internal cholinergic regulation of learning and recall in a model of olfactory processing. *Front Cell Neurosci* **10:** 1–14. doi:10.3389/fncel.2016.00256

Donahoe JW, Burgos JE, Palmer DC. 2006. A selectionist approach to reinforcement. *J Exp Anal Behav* **60:** 17–40. doi:10.1901/jeab.1993.60-17

Duveau A, Godinot F. 1988. Influence of the odorization of the rearing environment on the development of odor-guided behavior in rat pups. *Physiol Behav* **42:** 265–270. doi:10.1016/0031-9384(88)90080-7

Franks KM, Isaacson JS. 2005. Synapse-specific downregulation of NMDA receptors by early experience: a critical period for plasticity of sensory input to olfactory cortex. *Neuron* **47:** 101–114. doi:10.1016/j.neuron.2005.05.024

Franks KM, Isaacson JS. 2006. Strong single-fiber sensory inputs to olfactory cortex: implications for olfactory coding. *Neuron* **49:** 357–363. doi:10.1016/j.neuron.2005.12.026

Franks KM, Russo MJ, Sosulski DL, Mulligan AA, Siegelbaum SA, Axel R. 2011. Recurrent circuitry dynamically shapes the activation of piriform cortex. *Neuron* **72:** 49–56. doi:10.1016/j.neuron.2011.08.020

Ghosh A, Purchase NC, Chen X, Yuan Q. 2015. Norepinephrine modulates pyramidal cell synaptic properties in the anterior piriform cortex of mice: age-dependent effects of β-adrenoceptors. *Front Cell Neurosci* **9:** 450. doi:10.3389/fncel.2015.00450

Ghosh A, Mukherjee B, Chen X, Yuan Q. 2017. β-adrenoceptor activation enhances L-type calcium channel currents in anterior piriform cortex pyramidal cells of neonatal mice: implication for odor learning. *Learn Mem* **24:** 132–135. doi:10.1101/lm.044818.116

Gregory EH, Pfaff DW. 1971. Development of olfactory-guided behavior in infant rats. *Physiol Behav* **6:** 573–576. doi:10.1016/0031-9384(71)90208-3

Haddad R, Lanjuin A, Madisen L, Zeng H, Murthy VN, Uchida N. 2013. Olfactory cortical neurons read out a relative time code in the olfactory bulb. *Nat Neurosci* **16:** 949–957. doi:10.1038/nn.3407

Jensen O, Idiart MAP, Lisman JE. 1996. Physiologically realistic formation of autoassociative memory in networks with θ/γ oscillations: role of fast NMDA channels. *Learn Mem* **3:** 243–256. doi:10.1101/lm.3.2-3.243

Kasper EM, Larkman AU, Lübke J, Blakemore C. 1994. Pyramidal neurons in layer 5 of the rat visual cortex. II. Development of electrophysiological properties. *J Comp Neurol* **339:** 475–494. doi:10.1002/cne.903390403

Kepecs A, Uchida N, Mainen ZF. 2007. Rapid and precise control of sniffing during olfactory discrimination in rats. *J Neurophysiol* **98:** 205–213. doi:10.1152/jn.00071.2007

Kimura F, Nakamura S. 1985. Locus coeruleus neurons in the neonatal rat: electrical activity and responses to sensory stimulation. *Dev Brain Res* **23:** 301–305. https://doi.org/10.1016/0165-3806(85)90055-0

Lorenzon NM, Foehring RC. 1993. The ontogeny of repetitive firing and its modulation by norepinephrine in rat neocortical neurons. *Dev Brain Res* **73:** 213–223. https://doi.org/10.1016/0165-3806(93)90141-V

Maravall M, Stern EA, Svoboda K. 2004. Development of intrinsic properties and excitability of layer 2/3 pyramidal neurons during a critical period for sensory maps in rat barrel cortex. *J Neurophysiol* **92:** 144–156. https://doi.org/10.1152/jn.00598.2003

McCormick DA, Prince DA. 1987. Post-natal development of electrophysiological properties of rat cerebral cortical pyramidal neurones. *J Physiol* **393:** 743–762. https://doi.org/10.1113/jphysiol.1987.sp016851

Moriceau S, Sullivan RM. 2004. Unique neural circuitry for neonatal olfactory learning. *J Neurosci* **24:** 1182–1189. doi:10.1523/JNEUROSCI.4578-03.2004

Moriceau S, Sullivan RM. 2005. Neurobiology of infant attachment. *Dev Psychobiol* **47:** 230–242. doi:10.1002/dev.20093

Morrison GL, Fontaine CJ, Harley CW, Yuan Q. 2013. A role for the anterior piriform cortex in early odor preference learning: evidence for multiple olfactory learning structures in the rat pup. *J Neurophysiol* **110:** 141–152. https://doi.org/10.1152/jn.00072.2013

Oswald A-MM, Reyes AD. 2008. Maturation of intrinsic and synaptic properties of layer 2/3 pyramidal neurons in mouse auditory cortex. *J Neurophysiol* **99:** 2998–3008. doi:10.1152/jn.01160.2007

Pardo GVE, Lucion AB, Calcagnotto ME. 2018. Postnatal development of inhibitory synaptic transmission in the anterior piriform cortex. *Int J Dev Neurosci* **71:** 1–9. doi:10.1016/j.ijdevneu.2018.07.008

Perry RE, Al Aïn S, Raineki XC, Sullivan RM, Wilson DA. 2016. Development of odor hedonics : experience-dependent ontogeny of circuits supporting maternal and predator odor responses in rats. *J Neurosci* **36:** 6634–6650. doi:10.1523/JNEUROSCI.0632-16.2016

Polan HJ, Hofer MA. 1998. Olfactory preference for mother over home nest shavings by newborn rats. *Dev Psychobiol* **33:** 5–20. doi:10.1002/(SICI)1098-2302(199807)33:1<5::AID-DEV2>3.0.CO;2-P

Polan HJ, Milano D, Eljuga L, Hofer MA. 2002. Development of rats' maternally directed orienting behaviors from birth to day 2. *Dev Psychobiol* **40:** 81–103. doi:10.1002/dev.10015

Poo C, Isaacson JS. 2007. An early critical period for long-term plasticity and structural modification of sensory synapses in olfactory cortex. *J Neurosci* **27:** 7553–7558. doi:10.1523/JNEUROSCI.1786-07.2007

Poo C, Isaacson JS. 2009. Odor representations in olfactory cortex: "sparse" coding, global inhibition, and oscillations. *Neuron* **62:** 850–861. doi:10.1016/j.neuron.2009.05.022

Rangel S, Leon M. 1995. Early odor preference training increases olfactory bulb norepinephrine. *Dev Brain Res* **85:** 187–191. doi:10.1016/0165-3806(94)00211-H

Roth TL, Raineki C, Salstein L, Perry R, Sullivan-Wilson TA, Sloan A, Lalji B, Hammock E, Wilson DA, Levitt P, et al. 2013. Neurobiology of secure infant attachment and attachment despite adversity: a mouse model. *Genes Brain Behav* **12:** 673–680. doi:10.1111/gbb.12067

Stern M, Bolding KA, Abbott L, Franks KM. 2018. A transformation from temporal to ensemble coding in a model of piriform cortex. *Elife* **7:** e34831. doi:10.7554/elife.34831

Stokes CCA, Isaacson JS. 2010. From dendrite to soma: dynamic routing of inhibition by complementary interneuron microcircuits in olfactory cortex. *Neuron* **67:** 452–465. doi:10.1016/j.neuron.2010.06.029

Sullivan RM. 2001. Unique characteristics of neonatal classical conditioning: the role of the amygdala and locus coeruleus. *Integr Physiol Behav Sci* **36:** 293–307. doi:10.1007/bf02688797

Sullivan RM, Wilson DA. 1991a. Neural correlates of conditioned odor avoidance in infant rats. *Behav Neurosci* **105:** 307–312. doi:10.1037/0735-7044.105.2.307

Sullivan RM, Wilson DA. 1991b. The role of norepinephrine in the expression of learned olfactory neurobehavioral responses in infant rats. *Psychobiology* **19:** 308–312. doi:10.3758/bf03332084

Sullivan RM, Wilson DA. 1993. Role of the amygdala complex in early olfactory associative learning. *Behav Neurosci* **107:** 254–263. doi:10.1037/0735-7044.107.2.254

Sullivan RM, Wilson DA. 1995. Dissociation of behavioral and neural correlates of early associative learning. *Dev Psychobiol* **28:** 213–219. doi:10.1002/dev.420280403

Sullivan RM, Hofer MA, Brake SC. 1986. Olfactory-guided orientation in neonatal rats is enhanced by a conditioned change in behavioral state. *Dev Psychobiol* **19:** 615–623. doi:10.1002/dev.420190612

Sullivan RM, McGaugh JL, Leon M. 1991. Norepinephrine-induced plasticity and one-trial olfactory learning in neonatal rats. *Dev Brain Res* **60:** 219–228. doi:10.1016/0165-3806(91)90050-S

Sullivan RM, Zyzak DR, Skierkowski P, Wilson DA. 1992. The role of olfactory bulb norepinephrine in early olfactory learning. *Dev Brain Res* **70:** 279–282. doi:10.1016/0165-3806(92)90207-D

Sullivan RM, Wilson DA, Lemon C, Gerhardt GA. 1994. Bilateral 6-OHDA lesions of the locus coeruleus impair associative olfactory learning in newborn rats. *Brain Res* **643:** 306–309. doi:10.1016/0006-8993(94)90038-8

Sullivan RM, Stackenwalt G, Nasr F, Lemon C, Wilson DA. 2000. Association of an odor with activation of olfactory bulb noradrenergic β-receptors or locus coeruleus stimulation is sufficient to produce learned approach responses to that odor in neonatal rats. *Behav Neurosci* **114:** 957–962. doi:10.1037/0735-7044.114.5.957

Szerzenie V, Hsiao S. 1977. Development of locomotion toward home nesting material in neonatal rats. *Dev Psychobiol* **10:** 315–321. doi:10.1002/dev.420100405

Terry LM, Johanson IB. 1996. Effects of altered olfactory experiences on the development of infant rats' responses to odors. *Dev Psychobiol* **29:** 353–377. doi:10.1002/(SICI)1098-2302(199605)29:4<353::AID-DEV4>3.0.CO;2-P

Uchida N, Mainen ZF. 2003. Speed and accuracy of olfactory discrimination in the rat. *Nat Neurosci* **6:** 1224–1229. doi:10.1038/nn1142

Valiullina F, Akhmetshina D, Nasretdinov A, Mukhtarov M, Valeeva G, Khazipov R, Rozov A. 2016. Developmental changes in electrophysiological properties and a transition from electrical to chemical coupling between excitatory layer 4 neurons in the rat barrel cortex. *Front Neural Circuits* **10:** 1. doi:10.3389/fncir.2016.00001

Verhagen JV, Wesson DW, Netoff TI, White JA, Wachowiak M. 2007. Sniffing controls an adaptive filter of sensory input to the olfactory bulb. *Nat Neurosci* **10:** 631–639. doi:10.1038/nn1892

Wesson DW, Donahou TN, Johnson MO, Wachowiak M. 2008. Sniffing behavior of mice during performance in odor-guided tasks. *Chem Senses* **33:** 581–596. doi:10.1093/chemse/bjn029

Wilson DA, Sullivan RM. 1992. Blockade of mitral/tufted cell habituation to odors by association with reward: a preliminary note. *Brain Res* **594:** 143–145. doi:10.1016/0006-8993(92)91039-H

Received August 22, 2019; accepted in revised form November 12, 2019.

Capítulo 4

4.1 Artigo 2

O artigo intitulado **"*The maturational characteristics of the GABA input in the anterior piriform cortex may also contribute to the rapid learning of the maternal odor during the sensitive period*"** também apresenta uma atualização do modelo computacional proposto no artigo 1 com a integração das caraterísticas maturacionais das entradas GABAérgicas no córtex piriforme anterior, interneurônios de conexões de retroalimentação e Interneurônios de conexões pró-ação, e dados obtidos experimentalmente. No modelo, o trabalho explora o papel do GABA no aprendizado do odor maternal no período sensível e discute uma possível ação despolarizante do GABA no córtex piriforme anterior durante essa faixa do desenvolvimento, o qual contraria o papel GABA no aprendizado de preferência olfatória em ratos neonatos como descrito na literatura. Esse trabalho foi produzido de maneira colaborativa com a Grace Pardo, quem realizou o trabalho experimental no laboratório da professora Maria Elisa Calcagnotto e do professor Aldo Bolten Lucion como parte de sua tese de doutorado. O trabalho foi submetido no dia 21 de junho de 2020 à revista Learning and Memory e foi aceito para publicação no dia 27 de setembro de 2020. O artigo também foi capa da edição Vol 27 N° 12, 2020. O artigo pode ser citado como:

Oruro, E.M., Pardo, G.V.E., Lucion, A.B., Calcagnotto, M.E., Idiart, M.A.P., 2020. The maturational characteristics of the GABA input in the anterior piriform cortex may also contribute to the rapid learning of the maternal odor during the sensitive period. Learn. Mem. 2020, 27:493-502 https://doi.org/10.1101/lm.052217.120

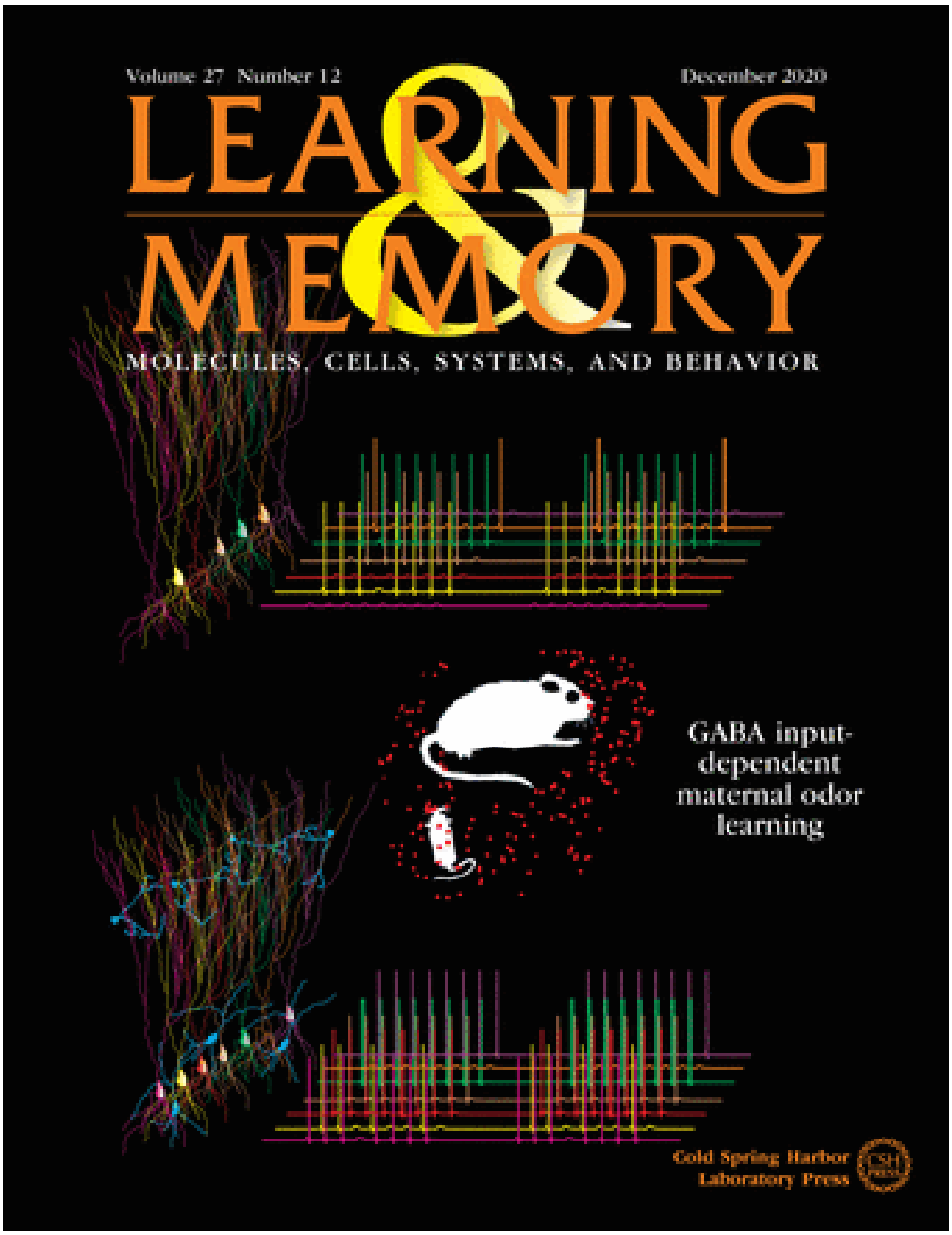

Figura na capa da revista Learning & Memory volume 27, número 12 de dezembro de 2020, preparada pelos autores.
Legenda da figura tirada de http://learnmem.cshlp.org/content/27/12.cover-expansion

Using a combined electrophysiological and computational approach, Oruro et al. (*LearnMem* **27:** 493–502) show that the GABAergic input enhances the olfactory bulb-anterior piriform cortex (OB-aPC) circuit's ability for maternal odor learning and amplifies its recall. Such an effect is due to the maturational characteristics of the GABAergic inputs that depolarize aPC pyramidal neurons during the sensitive period for attachment learning. The image shows that aPC circuits without (*top* figure) or with (*bottom* figure) GABAergic interneurons can learn maternal odor after conditioning. However, GABA-conditioned circuits are more likely to recruit more aPC pyramidal cells and engage them in more triggering activity in response to the conditioned maternal odor, thereby amplifying the entire circuit's response to maternal odor.

Research

The maturational characteristics of the GABA input in the anterior piriform cortex may also contribute to the rapid learning of the maternal odor during the sensitive period

Enver Miguel Oruro,[1,2,3,7] Grace V.E. Pardo,[3,4,5,6,7] Aldo Bolten Lucion,[2,4] Maria Elisa Calcagnotto,[2,3] and Marco A.P. Idiart[1,2]

[1]*Neurocomputational and Language Processing Laboratory, Institute of Physics, Universidade Federal do Rio Grande do Sul, Porto Alegre, Rio Grande do Sul 91501-970, Brazil;* [2]*Neuroscience Graduate Program, Universidade Federal do Rio Grande do Sul, Porto Alegre, Rio Grande do Sul 90050-170, Brazil;* [3]*Neurophysiology and Neurochemistry of Neuronal Excitability and Synaptic Plasticity Laboratory, Department of Biochemistry, Instituto de Ciências Básicas da Saúde (ICBS), Universidade Federal do Rio Grande do Sul, Porto Alegre, Rio Grande do Sul 90035-003, Brazil;* [4]*Department of Physiology, ICBS, Universidade Federal do Rio Grande do Sul, Porto Alegre, Rio Grande do Sul 90050-170, Brazil;* [5]*Centre for Interdisciplinary Science and Society Studies, Universidad de Ciencias y Humanidades, Los Olivos, Lima 15314, Peru;* [6]*Center for Biomedical Research, Universidad Andina del Cusco, San Jerónimo, Cuzco 08006, Peru*

During the first ten postnatal days (P), infant rodents can learn olfactory preferences for novel odors if they are paired with thermo-tactile stimuli that mimic components of maternal care. After P10, the thermo-tactile pairing becomes ineffective for conditioning. The current explanation for this change in associative learning is the alteration in the norepinephrine (NE) inputs from the locus coeruleus (LC) to the olfactory bulb (OB) and the anterior piriform cortex (aPC). By combining patch-clamp electrophysiology and computational simulations, we showed in a recent work that a transitory high responsiveness of the OB-aPC circuit to the maternal odor is an alternative mechanism that could also explain early olfactory preference learning and its cessation after P10. That result relied solely on the maturational properties of the aPC pyramidal cells. However, the GABAergic system undergoes important changes during the same period. To address the importance of the maturation of the GABAergic system for early olfactory learning, we incorporated data from the GABA inputs, obtained from in vitro patch-clamp experiment in the aPC of rat pups aged P5–P7 reported here, to the model proposed in our previous publication. In the younger than P10 OB-aPC circuit with GABA synaptic input, the number of responsive aPC pyramidal cells to the conditioned maternal odor was amplified in 30% compared to the circuit without GABAergic input. When compared with the circuit with other younger than P10 OB-aPC circuit with adult GABAergic input profile, this amplification was 88%. Together, our results suggest that during the olfactory preference learning in younger than P10, the GABAergic synaptic input presumably acts by depolarizing the aPC pyramidal neurons in such a way that it leads to the amplification of the pyramidal neurons response to the conditioned maternal odor. Furthermore, our results suggest that during this developmental period, the aPC pyramidal cells themselves seem to resolve the apparent lack of GABAergic synaptic inhibition by a strong firing adaptation in response to increased depolarizing inputs.

[Supplemental material is available for this article.]

Infants of altricial animals learn very rapidly to attach to their mothers. While essential for the immediate survival, these early experiences may also have long lasting consequences in adulthood. Understanding the mechanisms involved in the developing neural circuits underlying this first affiliative behavior is a critical step toward understanding the impact of the mother's care on the behavioral outcomes of the adult offspring, including mental health issues in the case of humans (Perry et al. 2017; Sullivan and Opendak 2018).

Newborn rodents are blind, deaf and possess limited motor skills. They are confined to the nest for the first 2 wk of postnatal life. Recognizing the mother's odor during this period is crucial for odor-guided behaviors such approaching the mother and attaching to a nipple (Farrell and Alberts 2002; Moriceau and Sullivan 2004; Kojima and Alberts 2009; Raineki et al. 2010; Meyer and Alberts 2016; Al Aïn et al. 2017). It is presumed that the pups learn the mother's odor by associating it with maternal care during the first 10 postnatal days (Moriceau and Sullivan 2005). This hypothesis has been extensively tested in an experimental paradigm where young rodents were subjected to pairings of an artificial odor (the unconditioned stimulus) with tactile stimulation, such as brush strokes, to mimic the presence of the mother

[7]**These authors contributed equally to this work.**
Corresponding author: envermiguel@gmail.com
Article is online at http://www.learnmem.org/cgi/doi/10.1101/lm.052217.120.

(the conditioned stimulus). Results shows that animals younger than P10 display orientation approximation behavior toward the artificial odor (Moriceau and Sullivan 2005; Morrison et al. 2013; Roth et al. 2013; Ghosh et al. 2015). However, pairing becomes ineffective for older than P10 age (Moriceau and Sullivan 2005; Morrison et al. 2013; Roth et al. 2013; Ghosh et al. 2015), but learning can be reinstated by direct application of NE in the OB or LC stimulation, which may suggest that the learning changes could be due to local LC changes (Sullivan et al. 2000).

It has been proposed that the olfactory circuit primarily including the OB and the aPC, both modulated by NE inputs from LC, is sufficient to support this learning (Sullivan et al. 1991, 1992, 1994; Morrison et al. 2013; Ghosh et al. 2017). In fact, in vivo studies show that the LC of neonate rats have large responses to somatosensory stimuli (Kimura and Nakamura 1985) and high levels of NE are released in the OB during odor-stroke conditioning in pups younger than P10, but this is no longer observed in pups older than P10 (Rangel and Leon 1995). Although, for pups older than P10, the pairing of an odor with electrical stimulation of NE fibers projecting to the OB results in preference for that odor (Wilson and Sullivan 1992). Moreover, in the aPC, NE release seems to be necessary and sufficient for the early odor preference learning. The pairing of an artificial odor with pharmacological activation of β-adrenoceptors, in the absence of any tactile stimulation or direct LC activation, induce behavioral olfactory preference in pups younger than P10. On the other hand, the blockage of the β-adrenoceptors before the odor-stroke pairing prevents the acquisition of odor preference (Morrison et al. 2013; Ghosh et al. 2015, 2017). In addition to the NE release, an elevated plasticity at the OB-aPC sensory synapses is present for ages younger than P10 (Franks and Isaacson 2005; Poo and Isaacson 2007) what has been considered critical to early olfactory learning (Yuan et al. 2014). The blockage of excitatory synaptic plasticity in the aPC before odor-stroke pairing, by blocking NMDA receptors, prevent the preference learning in pups younger than P10 (Morrison et al. 2013; Mukherjee and Yuan 2016; Ghosh et al. 2017).

In recent work, we proposed an alternative explanation based on a computational model of the OB-aPC circuit (Fig. 1) where we added aPC pyramidal cells age-dependent intrinsic properties obtained in our laboratory by in vitro patch-clamp electrophysiology of aPC slices from P5–P8 and P14–P17 infant rats (Oruro et al. 2020). We used the model to simulate a classical conditioning paradigm by pairing an odor (a random input to the network representing the maternal odor) with NE release (changes in neuronal properties, representing the maternal care) and then after the pairing protocol we measured the activity of the aPC pyramidal cells in response to the maternal odor exposition. We found that the OB-aPC circuit shows a higher aPC pyramidal activation to the maternal odor at ages P5–P8 than at ages P14–P17, and this can be explained by the changes in the intrinsic properties of the pyramidal cells due to maturation, indicated by our electrophysiological data. We also propose that, similarly, the experiments using artificial odors could be explained by an overlap between the novel odor neural representation at aPC (after pairing it with strokes) and the mother's odor neural representation at aPC, and this effect is prominent at P5–P8 and occur to a lesser extent at P14–P17 (Oruro et al. 2020).

In this work, we add yet another ingredient to our model. In addition to the age-dependent changes of aPC pyramidal cells, another intrinsic developmental mechanism could contribute to facilitate the higher responsiveness of pyramidal cells for the maternal odor at P5–P8. Previous study has shown that activation of $GABA_A$ receptor by local infusion of agonist prevents the olfactory conditioning learning in rat pups younger than P10 (Morrison et al. 2013). Recent experimental work had shown that the GABAergic inputs to the aPC pyramidal cells at the P5–P8 age are reduced compared to older ages (Pardo et al. 2018). In addition, we found in the present study that the $GABA_A$ receptor equilibrium potential (E_{GABA}) is more depolarized than the resting membrane potential and the threshold of the aPC pyramidal cells recorded in pups from the same age period. To address the impact of this developmental change to the maternal odor learning, we include a variable GABAergic synaptic input to our previous P5–P8 OB-aPC circuit model and simulate the maternal odor learning by pairing odor input with norepinephrine (NE) release. Simulations revealed that OB-aPC circuits modeled with GABAergic synaptic inputs present an even more significant number of active cells in response to the maternal odor, suggesting that during this period of development, the GABAergic synapses also contribute to support higher responsiveness to the maternal odor.

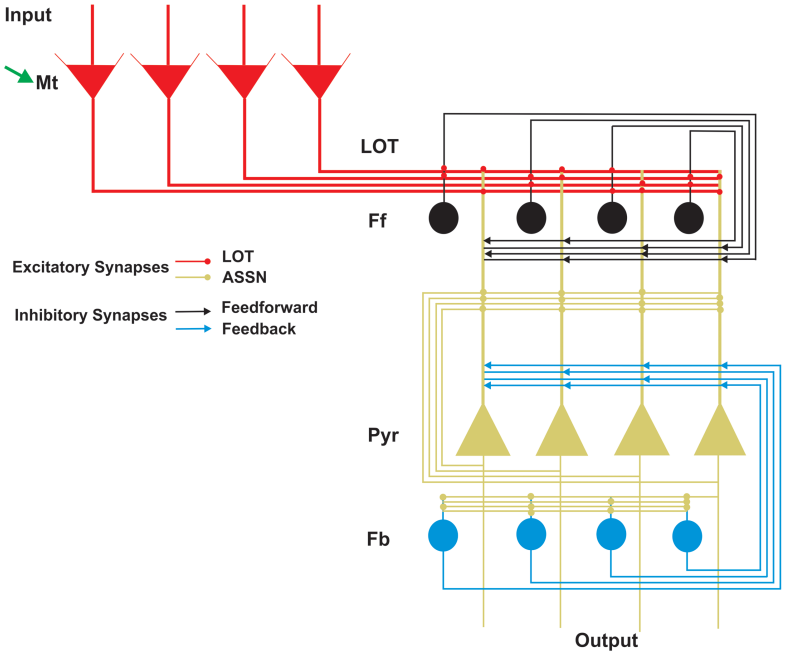

Figure 1. A simplified architecture of the artificial circuit of the olfactory system. The figure is a simplified structure of the olfactory bulb (OB), containing only the mitral cells (Mt; red), and the anterior piriform cortex (aPC) with principal kinds of cells: pyramidal cells (Pyr; yellow), feed-forward (Ff; black), and feedback (Fb; blue) interneurons. The axons of the Mt cells extend to the aPC forming the lateral olfactory tract (LOT; red). The LOT terminals make excitatory synapses (red dots) with the apical dendrites of the Pyr cells and with the Ff interneurons. In turn, the Ff interneurons make inhibitory synapses on the dendrites of Pyr cells (black arrows). The Pyr cells form an important associative input making excitatory synapses with another adjacent Pyr cells and with Fb interneurons (ASSN; yellow dots). In turn, Fb interneurons make inhibitory synapses with basal dendrites and soma of Pyr cells (blue arrows). Mt cells are modulated by NE (green arrow).

Results

Computational experiment I: GABAergic synaptic input enhances the learning of the maternal odor

The maturational characteristics of the GABAergic synaptic input in the aPC during the P5–P8 age period (the sensitive period for attachment learning) contributes to the maternal odor learning. Specifically, simulation results of classical conditioning of two P5–P8 OB-aPC circuits (Fig. 2A) revealed that circuits modeled with GABAergic input profile (see Table 1) increased their activity in response to the conditioned maternal odor. Figure 3 shows the activity profiles of the aPC before, during, and after conditioning in two situations with the introduction of GABA synapses and without the introduction of GABAergic synapses. Before conditioning, the P5–P8 OB-aPC circuit "with GABA" exhibited a slightly higher response to odor when compared to the circuit "without GABA." Over the seven sessions of odor-NE pairing, the activity of the circuit "with GABA" was twice higher than the circuit "without GABA" (Fig. 3B,C; red dots). At the last trial session, the number of spikes and the number of active cells reached their maximum increase of 179% and 134%, respectively (taking the maximal number of evoked spikes during the first trial as 100%, from 10 respiratory cycles).

After conditioning, the average maximum number of spikes (86 ± 2.07 vs. 46.50 ± 0.88) (Fig. 3B, inserted graph) and the average maximum number of active cells (83.16 ± 1.88 vs. 44.13 ± 0.13) (Fig. 3C, inserted graph) were higher when GABA was present [number of spikes: $t_{(14)} = 17.53$; number of active cells: $t_{(14)} = 20.75$; both $P < 0.0001$, unpaired t Student test]. These results indicate that both circuits, with and without GABAergic synaptic inputs, learn the maternal odor; however, in the presence of GABA inputs the pyramidal cells exhibit an enhanced response for the conditioned maternal odor. It could be the that the GABAergic contribution is restricted only to the training phase, by allowing a higher recruitment of pyramidal cells during odor pairing with NE, but with little effect afterward. To clarify that, in the next section we measured the effect of GABA during recall.

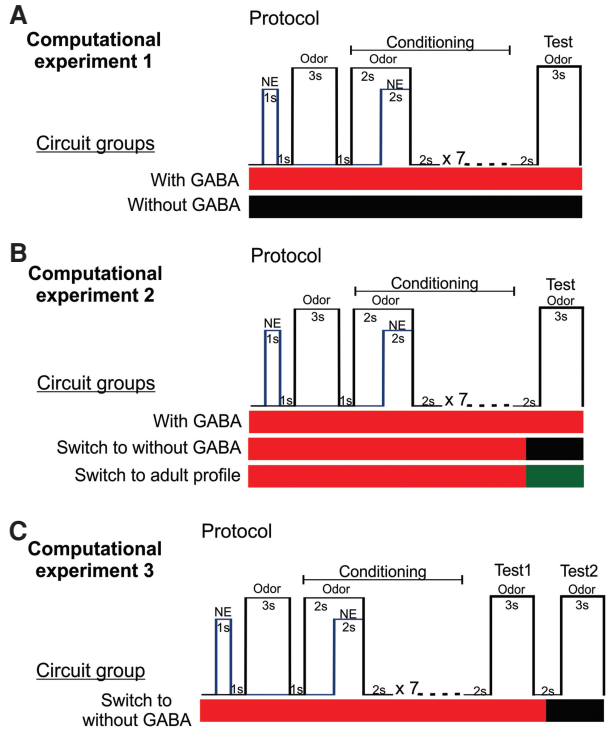

Figure 2. Computational experimental design and conditioning protocols. (*A*) Computational experiment 1. Two OB-aPC circuits groups, modeled with GABA (red horizontal bar) and without GABA (black horizontal bar) were separately conditioned using a delayed pairing procedure of odor and NE. In the protocol, the odor onset preceded the NE onset by 2 sec, odor-NE overlapping for 2 sec, after which the odor was terminated. This pairing was presented seven times with a 2-sec interval. Two seconds after the last pairing, the odor was presented alone during a 3-sec window. (*B*) Computational experiment 2. OB-aPC circuits modeled with GABA were conditioned (red horizontal bar) using the same previous protocol, and 1 sec after the last pairing, the GABAergic synaptic input was blocked (black horizontal bar), or switched to adult GABAergic input profile (green horizontal bar) and the recall (test) was measure in those conditions. (*C*) Computational experiment 3. OB-aPC circuits modeled with GABA (red horizontal bar) using the same odor-NE pairing protocol and 2 sec after the last pairing were tested for the recall 1 of the maternal odor (test 1). One second after the recall 1 was finished, the GABAergic input was blocked (black horizontal bar) and the plasticity of mitral cell and pyramidal cells was excluded. In those conditions, the activity of the circuits was measured during another 3 sec window to the recall 2 of the maternal odor (test 2).

Computational experiment 2: GABAergic synaptic input amplifies the recall of the maternal odor

In order to test the individual effect of GABA in recall, three groups of P5–P8 OB-aPC circuits "with GABA" were trained (Fig. 2B) and after the last pairing, three different recall conditions where explored (Fig. 4A): The GABA input properties remained the same ("with GABA"), were blocked ("without GABA"), or switched to adult GABAergic input profile ("with adult profile"). The aPC pyramidal cells activity in the "without GABA" ($n = 10$ circuits) (Fig. 4B, C; black dots) or "with adult profile" conditions ($n = 10$ circuits) (Fig. 4B,C; green dots) show a significant reduction in the number of spikes (one-way ANOVA, $F_{(2,21)} = 598.1$; $P < 0.0001$, followed by Tukey test; $n = 8$ respiratory cycles in each condition) when compared with the "with GABA" condition ($n = 10$ circuits). The same is true for the number of active cells (one-way ANOVA, $F_{(2,21)} = 597$; $P < 0.0001$, followed by Tukey test; $n = 8$ respiratory cycles in each condition) (Fig. 4B,C; red dots). Moreover, the circuit "with adult profile" has a dramatic reduction in the maximum number of spikes and a number of active cells when compared to the two other conditions (Fig. 4B,C, inserted graphs). These results indicate that the GABAergic input per se contributes to the amplified response during the recall of the maternal odor. Next, we investigated whether the individual variability of the circuits in the experimental groups (intersubject design) (see Fig. 2B), which was modeled by randomizing the connectivity, may have partly contributed to this result.

Computational experiment 3: GABAergic synaptic input amplifies the recall of the maternal odor independently of the variability of the circuit

To control possible effects of the variability of connections between the models, a group of P5–P8 OB-aPC circuits, modeled "with GABA" input ($n = 10$ circuits), was submitted to the conditioning protocol (Fig. 2C) where two recall phases 2 sec apart were tested. We found that all pyramidal cells that fired during the recall 1 phase reduced their spiking frequency significantly in the recall 2 phase (Fig. 5B shows a representative spiking profile from an aleatory aPC pyramidal cell). The mean of the number of spikes (recall 1: 94.69 ± 0.76, $n = 8$ respiratory cycles vs. recall 2: 76.23 ± 0.45, $n = 7$ respiratory cycles; $t_{(6)} = 15.57$; $P < 0.0001$; paired t Student test) (Fig. 5C, inserted graph) and the mean of the number of active cells (recall 1: 83.49 ± 0.52, $n = 8$ respiratory cycles vs. recall 2: 71.67 ± 0.35; $n = 7$ respiratory cycles; $t_{(6)} = 20.35$; $P <$

Table 1. Model parameters

Neurons	Parameters
Mitral (Mt) cells ($n=100$ cells)	$\tau = 20$ ms $\Theta_{min} = -0.0014$ V; $\Theta_{max} = 0.009$ V[a] $\Theta_{min} = -0.0014$ V; $\Theta_{max} = 0.002$ V[b] $V_{hyper} = -0.01$ V; $t^{refrac} = 2$ msec
Pyramidal (Pyr) cells ($n=200$ cells)	$\Theta_{min} = -0.03922$ V; $\Theta_{max} = -0.03663$ V[c] $V^{hype} = \Theta_{min}$; $t^{refrac} = 2$ msec $\tau = 42.78$ msec[c] $C_m = 98.21$ pF[c] $R_{inp} = \tau/C_m$ MΩ[c] $AP_{ampl} = 0.07690$ V[c] $E_{ahc} = -0.060$ V[d] $\tau_{ahc} = 1$[d] $A_{ahc} = 30$[d] $Rm_{adapt} = 0.12$[e] $W_{Mt\ to\ Pyr} = 35$[e] $g^{max}_{Pyr\ to\ Pyr} = 10$[e] $W_{Pyr\ to\ Pyr} = 35$[e] $g^{max}_{Mt\ to\ Pyr} = 10$[e] $E_{glu} = 0$ V $\tau_{2\ Mt\ to\ Pyr} = 1$ msec; $\tau_{2\ Mt\ to\ Pyr} = 2$ msec $\tau^{pp} = 12$ msec $\tau^{pnp} = \tau^{npp} = 500$ msec $W_{LTP} = 62.2$ $W_{LTD} = 12.25$ $E_{GABA} = -0.02458$ V[c] $\tau_{2\ Ff\ to\ Pyr} = 4.8$ msec; $\tau_{2\ Ff\ to\ Pyr} = 5.36$ msec[c] E_{GABA} adult $= -0.070$ V
Feed-forward (Ff) interneurons ($n=100$ cells)	$\tau = 15$ msec $\Theta_{min} = 0$ V; $\Theta_{max} = 0.015$ V $V^{hyper} = -0.01$ V $g^{max}_{Ff\ to\ Pyr} = 13693, 7096$[d] $E_{Glu} = 0$ V $\tau_{2\ Py\ toff} = 1$ msec; $\tau_{2\ Pyr\tau\ to\ ff} = 2$ msec[c]
Feedback interneurons (Fb) ($n=100$ cells)	$\tau = 5$ msec $\Theta_{min} = 0$ V; $\Theta_{max} = 0.013$ V $V^{hyper} = -0.01$ V $g^{max}_{Fb\ to\ Pyr} = 13693, 7096$[d] $E_{Glu} = 0$ V $\tau_{2\ Pyr\ to\ Fb} = 1$ ms; $\tau_{2\ Pyr\tau\ to\ Fb} = 2$ msec

[a]Values without NE modulation.
[b]Values with NE modulation.
[c]Values from electrophysiological data.
[d]Values inferred from electrophysiological data reported in this study.
[e]Values inferred from electrophysiological data reported in the literature.

0.0001; paired *t* Student test) (Fig. 5D, inserted graph) were significantly reduced in the recall 2 phase when compared with recall 1. Moreover, we observed that onset of the pyramidal cell activity was closer to the rising phase of inhalation during recall 1, but was delayed to the middle of the inhalation phase during recall 2. This computational experiment (intrasubject design) (see Fig. 2C) confirms that the GABAergic input per se contributes to the amplification of the response of the P5–P8 OB-aPC circuit for the conditioned maternal odor.

Discussion

Previous studies of early olfactory learning in infant rodents (mostly rats and mice) have pointed the OB and aPC as crucial areas, in which NE release is both necessary and sufficient for infant olfactory learning (for a revision, see Moriceau and Sullivan 2005; Yuan et al. 2014). The main contributions of the present study are (1) to propose a model of the OB-aPC circuit for the maternal odor learning during the sensitive period based on the GABAergic synaptic input profile, in addition to the aPC experimental intrinsic electric properties of pyramidal cells, and (2) to reveal that the GABAergic synaptic input profile during this period also contributes to supporting the maternal odor learning and the recall process.

Does GABAergic input in aPC contributes to the maternal odor learning during the sensitive period?

In this work, we investigate the possible contribution of GABAergic synapses into our model for early olfactory learning. We found that adding GABAergic inputs increased by 47% both the number of active pyramidal cells in aPC and their spiking activity in response to the conditioned odor (Fig. 3). Moreover, we found that GABA is not only relevant during learning but also in the recall phase (Fig. 4). The contribution for immature GABA cells was able to increase in 70% the number of pyramidal cells in aPC that were responsive to the learned odor when compared to the scenario where these cells have the adult profile (Fig. 4). Finally, after eliminating any possible effect of random connections in the OB-aPC circuit on the effect of GABAergic input in the maternal odor recall, we tested the circuit for two recall scenarios (with intact or blocked GABA input) after odor conditioning. We found that blocking GABA input reduced the number of active cells (15%) and spiking activity (20%), suggesting that the GABAergic input in the aPC amplifies the ability of the circuit to support the recall process of the maternal odor (Fig. 5). Therefore, we showed that GABAergic input characteristic of P5–P7 contributes to the maternal odor learning and this contribution resides in the ability to amplify the response of the OB-aPC circuit to the conditioned maternal odor in terms of both numbers of active cells and spikes.

How does the GABAergic input in aPC manage to amplify the activity of pyramidal cells during the sensitive period?

We found that the E_{GABA} of the aPC pyramidal cells from P5–P8 animals was more depolarized (−24.58 mV) (reported in the present study) in comparison with the resting membrane potential and the voltage threshold potential of the same type of cells (−40.27 mV and −35.94 mV, reported in our previous work (see Fig. 6; Oruro et al. 2020). The E_{GABA} of the aPC pyramidal cells from P5–P8 animals was also ∼18 mV more depolarized than the value obtained in older pups (GVE Pardo, AB Lucion, ME Calcagnotto, et al. unpubl.). This result strongly suggests that during the sensitive period of attachment learning, the activation of GABA synapses produces depolarization in the aPC pyramidal cells instead of the characteristic hyperpolarization. It is not uncommon phenomena in developing cortices. Excitatory GABA has been reported for many immature brain areas attributed to the positive switch in the chloride reversal potential due to elevated intracellular chloride concentration (Rivera et al. 1999; Rheims et al. 2008; Ehrlich et al. 2013; Tyzio et al. 2014) and for revision see (Ben-Ari 2014)).

If GABAergic input to aPC pyramidal cells is excitatory during this period, as we are suggesting, why is that the local infusion of GABA receptor agonist (muscimol) into the aPC 10 min before odor-stroke training has shown to prevent the olfactory preference learning in P7 age rat pups?

A possible answer to this question arises from our experimental observation of the active membrane properties of the aPC pyramidal cells during this period of development. In the experiment by

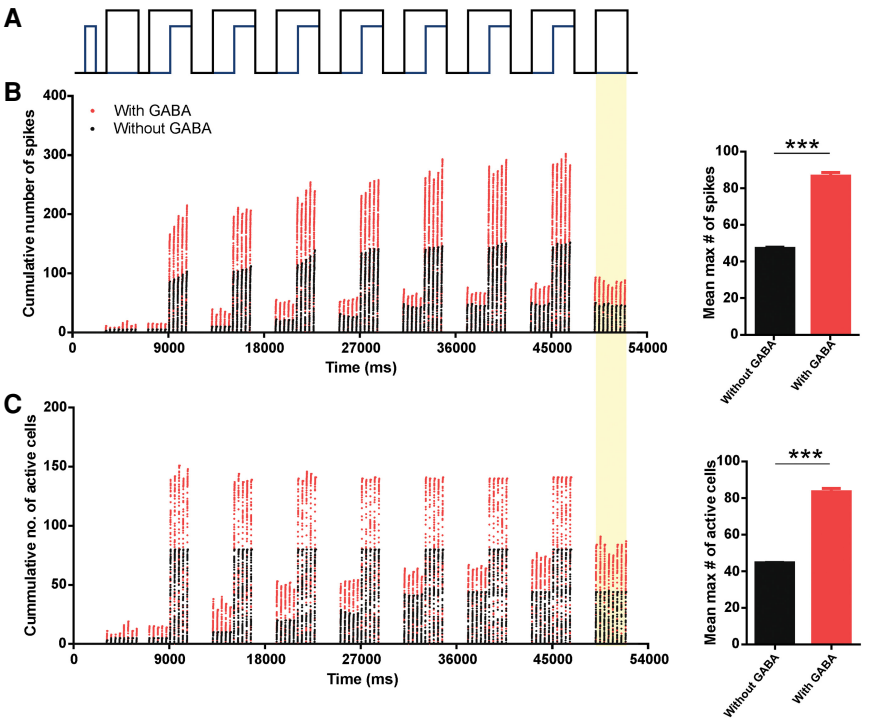

Figure 3. Cumulative number of spikes and number of active aPC pyramidal cells during maternal odor conditioning in the P5–P8 OB-aPC circuit with and without GABA synaptic input. (*A*) Protocol for odor conditioning. A delayed pairing procedure was used in which the odor (black trace) onset preceded the NE (blue trace) by 2 sec and odor and NE overlapped for 2 sec, after which the odor was terminated. The odor-NE pairing was presented seven times with 2 sec intervals. Plot of cumulative number of spikes (*B*) and number of active cells (*C*) during odor-NE pairing and odor test are showed for the P5–P8 OB-aPC circuit with GABA input (red dots) superimposed to the circuit without GABA input (black dots). Data were collected at every 0.5 msec in a 200-msec window of simulation. Simulation (from 0 msec to 54,000 msec) was carried out over several respiratory cycles modulating the activity of the mitral cells, starting with 200 msec of the exhalation phase followed by 200-msec inhalation phase. Activity was measured during inhalation and exhalation phase. After conditioning, the test of the odor (yellow background) evoked a higher cumulative number of spikes and number of active cells for the circuit with GABA input compared to the cells for the circuit without GABA input (inserted graphs). Asterisks represent statistically significant unpaired *t* Student test comparison between the groups during the odor test. (***) $P < 0.001$. Bin: 0.5 msec.

Morrison et al. (2013), the injection of muscimol into the aPC was used to increase the inhibitory synaptic effect of GABA onto the pyramidal cells. The effect of muscimol can be interpreted as a constant excitatory synaptic effect of GABA similar to the effect of the sustained depolarizing current into the pyramidal cells on in vitro current clamp experiment, as we have observed in our previous experiments (Oruro et al. 2020). The aPC pyramidal cells of P5–P8 pups exhibit adaptation properties to increasing depolarizing inputs but this is no longer observed in older pups (Supplemental Fig. S1). In Figure 7, pyramidal cells respond maintaining constant or reducing their firing to increasing inputs, which suggest that aPC pyramidal cells can eventually reduce or interrupt their activity in response to increasing GABAergic input. Thus, the local infusion of muscimol into the aPC may be equivalent to the synaptic activity of all GABAergic neurons at the same time, which in physiological conditions is unlikely to occur. Therefore, if the aPC pyramidal cells show adaptation, the resulting increase in depolarizing inputs could have inhibitory effect in their activity. This effect could be progressively reduced with development, as data from older pups seem to indicate, since E_{GABA} tends to change to more hyperpolarized values (GVE Pardo, AB Lucion, ME Calcagnotto, et al., unpubl.). This also suggests that the firing adaptation properties of the aPC pyramidal cells could be the way to manage the lack of synaptic inhibition in the circuit during early development period.

It is interesting to think that during the P5–P8 age period, the inhibition in the aPC is provided by the action potential properties of pyramidal cells itself and not by the GABA synaptic conductance. However, it remains to be verified if indeed the GABAergic synaptic transmission in the aPC during the sensitive period of attachment learning is excitatory, how the depolarizing GABA could influence the pyramidal cells' excitability and how it could amplify the response to the entrance of odor remains for future work. Interestingly, inhibitory action of GABA has been proposed to be critical for the emergence of aversive conditioned responses induced by odor-shock pairing. In P11 rodents, $GABA_B$ receptor activation prevents the acquisition of olfactory preference learning induced by pairing odor with electric shock, and its pharmacological blocking paired with an odor induce an aversive response to that odor (Okutani et al. 2003). $GABA_A$ receptor activation also has been reported to be critical for the long-term depression in excitatory synapsis in the basolateral amygdala, which correlates with the emergence of conditioned odor aversion in rodent pups older than P10 (Thompson et al. 2008). For an excellent revision in the matter see (Ross and Fletcher 2019).

In conclusion, our computational experiments show that the GABAergic input enhances the OB-aPC circuit's ability for maternal odor learning and amplifies its recall. Such effect is due to the maturational characteristics of the GABAergic inputs that depolarize aPC pyramidal neurons at age younger than P10. Furthermore, in this developing circuit, the apparent lack of synaptic inhibition mediated by GABA appears to be compensated by the adaptive firing properties of aPC immature pyramidal neurons. The depolarizing GABA input may contribute, at least in part, to induce the immature pyramidal neuron to reach its adaptive firing pattern therefore preventing runaway excitation in the circuit. The panorama unfolded here indicates that although an immature circuit may present very different properties regarding its individual cell types, this does not render the circuit useless. On the contrary, immature cells may provide the circuit with important computational properties while the stability of the circuit as a whole remains unchanged.

Materials and Methods

Circuit model and connectivity

The model presented here is an extension of our previous work (Oruro et al. 2020). The OB and aPC are implemented in separate subnetworks (de Almeida et al. 2013, 2016). Only the mitral cells (Mt) were implemented in the OB, which projects to the aPC by the lateral olfactory tract (LOT), as shown in Figure 1. The aPC was implemented with three cell types: pyramidal (Pyr) cells, feedforward (Ff) interneurons, and feedback (Fb) interneurons (Stokes

and Isaacson 2010; Bekkers and Suzuki 2013), with parameters listed in Table 1.

The present model contains 100 neurons of Mt cells, 200 neurons of Pyr cells, and 100 neurons of each type of interneurons (Ff and Fb). In our previous work, we adjusted the parameters for connectivity of Mt and Pyr cells to best match the experimentally reported data (Oruro et al. 2020). We assume that each Pyr cell is randomly connected with ~15–45 Mt cells. For the autoassociative Pyr–Pyr connectivity, we considered that each Pyr cell is randomly connected with five to 15 Pyr cells. This model does not consider the feedback interaction between the aPC and OB. The Ff interneurons receive excitatory input from Mt cells via the lateral olfactory tract (LOT) and connect the distal apical dendrites of the L2/3 Pyr cells (Suzuki and Bekkers 2007; Bekkers and Suzuki 2013). In our model, each Pyr cell is connected to 40% of the Ff interneurons population. Each Fb cell is excited by 25% random Pyr cells, and each Pyr cell is connected to 40% of the Fb cells. The parameters for the connectivity of Ff and Fb interneurons were adjusted using experimental data reported in our previous work (Pardo et al. 2018) and with data reported here (Table 2). To assure continuity between models, the architecture and parameters in the model, other than those related to the function of GABAergic input investigated here, were kept the same as the previous model (Oruro et al. 2020), as detailed in Table 2. Details about connectivity can be found in Figure 1, and all neural and synaptic parameters are detailed in Table 1.

The computational model and simulations were developed using NetLogo 6.0.4 software (NetLogo, http://ccl.northwestern.edu/netlogo, June 4, 2018). In the framework of NetLogo, each neuron was represented as an individual agent that processes information.

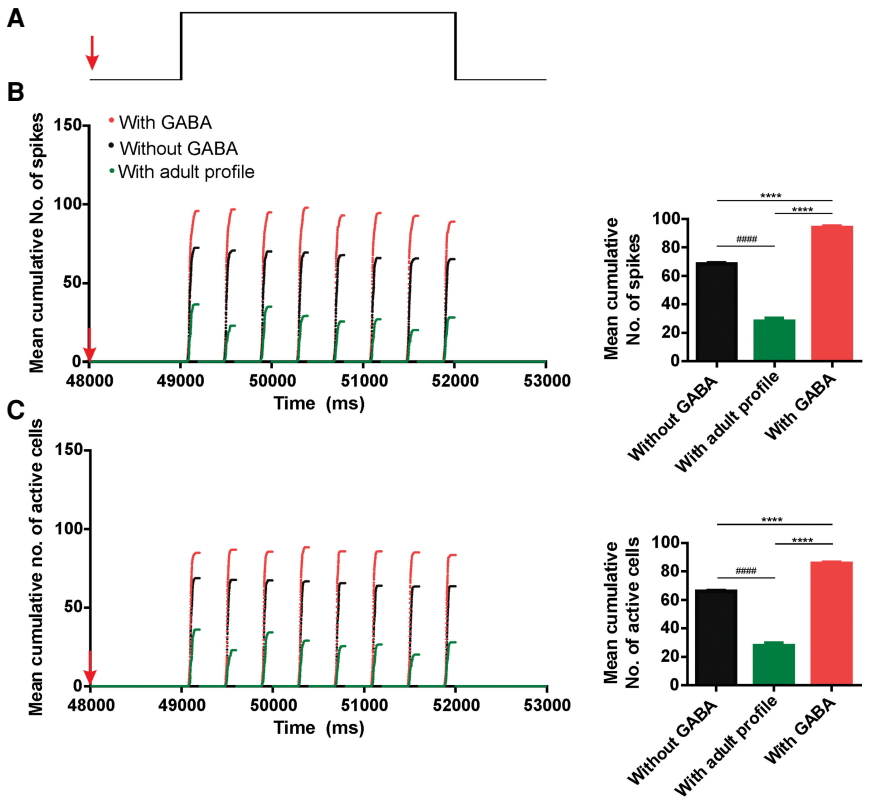

Figure 4. Comparative cumulative number of spikes and active number of cells during maternal odor recall in the P5–P8 OB-aPC circuit with GABA, without GABA and adult GABAergic input profile. (*A*) Illustration of the protocol of recall of CS (during 3 sec), which onset 2 sec after the last odor-NE pairing. Superimposed plot of cumulative number of spikes (*B*) and number of active cells (*C*) (average of 10 simulations) of the P5–P8 OB-aPC circuits with GABA input (red dots), without GABA input (black dots), and adult GABA input profile (green dots), collected at every 0.5 msec in a 200-msec window of simulation. The simulation (from 0 msec to 53,000 msec) was carried out over several respiratory cycles modulating the activity of the mitral cells, starting with 200 msec of the exhalation phase followed by 200-msec inhalation phase. Activity was measured during the inhalation and exhalation phase. The circuit P5–P8 OB-aPC with GABA input was submitted to seven trials of odor-NE pairing (simulation carried out from 0 msec to 47,000 msec) and 1 sec after the last pairing the GABA synaptic input ($E_{GABA} = -25$ mV) was switched to adult profile ($E_{GABA} = -70$ mV, approximate value based on experimental data reported in Kapur et al. 1997; Whalley and Constanti 2006; Kfir et al. 2020) or blocked (without GABA) (red arrows indicate the beginning of the switch; simulation carried out from 48,000 msec to 53,000 msec). Under those conditions, the mean of cumulative number of spikes and the number of active cells were significant higher in the circuits with GABA input than in the circuits without or with adult profile (inserted graphs). Asterisks represent statistically significant one-way ANOVA comparison among the three condition groups followed by Tukey's multiple comparisons test. (****) $P < 0.0001$. Bin: 0.5 msec.

Neuron model

All neurons were modeled as single compartment leaky integrate-and-fire neurons, in which the change in the membrane voltage is described by Equation 1:

$$\frac{dV(t)}{dt} = \frac{1}{C}\{I_e(t) - g_L[V(t) - E_L]\}, \quad (1)$$

where V (t) is the membrane potential, C is the capacitance, g_L is the leaky membrane conductance, E_L is the resting potential, and I_e is the time-dependent external current input adapted from previous work (Oruro et al. 2020). A particular external input (I_e^{ij}) that a neuron i receives from a presynaptic neuron j at time t is given by Equation 2:

$$I_e^{ij}(t) = W_{ij}g_{ij}(t)[E_{N,ij} - V_i(t)], \quad (2)$$

where W_{ij} is the synaptic strength of the synapse connecting neurons i and j, g_{ij} (t) is the change of channel conductance at time t, $E_{N,ij}$ is the reversal potential of the specific channel type and V_i (t) is the membrane potential of the postsynaptic neuron at time t. The firing probability of the model neuron at voltage V is described by Equation 3:

$$F_i(\mathrm{V}) = \begin{cases} 0 & \text{if } \mathrm{V} < \theta^{\min} \\ \left(\dfrac{\mathrm{V} - \theta^{\min}}{\theta^{\max} - \theta^{\min}}\right)^{\beta} & \text{if } \mathrm{V} \in [\theta^{\min}, \theta^{\max}] \\ 1 & \text{if } \mathrm{V} > \theta^{max} \end{cases}, \quad (3)$$

where θ^{max} represents the saturation value of the threshold, $\theta^{\min}$ is the minimum value of the threshold, and β is a constant defining the nonlinearity of F_i (V). At each spike of the presynaptic neuron j the corresponding conductance in the postsynaptic neuron i changes according to Equation 4:

$$g_{ij}(t) = g_{ij}^{max}\left[exp\left(\frac{-t + t_j^{fire}}{\tau_{1,ij}}\right) - exp\left(\frac{-t + t_j^{fire}}{\tau_{2,ij}}\right)\right], \quad (4)$$

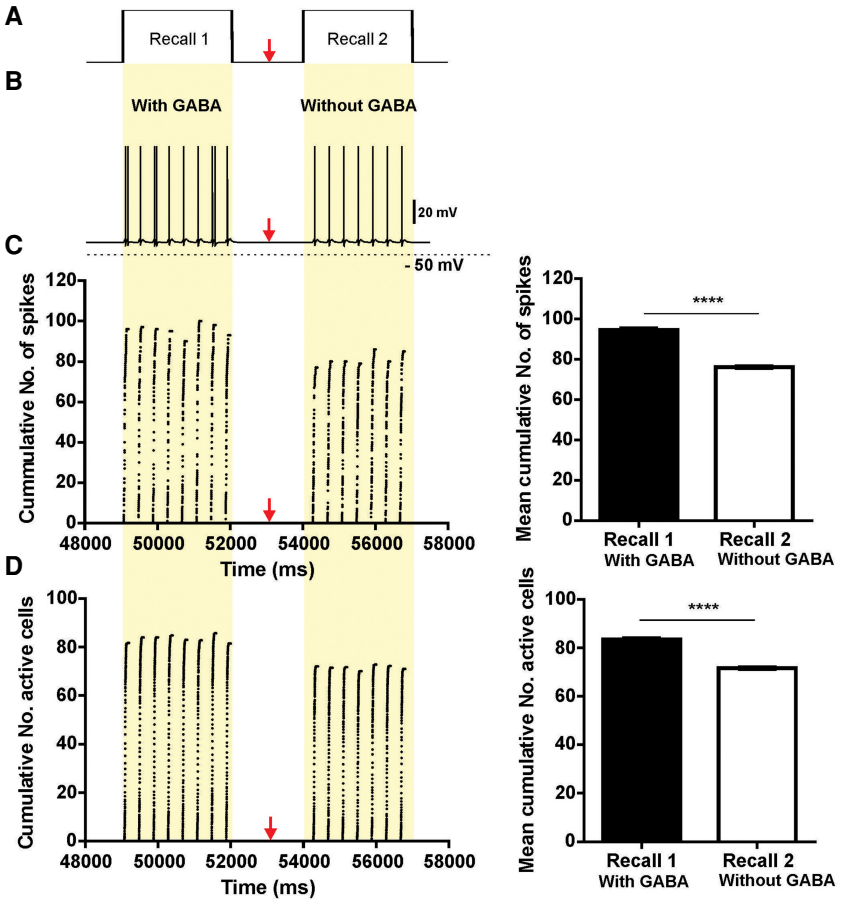

Figure 5. Activity of pyramidal cells during maternal odor recall in the P5–P8 OB-aPC circuit with and without GABA synaptic input. (*A*) Protocol of two periods of maternal odor recall. Two seconds after the last odor-NE pairing (simulation carried out from 0 msec to 47,000 msec), the circuit was exposed to the odor for 3 sec (recall 1) and 2 sec after it has finished, the circuit was exposed again to the odor for 3 sec (recall 2) (simulation carried out from 48,000 msec to 57,000 msec). At the middle of the interval, the circuits have their GABA input profile blocked (red arrows indicate the beginning of the switch, corresponding to 53,000 msec of simulation). The simulation (from 0 msec to 57,000 msec) was carried out over several respiratory cycles modulating the activity of the mitral cells, starting with 200 msec of the exhalation phase followed by 200-msec inhalation phase. Activity was measured during the inhalation and exhalation phase and date were collected at every 0.5 msec in a 200-msec window of simulation. (*B*) Action potential traces of one pyramidal cell during the recall 1 and recall 2. Note that during recall 2 the cell reduced its firing frequency. Plot of cumulative number of spikes (*C*) and number of active cells (*D*) (average of 10 simulations) of the P5–P8 OB-aPC circuits during recall 1 and recall 2. Note that during the recall 2 (circuits without GABA synaptic input) the number of spikes and number of active pyramidal reduced significantly (inserted graphs). Asterisks represent statistically significant unpaired *t* Student test comparison between recall 1 and recall 2. (****) $P<0.0001$. Bin: 0.5 msec.

where t_j^{fire} is the spike time of neuron *j*, g_{ij}^{max} represents the maximum conductance of the corresponding channel, while $\tau_{1,ij}$ and $\tau_{2,ij}$ are its rise and fall. Following an action potential, the voltage of each neuron is reset to the hyperpolarization potential V^{hyper}, where it remains clamped for the refractory period $t^{refract}$.

In the model, Pyr cells adaptation was implemented as a change in the voltage $V_i^{ahc}(t)$ due to a hyperpolarizing current that increases the firing threshold for the recently activated Pyr neuron *i*, described by Equation 5:

$$\tau^{ahc}\frac{dV_i^{ahc}}{dt} + V_i^{ahc} = A^{ahc}X_i, \quad (5)$$

where X_i is equal to 1 in the time-step after neuron *i* spikes and 0 otherwise. Accordingly, V^{ahc} increases with the constant A^{ahc} and decays with the characteristic time τ^{ahc}.

The output from Mt cells is modulated by a sinusoidal wave of 2 Hz, which mimics the respiratory rhythm (Uchida and Mainen 2003; Kepecs et al. 2007; Verhagen et al. 2007; Wesson et al.

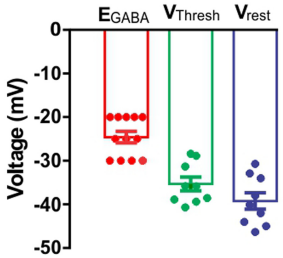

Figure 6. The reversal potential for the $GABA_AR$- mediated synaptic currents in P5–P8 L2/3 aPC pyramidal cells are more depolarized than the V_{rest} and V_{Thresh}. Bar graph showing comparison of mean (±SEM) values of reversal potential for the $GABA_AR$-mediated synaptic currents (E_{GABA}), resting membrane potential (V_{rest}) and the threshold potential (V_{Thresh}). The value for E_{GABA} is more positive than V_{rest} and V_{Thresh}, suggesting that during the P5–P8 age period, the GABAergic synaptic transmission mediated by $GABA_A$ receptors could result in the depolarization of the membrane potentials of the L2/3 aPC pyramidal cells. The bar graph was generated using data described in Table 2.

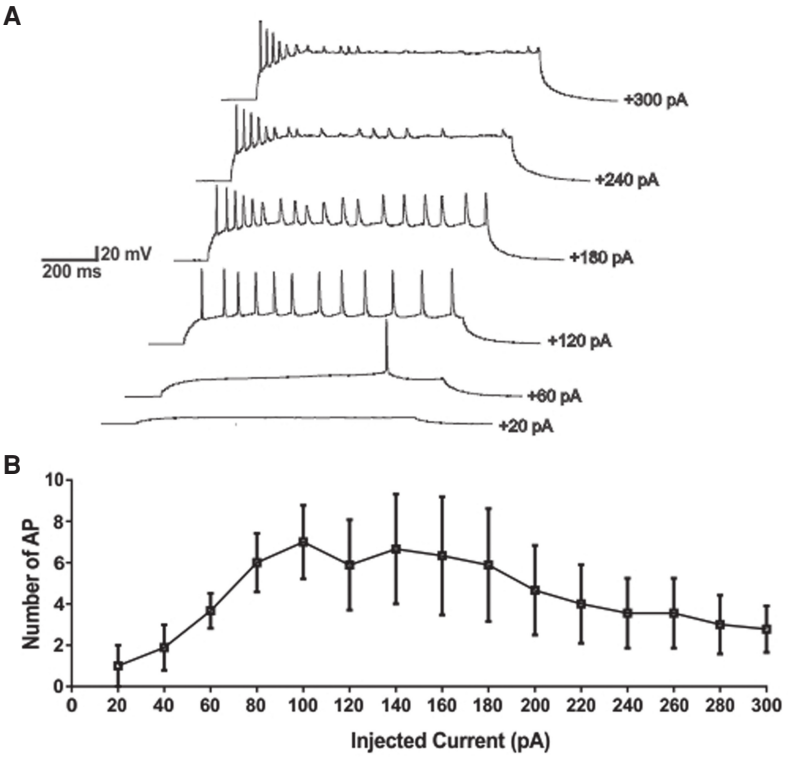

Figure 7. In P5–P8, the firing responses of L2/3 aPC pyramidal cells show adaptive properties to increasing depolarizing currents. Firing properties of the L2/3 aPC pyramidal cells were estimated in the current-clamp mode by applying depolarizing current steps (1 sec of constant current injection). (*A*) Representative traces of pyramidal cell responding to steps of depolarizing currents. Note how the cells reduced its firing at higher intensities of injected currents. (*B*) For depolarizing currents >180 pA, the cells responded by reducing their spike rates. Data are mean (± SEM) values from nine cells. The graphs were generated based in our previous work (Oruro et al. 2020).

2008; Poo and Isaacson 2009). Based on in vivo experimental studies in rodents (Poo and Isaacson 2009; Haddad et al. 2013; Stern et al. 2018) we simulated the activity of mitral cells over the course of several respiratory cycles, with a single respiratory cycle consisting of a 200-msec exhalation followed by a 200-msec inhalation. The onset of odor stimulation was set to coincide with the beginning of the exhalation phase. In the model, only Mt cells received NE modulation.

Synaptic plasticity model

Similar to de Almeida et al. (2013, 2016), activity-dependent synaptic plasticity (Hebbian learning) was implemented for synapses from Mt to Pyr and from Pyr to Pyr. The synaptic strength W_{ij} is increased if both presynaptic and postsynaptic neurons fire together; otherwise, it is reduced to a plasticity rate of 0.25, which multiplies the change of W. This change described by Equation 6:

$$\frac{dW_{ij}}{dt} = (W_{LTP} - W_{ij})\frac{i^{post}\left(t - t_i^{fire}\right)b^{glu}\left(t - t_j^{fire} - t^{delay}\right)}{\tau^{pp}} + (W_{LTD} - W_{ij})\left[\frac{i^{post}\left(t - t_i^{fire}\right)}{\tau^{npp}} + \frac{b^{glu}\left(t - t_j^{fire} - t^{delay}\right)}{\tau^{pnp}}\right], \quad (6)$$

where t^{delay} is the time it takes for the action potential to travel from the soma to the recurrent collateral connections, and i^{post} is the postsynaptic depolarization attributed to retropropagated action potential of postsynaptic neurons described by Equation 7:

$$i^{post}(t) = \frac{t}{\tau^{post}} exp\left(1 - \frac{t}{\tau^{post}}\right), \quad (7)$$

where the time course of the depolarization at the postsynaptic neuron (τ^{post}) is of 2 msec. b^{glu} is the time course of the kinetics of the binding of glutamate on NMDA receptors (de Almeida et al. (2013, 2016) is described by Equation 8.

$$b^{glu}(t) = exp\left(\frac{-t}{\tau^{NMDAf}}\right) \times \left[1 - exp\left(\frac{-t}{\tau^{NMDAr}}\right)\right], \quad (8)$$

where τ^{NMDAf} (7 msec) and τ^{NMDAr} (1 msec) characterize the NMDA receptor kinetics.

During early postnatal weeks, NMDA receptors predominate at the LOT-aPC synapses (Mt-Pyr) (Franks and Isaacson 2005), and these synapses express a robust NMDA-dependent LTP plasticity with strength declining by the first postnatal month. However, the associative synapses (Pyr to Pyr) plasticity do not lose strength in the same period (Poo and Isaacson 2007). The maximum weight for LTP (W_{LTP}) was set initially to 62.2 and the minimal weight for LTD (W_{LTD}) was set initially to 12.25. If i^{post} and i^{post} peak together, then the synaptic weight between the neurons *i* and *j* is driven to (W_{LTP}) with the characteristics time τ^{pp} (12 msec) otherwise, in the case of unsynchronized firing, it is reduced to (W_{LTD})_with the time constant $\tau^{pnp} = \tau^{npp} = 500$ msec.

Experimental data

In our previous work, we reported characteristics of the $GABA_A$ receptor-mediated spontaneous inhibitory postsynaptic currents (sIPSC) obtained by patch-clamp recordings in voltage-clamp mode from pyramidal neurons in layer 2/3 (L2/3) of the aPC in vitro slice preparation of the P5–P8 rat brain slices (Pardo et al. 2018). In some of those recordings from control animals, we identified the $GABA_A$ receptor equilibrium potential (E_{GABA}) by systematically varying the holding potential from 0 to −100 mV in 5-mV-steps. The holding potential where the E_{GABA} has its current zero was considered as a potential for reversion. The analysis of E_{GABA} was carried out by pClamp 10.0 software, through the measurement of the amplitude (pA) of the sIPSC in each step of holding potential tested. Results from this experiment are reported in Table 2.

Acknowledgments

E.M.O. is supported by Coordenação de Aperfeiçoamento de Pessoal de Nível Superior (CAPES; process no. 1608346). G.V.E.P. is supported by a doctoral scholarship from Conselho Nacional de Pesquisa e Desenvolvimento Cientifico e Tecnológico (CNPq; process no. 141727/2014-4). A.B.L. and M.E.C. are funded by CNPq (process no. 465671/2014-4). M.A.P.I. is supported by CNPq (process no. 423843/2016-8). Other funding that partly contributed to the end of this work is provided to G.V.E.P. by Universidad de Ciencias y Humanidades (UCH) under research grant "Exploración teórico-experimental neurocomportamental de la formación del apego madre-infante en el desarrollo temprano" (resolución no. 012-2019-CU-UCH).

Table 2. Experimental data obtained by recording L2/3 aPC pyramidal cells during P5–P8 age

Passive and active membrane properties (mean data)		GABAergic synaptic properties (sIPSC) (mean data)	
V_{res}	−39.22 mV[a]	sIPSC amplitude	11.61 pA[b]
R_{inp}	438.6 MΩ[a]	sIPSC 10%–90% rise time	4.88 msec[b]
Tm	42.78 ms[a]	sPSC Decay-time constant	5.36 msec[b]
Capacitance	98.21 pF[a]	E_{GABA}	−24.58 ± 1.3 mV[c]
AP threshold (mV)	−36.63 mV[a]		
AP amplitude (mV)	76.90 mV[a]		

[a]Data are from Oruro et al. 2020.
[b]Data are from Pardo et al. 2018.
[c]Mean value (±SEM) from 12 pyramidal cells recorded.

References

Al Aïn S, Perry RE, Nuñez B, Kayser K, Hochman C, Brehman E, LaComb M, Wilson DA, Sullivan RM. 2017. Neurobehavioral assessment of maternal odor in developing rat pups: implications for social buffering. *Soc Neurosci* **12:** 32–49. doi:10.1080/17470919.2016.1159605

Bekkers JM, Suzuki N. 2013. Neurons and circuits for odor processing in the piriform cortex. *Trends Neurosci* **36:** 429–438. doi:10.1016/j.tins.2013.04.005

Ben-Ari Y. 2014. The GABA excitatory/inhibitory developmental sequence: a personal journey. *Neuroscience* **279:** 187–219. doi:10.1016/j.neuroscience.2014.08.001

de Almeida L, Idiart M, Linster C. 2013. A model of cholinergic modulation in olfactory bulb and piriform cortex. *J Neurophysiol* **109:** 1360–1377. doi:10.1152/jn.00577.2012

de Almeida L, Idiart M, Dean O, Devore S, Smith DM, Linster C. 2016. Internal cholinergic regulation of learning and recall in a model of olfactory processing. *Front Cell Neurosci* **10:** 256. doi:10.3389/fncel.2016.00256

Ehrlich DE, Ryan SJ, Hazra R, Guo J-D, Rainnie DG. 2013. Postnatal maturation of GABAergic transmission in the rat basolateral amygdala. *J Neurophysiol* **110:** 926–941. doi:10.1152/jn.01105.2012

Farrell WJ, Alberts JR. 2002. Stimulus control of maternal responsiveness to Norway rat (Rattus norvegicus) pup ultrasonic vocalizations. *J Comp Psychol* **116:** 297–307. doi:10.1037/0735-7036.116.3.297

Franks KM, Isaacson JS. 2005. Synapse-specific downregulation of NMDA receptors by early experience: a critical period for plasticity of sensory input to olfactory cortex. *Neuron* **47:** 101–114. doi:10.1016/j.neuron.2005.05.024

Ghosh A, Purchase NC, Chen X, Yuan Q. 2015. Norepinephrine modulates pyramidal cell synaptic properties in the anterior piriform cortex of mice: age-dependent effects of β-adrenoceptors. *Front Cell Neurosci* **9:** 450. doi:10.3389/fncel.2015.00450

Ghosh A, Mukherjee B, Chen X, Yuan Q. 2017. β-Adrenoceptor activation enhances L-type calcium channel currents in anterior piriform cortex pyramidal cells of neonatal mice: implication for odor learning. *Learn Mem* **24:** 132–135. doi:10.1101/lm.044818.116

Haddad R, Lanjuin A, Madisen L, Zeng H, Murthy VN, Uchida N. 2013. Olfactory cortical neurons read out a relative time code in the olfactory bulb. *Nat Neurosci* **16:** 949–957. doi:10.1038/nn.3407

Kapur A, Pearce RA, Lytton WW, Haberly LB. 1997. GABA(A)-mediated IPSCs in piriform cortex have fast and slow components with different properties and locations on pyramidal cells. *J. Neurophysiol* **78:** 2531–2545. doi:10.1152/jn.1997.78.5.2531

Kepecs A, Uchida N, Mainen ZF. 2007. Rapid and precise control of sniffing during olfactory discrimination in rats. *J Neurophysiol* **98:** 205–213. doi:10.1152/jn.00071.2007

Kfir A, Awasthi R, Ghosh S, Kundu S, Paul B, Lamprecht R, Barkai E. 2020. A cellular mechanism of learning-induced enhancement of synaptic inhibition: PKC-dependent upregulation of KCC2 activation. *Sci Rep* **10:** 962. doi:10.1038/s41598-020-57626-2

Kimura F, Nakamura S. 1985. Locus coeruleus neurons in the neonatal rat: electrical activity and responses to sensory stimulation. *Brain Res* **355:** 301–305. doi:10.1016/0165-3806(85)90055-0

Kojima S, Alberts JR. 2009. Maternal care can rapidly induce an odor-guided huddling preference in rat pups. *Dev Psychobiol* **51:** 95–105. doi:10.1002/dev.20349

Meyer PM, Alberts JR. 2016. Non-nutritive, thermotactile cues induce odor preference in infant mice (Mus musculus). *J Comp Psychol* **130:** 369–379. doi:10.1037/com0000044

Moriceau S, Sullivan RM. 2004. Unique neural circuitry for neonatal olfactory learning. *J Neurosci* **24:** 1182–1189. doi:10.1523/JNEUROSCI.4578-03.2004

Moriceau S, Sullivan RM. 2005. Neurobiology of infant attachment. *Dev Psychobiol* **47:** 230–242. doi:10.1002/dev.20093

Morrison GL, Fontaine CJ, Harley CW, Yuan Q. 2013. A role for the anterior piriform cortex in early odor preference learning: evidence for multiple olfactory learning structures in the rat pup. *J Neurophysiol* **110:** 141–152. doi:10.1152/jn.00072.2013

Mukherjee B, Yuan Q. 2016. NMDA receptors in mouse anterior piriform cortex initialize early odor preference learning and L-type calcium channels engage for long-term memory. *Sci Rep* **6:** 35256. doi:10.1038/srep35256

Okutani F, Zhang JJ, Otsuka T, Yagi F, Kaba H. 2003. Modulation of olfactory learning in young rats through intrabulbar GABAB receptors. *Eur J Neurosci* **18:** 2031–2036. doi:10.1046/j.1460-9568.2003.02894.x

Oruro EM, Pardo GVE, Lucion AB, Calcagnotto ME, Idiart MAP. 2020. Maturation of pyramidal cells in anterior piriform cortex may be sufficient to explain the end of early olfactory learning in rats. *Learn Mem* **27:** 20–32. doi:10.1101/lm.050724.119

Pardo GVE, Lucion AB, Calcagnotto ME. 2018. Postnatal development of inhibitory synaptic transmission in the anterior piriform cortex. *Int J Dev Neurosci* **71:** 1–9. doi:10.1016/j.ijdevneu.2018.07.008

Perry RE, Blair C, Sullivan RM. 2017. Neurobiology of infant attachment: attachment despite adversity and parental programming of emotionality. *Curr Opin Psychol* **17:** 1–6. doi:10.1016/j.copsyc.2017.04.022

Poo C, Isaacson JS. 2007. An early critical period for long-term plasticity and structural modification of sensory synapses in olfactory cortex. *J Neurosci* **27:** 7553–7558. doi:10.1523/JNEUROSCI.1786-07.2007

Poo C, Isaacson JS. 2009. Odor representations in olfactory cortex: 'sparse' coding, global inhibition, and oscillations. *Neuron* **62:** 850–861. doi:10.1016/j.neuron.2009.05.022

Raineki C, Moriceau S, Sullivan RM. 2010. Developing a neurobehavioral animal model of infant attachment to an abusive caregiver. *Biol Psychiatry* **67:** 1137–1145. doi:10.1016/j.biopsych.2009.12.019

Rangel S, Leon M. 1995. Early odor preference training increases olfactory bulb norepinephrine. *Brain Res Dev Brain Res* **85:** 187–191. doi:10.1016/0165-3806(94)00211-H

Rheims S, Minlebaev M, Ivanov A, Represa A, Khazipov R, Holmes GL, Ben-Ari Y, Zilberter Y. 2008. Excitatory GABA in rodent developing neocortex in vitro. *J Neurophysiol* **100:** 609–619. doi:10.1152/jn.90402.2008

Rivera C, Voipio J, Payne JA, Ruusuvuori E, Lahtinen H, Lamsa K, Pirvola U, Saarma M, Kaila K. 1999. The K+/Cl− co-transporter KCC2 renders GABA hyperpolarizing during neuronal maturation. *Nature* **397:** 251–255. doi:10.1038/16697

Ross JM, Fletcher ML. 2019. Aversive learning-induced plasticity throughout the adult mammalian olfactory system: insights across development. *J Bioenerg Biomembr* **51:** 15–57. doi:10.1007/s10863-018-9770-z

Roth TL, Raineki C, Salstein L, Perry R, Sullivan-Wilson TA, Sloan A, Lalji B, Hammock E, Wilson DA, Levitt P, et al. 2013. Neurobiology of secure infant attachment and attachment despite adversity: a mouse model. *Genes Brain Behav* **12:** 673–680. doi:10.1111/gbb.12067

Stern M, Bolding KA, Abbott L, Franks KM. 2018. A transformation from temporal to ensemble coding in a model of piriform cortex. *Elife* **7:** e34831. doi:10.7554/elife.34831

Stokes CCA, Isaacson JS. 2010. From dendrite to soma: dynamic routing of inhibition by complementary interneuron microcircuits in olfactory cortex. *Neuron* **67:** 452–465. doi:10.1016/j.neuron.2010.06.029

Sullivan RM, Opendak M. 2018. Developmental and neurobehavioral transitions in survival circuits. *Curr Opin Behav Sci* **24:** 50–55. doi:10.1016/j.cobeha.2018.03.005

Sullivan RM, McGaugh JL, Leon M. 1991. Norepinephrine-induced plasticity and one-trial olfactory learning in neonatal rats. *Brain Res Dev Brain Res* **60:** 219–228. doi:10.1016/0165-3806(91)90050-S

Sullivan RM, Zyzak DR, Skierkowski P, Wilson DA. 1992. The role of olfactory bulb norepinephrine in early olfactory learning. *Brain Res Dev Brain Res* **70:** 279–282. doi:10.1016/0165-3806(92)90207-D

Sullivan RM, Wilson DA, Lemon C, Gerhardt GA. 1994. Bilateral 6-OHDA lesions of the locus coeruleus impair associative olfactory learning in newborn rats. *Brain Res* **643:** 306–309. doi:10.1016/0006-8993(94)90038-8

Sullivan RM, Stackenwalt G, Nasr F, Lemon C, Wilson DA. 2000. Association of an odor with activation of olfactory bulb noradrenergic β-receptors or locus coeruleus stimulation is sufficient to produce learned approach responses to that odor in neonatal rats. *Behav Neurosci* **114:** 957–962. doi:10.1037/0735-7044.114.5.957

Suzuki N, Bekkers JM. 2007. Inhibitory interneurons in the piriform cortex. *Clin Exp Pharmacol Physiol* **34:** 1064–1069. doi:10.1111/j.1440-1681.2007.04723.x

Thompson JV, Sullivan RM, Wilson DA. 2008. Developmental emergence of fear learning corresponds with changes in amygdala synaptic plasticity. *Brain Res* **1200:** 58–65. doi:10.1016/j.brainres.2008.01.057

Tyzio R, Nardou R, Ferrari DC, Tsintsadze T, Shahrokhi A, Eftekhari S, Khalilov I, Tsintsadze V, Brouchoud C, Chazal G, et al. 2014. Oxytocin-mediated GABA inhibition during delivery attenuates autism pathogenesis in rodent offspring. *Science* **343:** 675–679. doi:10.1126/science.1247190

Uchida N, Mainen ZF. 2003. Speed and accuracy of olfactory discrimination in the rat. *Nat Neurosci* **6:** 1224–1229. doi:10.1038/nn1142

Verhagen JV, Wesson DW, Netoff TI, White JA, Wachowiak M. 2007. Sniffing controls an adaptive filter of sensory input to the olfactory bulb. *Nat Neurosci* **10:** 631–639. doi:10.1038/nn1892

Wesson DW, Donahou TN, Johnson MO, Wachowiak M. 2008. Sniffing behavior of mice during performance in odor-guided tasks. *Chem Senses* **33:** 581–596. doi:10.1093/chemse/bjn029

Whalley BJ, Constanti A. 2006. Developmental changes in presynaptic muscarinic modulation of excitatory and inhibitory neurotransmission in rat piriform cortex in vitro: relevance to epileptiform bursting susceptibility. *Neuroscience* **140:** 939–956. doi:10.1016/j.neuroscience.2006.02.046

Wilson DA, Sullivan RM. 1992. Blockade of mitral/tufted cell habituation to odors by association with reward: a preliminary note. *Brain Res* **594:** 143–145. doi:10.1016/0006-8993(92)91039-H

Yuan Q, Shakhawat AMD, Harley CW. 2014. Mechanisms underlying early odor preference learning in rats. *Prog Brain Res* **208:** 115–156. doi:10.1016/B978-0-444-63350-7.00005-X

Received June 21, 2020; accepted in revised form September 27, 2020.

Material suplementar

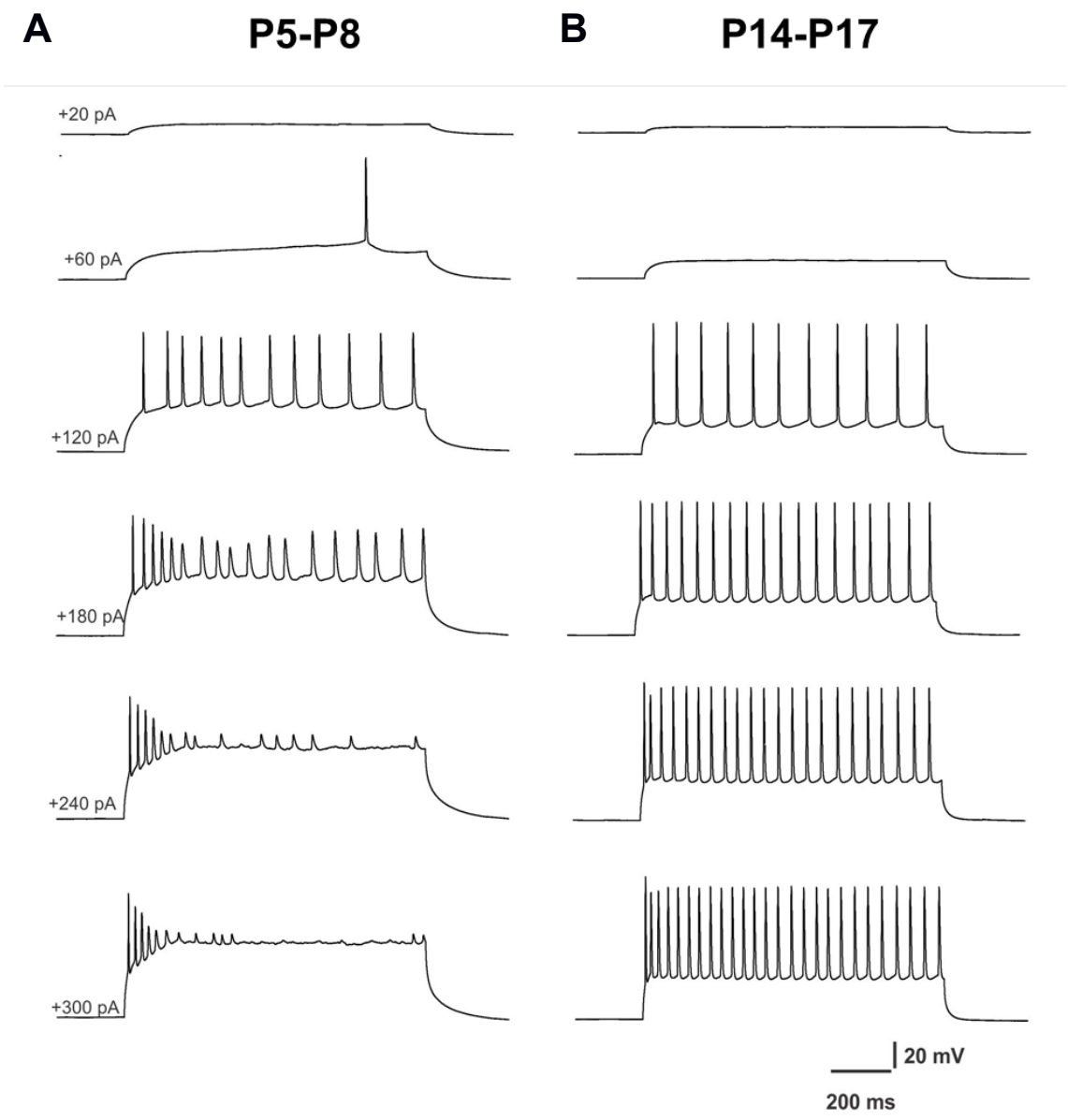

Figure S1. **Representative voltage traces from aPC pyramidal cells of P5-P8 and P14-P17 age period at depolarizing current injections.**

Note how the cell from P5-P8 animals start to fire at lower intensities of injected currents (a pulse of square-wave current with a one-second duration) and reduced its firing at higher intensities and show adaptation (**A**) compared to cells from P14-P17 animals, which start to firing at relative higher intensities of the injected currents and increase their firing with the increase of the intensity of injected currents, with no apparent adaptation (**B**). Amplitude of injected currents are indicated at the beginning of each trace. Representative voltage traces are from current-clamp recordings from aPC pyramidal cells reported in our previous work (Oruro et al., 2020).

Capítulo 5

Discussão geral e conclusão

5.1 Principais contribuições do trabalho

5.1.1 Abordagem integrativa da neuroetologia e neurociencia computacional no estúdio de fenômenos comportamentais

A presente tese apresenta um modelo computacional que integra dados experimentais, simulando o aprendizado do odor maternal durante o período sensível do apego. Propomos uma hipótese sobre o final do período sensível e, igualmente, avaliamos a função das correntes GABAérgicas durante o período sensível. Nossa estratégia de trabalho é nova no campo do aprendizado olfatório de recém-nascidos, pois nos permite integrar níveis de análise.

Os problemas de integração em vários níveis foram estudados por cientistas da complexidade. Com o objetivo de estudar em vários níveis, grupos de pesquisa de sistemas complexos e sociedades surgiram em todo o mundo, sendo o mais importante o Instituto de Santa Fé (SFI), nos Estados Unidos de América, fundado por cientistas de prestígio de diferentes áreas, incluindo vencedores de prêmio Nobel. Outro movimento é a Sociedade de Sistemas Complexos, fundada na Europa em 2004. Atualmente, a CSS se encarrega de organizar o evento mais importante em sistemas complexos, a Conferência sobre Sistemas Complexos (Conference on Complex System, CCS). O evento CCS foi influenciado pelos grupos da complexidade da França, organizados em Roadmaps (French Roadmap for Complex Systems 2008-2009 https://hal.archives-ouvertes.fr/hal-00392486). Uma peculiaridade que torna o CCS especial foi a promoção do método de modelagem baseado em agentes (**Figura 6**) para resolver os problemas em vários níveis (para obter mais detalhes, consulte: The CSS Roadmap for Complex Systems Science and its Applications 2012 – 2020" Edited by Paul Bourgine, Jeffrey Johnson, and Davis Chavalarias).

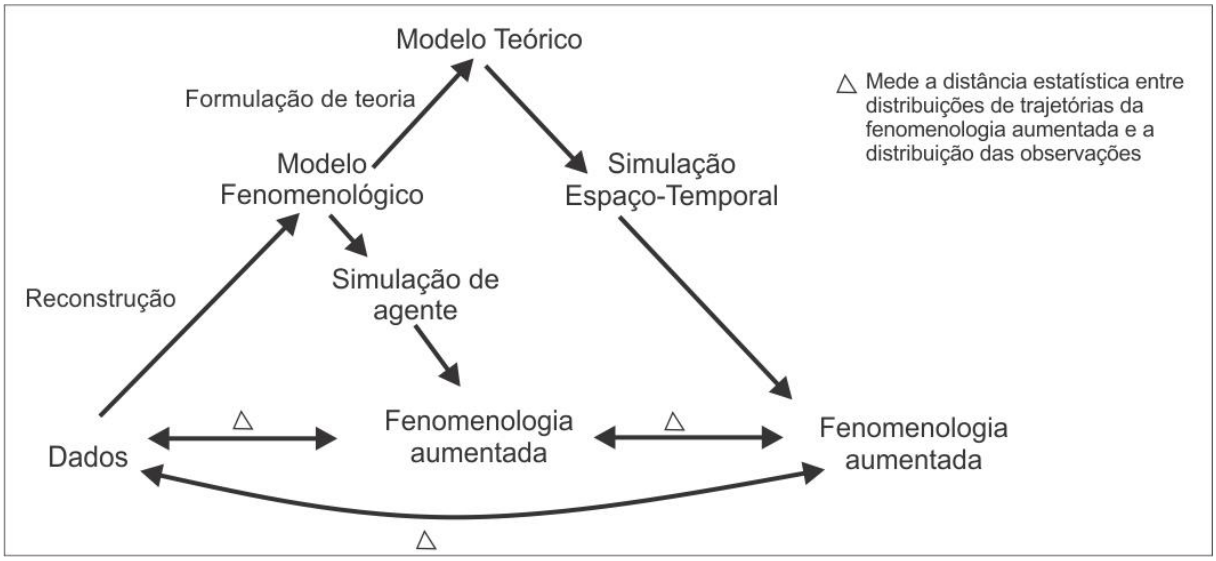

Figura 6. **Metodologia de sistemas complexos para a reconstrução de modelos a partir de dados.**

Nossa proposta foi integrar a organização conceitual da abordagem biocomportamental com uma visão experimental no nível neural, todavia considerando a emergência no mesmo nível neural (aparecimento de um novo padrão na organização do nível neural), contrariando a proposta biobehaviorista.

O princípio unificado do reforço é uma proposta teórica computacional de Donahoe, Burgos e Palmer (1993) para um dos problemas abertos do behaviorismo, que é a distinção operante/respondente. Nesse trabalho não queremos abordar o caráter histórico nem discutir as soluções para esse problema. A proposta do grupo Biobehaviorista já foi discutida na edição especial da revista behaviorista Journal of Experimental Analisys of Behavior na edição de março 1997, volume 67 (DOMJAN, 2016); e no trabalho de Burgos (2010). Para essa tese, consideramos a proposta de princípio unificado do reforço como esquema conceitual para estudar o aprendizado de preferência ao odor da mãe.

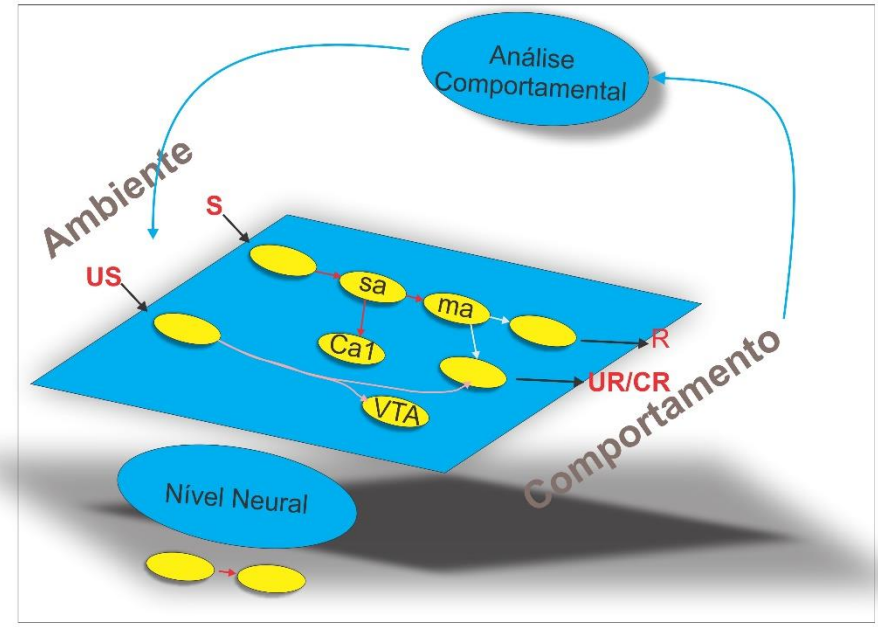

Figura 7. **Esquema de integração**. Figura adaptada de Oruro, PE; Pardo, G.E, do trabalho " A hipótese da seleção por reforço em resposta à emergência do problema dos sistemas complexos adaptativos". Título original em Inglês: "The hypothesis of selection by reinforcement in response to the emergence problem of complex adaptive systems in computational neuroethology" (trabalho apresentado na seção de pôster no congresso da *International Brain Research Organization*, IBRO, Rio de Janeiro, agosto, 2015).

Uma aplicação do princípio do reforço unificado foi distinguir que comportamentos respondentes e operantes são adquiridos simultaneamente e podem ter diferentes saídas do sistema (**Figura 7**). Isso pode estar acontecendo durante o aprendizado do odor da mãe no período sensível, ocorrendo naturalmente no momento em que o filhote recebe o cuidado materno. Por tanto, sabemos que durante o condicionamento para o aprendizado de preferência olfatória de um odor artificial, usando o protocolo de condicionamiento clássico em filhotes com DPN 5-7, uma reposta operante de aproximação não é reforçada, mas essa resposta já existe no circuito do filhote dessa idade e durante o condicionamento clássico ela é ativada no circuito. Agora entendemos que ele é ativado simultaneamente com o procedimento de condicionamento clássico, sendo por isso que o filhote se aproxima durante o teste de preferência olfatória. Após o período sensível, o circuito operante não é recrutado. A questão do que acontece no nível neural ao final do período sensível foi estudada no artigo 1. Consequentemente, esta proposta do princípio unificado do reforço nós permitiu integrar os níveis de comportamento e da neurociência com conteúdo teórico da análise do comportamento.

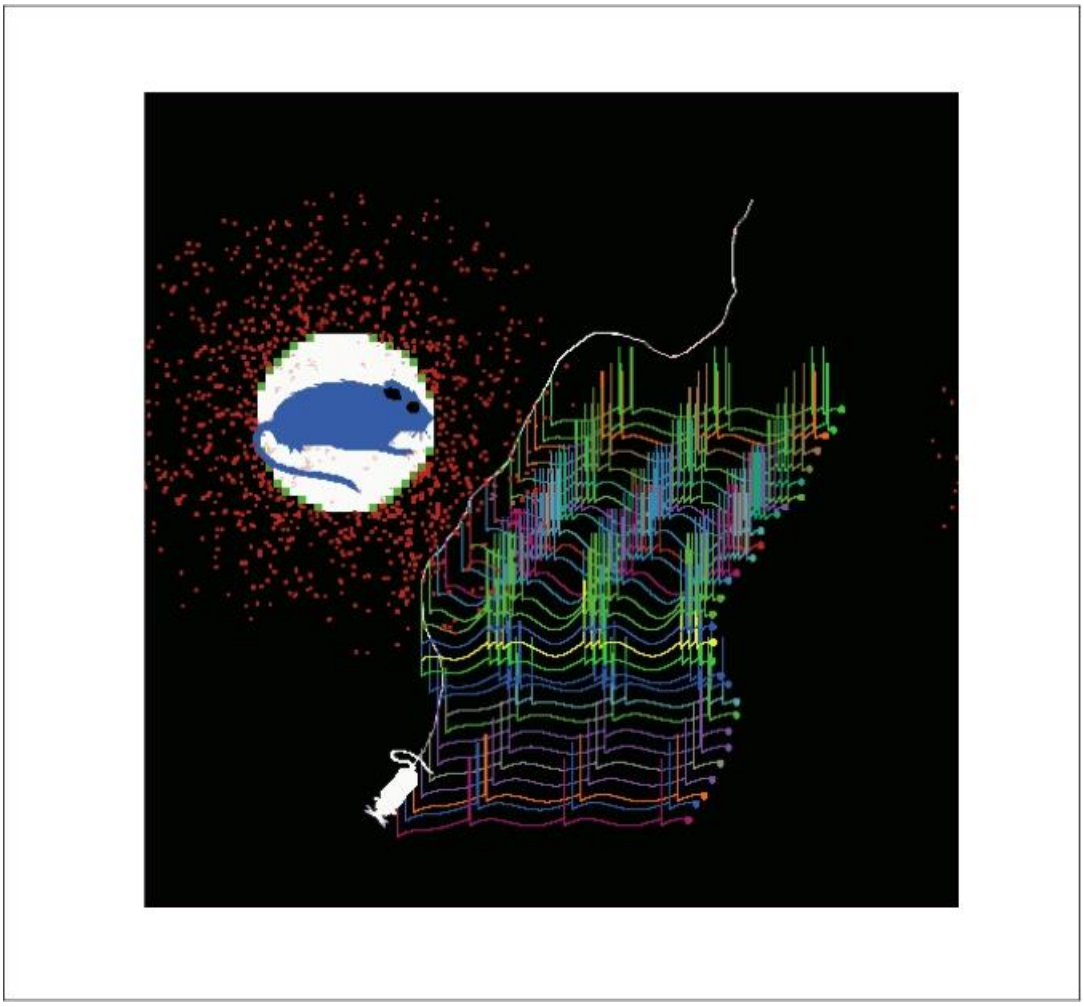

Figura 8. **A figura é uma simulação baseada em agentes feita com Netlogo.** A rata mãe é fonte de calor (em branco) e fonte de odor (vermelho), o filhote pode se mexer no espaço, a resposta dos neurônios incrementa quanto mais perto ele estiver do odor da mãe. Na simulação os agentes são a mãe, a molécula de odor, o filhote e os neurônios

5.1.2 O aprendizado da preferência do odor maternal e o aprendizado precoce de preferência olfatória para um odor artificial

Uma das principais contribuições da presente tese para o entendimento do aprendizado de preferências olfatórias nos roedores neonatos é a proposta de que a preferência do aprendizado do odor maternal é mediada pelo mesmo circuito envolvido no aprendizado precoce de preferência olfatória para um odor artificial. Os dois artigos fazem contribuições nesse ponto baseado em experimentos de simulação computacional com dados das caraterísticas eletrofisiológicas maturacionais dos neurônios piramidais e da transmissão sináptica GABAérgica no CPa. Os dois trabalhos de simulação representam o entendimento atual de que os roedores

neonatos aprendem o odor maternal mediante as experiências com mãe dentro do ninho durante a primeira semana pós-natal.

Os resultados da presente tese podem ajudar na compreensão dos desfechos comportamentais do condicionamento odor-estimulação táctil de filhotes de rato antes e depois do DPN 10, em um nível neural. No paradigma do condicionamento clássico usado para filhotes com DPN 5-8 para induzir preferência olfatória para odores artificiais, o estímulo incondicionado é uma pincelada vigorosa no dorso dos filhotes, o qual depois de repetidos pareamentos com um odor artificial (o estímulo neutro), induz uma resposta comportamental de aproximação para o odor artificial (agora estímulo condicionado). Curiosamente, a estimulação táctil no dorso do filhote não induz essa resposta de aproximação antes do pareamento, apenas induz um incremento na atividade locomotora basal dos filhotes (Sullivan et al., 1986; Sullivan and Wilson, 1993). Porém, como pode ser que um odor artificial induza uma resposta de aproximação depois de ter sido pareado com a estimulação táctil, o qual não induz uma resposta de aproximação? A presente tese oferece uma resposta para essa pergunta, discutida na seguinte seção.

5.1.3 O papel das caraterísticas maturacionais dos neurônios piramidais do CPa no aprendizado da preferência do odor maternal e implicâncias para o aprendizado precoce de preferência olfatória para um odor artificial

A resposta para a pergunta na seção anterior está baseada na consideração de que o pareamento de um odor artificial com a estimulação táctil é possível porque esse novo aprendizado aproveita um circuito no CPa previamente formado durante a interação mãe-filhote dentro do ninho. Ou seja, as propriedades das células piramidais imaturas do CPa permitem que o condicionamento de um odor artificial- estimulação táctil recrute um circuito neural que parcialmente se encontra superposto com o circuito que suporta o comportamento de aproximação para o odor da mãe. Conforme amadurecem as células piramidais do CPa, a superposição do circuito não é mais possível. Assim o pareamento do odor artificial- estimulação táctil em filhotes > DPN 10 não é mais efetivo em induzir aprendizado de preferência olfatória.

Pensamos que essa hipótese oferecida é a mais simples, dado o conhecimento da circuitaria que se tem até o momento. Além disso a hipótese proposta é possível de ser testada experimentalmente. Por outro lado, a proposta poderia ser explicada pelo princípio unificado do condicionamento proposto por Donahoe e colaboradores,

(1993), no qual os comportamentos operantes e respondentes emergem simultaneamente. Desde essa perspectiva, os neurônios recrutados para o odor maternal condicionado no CPa podem ser os mesmos que são ativados durante o condicionamento do odor- estimulação táctil, e esses neurônios coincidentes poderiam ser os que se encontram reduzidos no circuito BO-CPa P14-P17 na simulação da exposição do odor maternal (resultados do artigo 1).

Em suma, o nosso modelo apresentado no primeiro artigo sugere duas distintas funções para o processamento no circuito BO-CPa no aprendizado associativo em filhotes de ratas com idades antes e depois do DPN 10, isso baseado no desenvolvimento das propriedades intrínsecas das células piramidais do CPa. Para os dos circuitos BO-CPa em desenvolvimento, o sucesso para o pareamento odor-estimulação táctil é dependente da ativação coincidente das células piramidais do CPa responsivas para o odor maternal, promovendo o comportamento de aproximação-orientação. As mudanças nas propriedades intrínsecas das células piramidais do CPa reduzem a disponibilidade das células responsivas para o odor maternal durante a exposição desse odor.

5.1.4 O papel das caraterísticas maturacionais das entradas GABAérgicas no CPa no aprendizado de preferência do odor maternal

Além do papel das propriedades intrínsecas das células piramidais do CPa, os nossos experimentos computacionais têm mostrado que as entradas GABAérgicas melhoram a habilidade do circuito BO-CPa para aprender o odor mãe e amplificar o recordo de esse odor. Esse efeito é devido às caraterísticas maturacionais das entradas GABAérgicas que despolarizam os neurônios piramidais do CPa em filhotes com idades menores ao DPN 10. Esses resultados publicados no segundo artigo sugerem que durante o aprendizado de preferência olfatória em filhotes menores do DPN 10, as entradas sinápticas GABAérgicas possivelmente atuam depolarizando os neurônios piramidais do CPa, de modo que isso leva para uma amplificação na resposta dos neurônios piramidais para o odor maternal condicionado. Contribuindo assim para um rápido aprendizado do odor maternal durante esse período do desenvolvimento.

5.2 Conclusões

Nosso trabalho é o primeiro na literatura de simulação na área de estudo do apego mãe-filhote. Apresentamos novidades para a literatura do aprendizado do odor maternal, como:

1. Incluir a técnica da modelagem baseada em agentes e sistemas de equações para modelar neurônios e comportamento usando o software Netlogo;
2. Identificar componentes importantes no sistema olfatório para o aprendizado precoce de preferência olfatória;
3. Integrar modelos de registro etológicos e eletrofisiológico no campo da neuroetologia computacional;
4. Usar abordagens teóricas da análise do comportamento para estudar a distinção operante/respondente no aprendizado precoce de preferência olfatória;
5. Uma explicação para o fim do período sensível para o aprendizado de preferência olfatória em filhotes de roedor, rato ou camundongo, depois do DPN 10, é que a mudança nas propriedades intrínsecas das células piramidais do CPa reduz a disponibilidade de células piramidais que respondem ao odor materno durante a exposição a esse estímulo. Assim, o número reduzido de neurônios que respondem ao odor condicionado (materno) pode não coincidir com os neurônios que respondem a um segundo odor condicionado;
6. As entradas GABAérgicas melhoram a capacidade do circuito BO-CPa para aprender o odor materno durante o período sensível. Esse efeito é devido às características maturacionais das entradas GABAérgicas que despolarizam os neurônios piramidais do CPa em idades menores a DPN 10. Além disso, nesse circuito em desenvolvimento, a aparente falta de inibição sináptica mediada por GABA parece ser compensada pelas propriedades de ativação adaptativa de neurônios piramidais imaturos do CPa;
7. A preferência ao odor maternal tem circuitos que são coincidentes com a preferência a um segundo odor condicionado, o qual só é possível adquiri-lo durante uma janela temporal do desenvolvimento. Nosso modelo computacional, desenhado usando estratégias que vão da neuroetologia à biofísica, permitiu estudar o circuito neural da preferência do odor maternal e permitirá explorar novas hipóteses sobre como mudanças ambientais podem

gerar mudanças no padrão da conectividade neural no circuito em desenvolvimento.

5.3 Futuras perspectivas da neuroetologia computacional

No pôster “Computational Simulation of Maternal Odor on Neonatal Learning in the Nest” apresentado no congresso da Sociedade para a Neurociência dos Estados Unidos (Society for Neuroscience) do ano 2017(**anexo**), realizamos um estudo sobre como as diferentes mudanças ambientais em cada período de cuidado maternal (variações naturais no padrão do comportamento maternal durante o pós-parto) pode ter um efeito diferente ao aprender o odor materno. Este tipo de desenho experimental para simular o aprendizado pode ser usado para trabalhar em neuroetologia.

Outra característica importante que nosso modelo preserva é que o mesmo sujeito possui propriedades de estímulo neutro/condicionado e estímulo incondicionado, como proposto por Domjam como característica do aprendizado em condições naturais (DOMJAN, 2005); nesse caso, a mãe é fonte do estímulo neutro e incondicionado simultaneamente para o filhote. Para tanto, o desenho mais apropriado para condicionar o circuito foi apresentar o odor primeiro e após alguns segundos o efeito da NA, representando assim a aproximação da mãe para o filhote e o contato materno, respectivamente. Na **Figura 8** mostramos uma representação ideal para simulação em neuroetologia. Essa perspectiva pode crescer ainda mais na Neuroetologia. Por exemplo, para explorar como as mudanças do cuidado materno dois dias antes e depois ao período sensível organizam o circuito. Progressivamente, entendendo as propriedades do nível neural durante o condicionamento, estaremos no caminho de estudar situações de maior complexidade comportamental. Neste trabalho, portanto, introduzimos uma estratégia de simulação da Neuroetologia à biofísica com dados experimentais.

Referências

Alberts, J. R. and Brunjes, P. C. (1978) ‘Ontogeny of thermal and olfactory determinants of huddling in the rat’, *Journal of Comparative and Physiological* Psychology. doi: 10.1037/h0077533.

Burgos, J. E. (2010) ‘The operant/respondent distinction: A computational neural-network analysis’, in Computational Models of Conditioning. doi: 10.1017/CBO9780511760402.009.

de Almeida, L. et al. (2015) ‘Computational modeling suggests distinct, location-specific function of norepinephrine in olfactory bulb and piriform cortex’, Frontiers in Computational Neuroscience. doi: 10.3389/fncom.2015.00073.

de Almeida, L., Idiart, M. and Linster, C. (2013) ‘A model of cholinergic modulation in olfactory bulb and piriform cortex’, Journal of Neurophysiology. doi: 10.1152/jn.00577.2012.

Domjan, M. (2005) ‘Pavlovian Conditioning: A Functional Perspective’, Annual Review of Psychology. doi: 10.1146/annurev.psych.55.090902.141409.

Domjan, M. (2016) ‘Elicited versus emitted behavior: Time to abandon the distinction’, Journal of the Experimental Analysis of Behavior. doi: 10.1002/jeab.197.

Donahoe, J. W., Burgos, J. E. and Palmer, D. C. (1993) ‘A SELECTIONIST APPROACH TO REINFORCEMENT’, Journal of the Experimental Analysis of Behavior. doi: 10.1901/jeab.1993.60-17.

Franks, K. M. and Isaacson, J. S. (2005) ‘Synapse-specific downregulation of NMDA receptors by early experience: a critical period for plasticity of sensory input to olfactory cortex.’, Neuron, 47(1), pp. 101–14. doi: 10.1016/j.neuron.2005.05.024.

Ghosh, A. *et al.* (2015) ‘Norepinephrine Modulates Pyramidal Cell Synaptic Properties in the Anterior Piriform Cortex of Mice: Age-Dependent Effects of β-adrenoceptors.’, *Frontiers in cellular neuroscience*, 9(November), p. 450. doi: 10.3389/fncel.2015.00450.

Jensen, O., Idiart, M. A. P. and Lisman, J. E. (1996) ‘Physiologically realistic formation of autoassociative memory in networks with theta/gamma oscillations: Role of fast NMDA channels’, Learning Memory, 3(2–3), pp. 243–256. doi: 10.1101/lm.3.2-3.243.

Kojima, S. and Alberts, J. R. (2009) ‘Maternal care can rapidly induce an odor-guided huddling preference in rat pups’, Developmental Psychobiology, 51(1), pp. 95–105. doi: 10.1002/dev.20349.

Li, G., Linster, C. and Cleland, T. A. (2015) ‘Functional differentiation of cholinergic and noradrenergic modulation in a biophysical model of olfactory bulb granule cells’, Journal of Neurophysiology. doi: 10.1152/jn.00324.2015.

Meyer, P. M. and Alberts, J. R. (2016) ‘Non-Nutritive, Thermotactile Cues Induce Odor Preference in Infant Mice (Mus musculus)’, *Journal of Comparative Psychology*, 130(4), pp. 369–379. doi: 10.1037/com0000044.

Moriceau, S. and Sullivan, R. M. (2004) ‘Unique neural circuitry for neonatal olfactory learning.’, The Journal of neuroscience: the official journal of the Society for Neuroscience. United States, 24(5), pp. 1182–1189. doi: 10.1523/JNEUROSCI.4578-03.2004.

Moriceau, S. and Sullivan, R. M. (2005) ‘Neurobiology of infant attachment’, *Developmental Psychobiology*. doi: 10.1002/dev.20093.

Moriceau, S. and Sullivan, R. M. (2006) ‘Maternal presence serves as a switch between learning fear and attraction in infancy’, Nature Neuroscience. doi: 10.1038/nn1733.

Morrison, Gillian L. et al. (2013) ‘A role for the anterior piriform cortex in early odor preference learning: Evidence for multiple olfactory learning structures in the rat pup’, Journal of Neurophysiology. doi: 10.1152/jn.00072.2013.

Poo, C. and Isaacson, J. S. (2007) ‘An early critical period for long-term plasticity and structural modification of sensory synapses in olfactory cortex.’, The Journal of neuroscience: the official journal of the Society for Neuroscience, 27(28), pp. 7553–8. doi: 10.1523/JNEUROSCI.1786-07.2007.

Raineki, C. *et al.* (2009) ‘Ontogeny of odor-LiCl vs. odor-shock learning: Similar behaviors but divergent ages of functional amygdala emergence’, *Learning and Memory*, 16(2), pp. 114–121. doi: 10.1101/lm.977909.

Roth, T. L., Moriceau, S. and Sullivan, R. M. (2006) ‘Opioid modulation of Fos protein expression and olfactory circuitry plays a pivotal role in what neonates remember.’, Learning & memory (Cold Spring Harbor, N.Y.), 13(5), pp. 590–8. doi: 10.1101/lm.301206.

Roth, T. L. *et al.* (2013) ‘Neurobiology of secure infant attachment and attachment despite adversity: A mouse model’, *Genes, Brain and Behavior*. doi: 10.1111/gbb.12067.

Sullivan, R. M. (2003) ‘Developing a Sense of Safety: The Neurobiology of Neonatal Attachment’, Annals of the New York Academy of Sciences, 1008, pp. 122–131. doi: 10.1196/annals.130.013.

Sullivan, R. M. and Wilson, D. a (2003) ‘Molecular biology of early olfactory memory.’, Learning & memory (Cold Spring Harbor, N.Y.), 10(1), pp. 1–4. doi: 10.1101/lm.58203.

Sullivan, R. M., Stackenwalt, G., Nasr, F., Lemon, C. and Wilson, D. A. (2000) ‘Association of an odor with activation of olfactory bulb noradrenergic β-receptors or locus coeruleus stimulation is sufficient to produce learned approach responses to that odor in neonatal rats’, Behavioral Neuroscience, 114(5), pp. 957–962. doi: 10.1037/0735-7044.114.5.957.

Thiele, J. C. and Grimm, V. (2010) ‘NetLogo meets R: Linking agent-based models with a toolbox for their analysis’, Environmental Modelling and Software. doi: 10.1016/j.envsoft.2010.02.008.

Thiele, J. C., Kurth, W. and Grimm, V. (2012) ‘RNetLogo: An R package for running and exploring individual-based models implemented in NetLogo’, Methods in Ecology and Evolution. doi: 10.1111/j.2041-210X.2011.00180.x. de Almeida, L., Reiner, S.J., Ennis, M., Linster, C., 2015. Computational modeling suggests distinct, location-specific function of norepinephrine in olfactory bulb and piriform cortex. Front. Comput. Neurosci. https://doi.org/10.3389/fncom.2015.00073

Donahoe, J.W., Burgos, J.E., Palmer, D.C., 2006. A selectionist approach to reinforcement. J. Exp. Anal. Behav. 60, 17–40. https://doi.org/10.1901/jeab.1993.60-17

Donahoe, J.W., Burgos, J.E., Palmer, D.C., 1993. A SELECTIONIST APPROACH TO REINFORCEMENT. J. Exp. Anal. Behav. https://doi.org/10.1901/jeab.1993.60-17

Ghosh, A., Purchase, N.C., Chen, X., Yuan, Q., 2015. Norepinephrine Modulates Pyramidal Cell Synaptic Properties in the Anterior Piriform Cortex of Mice: Age-Dependent Effects of β-adrenoceptors. Front. Cell. Neurosci. 9, 450. https://doi.org/10.3389/fncel.2015.00450

Meyer, P.M., Alberts, J.R., 2016. Non-Nutritive, Thermotactile Cues Induce Odor Preference in Infant Mice (Mus musculus). J. Comp. Psychol. 130, 369–379. https://doi.org/10.1037/com0000044

Moriceau, S., Sullivan, R.M., 2005. Neurobiology of infant attachment. Dev. Psychobiol. https://doi.org/10.1002/dev.20093

Morrison, G.L., Fontaine, C.J., Harley, C.W., Yuan, Q., 2013. A role for the anterior piriform cortex in early odor preference learning: Evidence for multiple olfactory learning structures in the rat pup. J. Neurophysiol. https://doi.org/10.1152/jn.00072.2013

Raineki, C., Shionoya, K., Sander, K., Sullivan, R.M., 2009. Ontogeny of odor-LiCl vs. odor-shock learning: Similar behaviors but divergent ages of functional amygdala emergence. Learn. Mem. 16, 114–121. https://doi.org/10.1101/lm.977909

Roth, T.L., Raineki, C., Salstein, L., Perry, R., Sullivan-Wilson, T.A., Sloan, A., Lalji, B., Hammock, E., Wilson, D.A., Levitt, P., Okutani, F., Kaba, H., Sullivan, R.M., 2013. Neurobiology of secure infant attachment and attachment despite adversity: A mouse model. Genes, Brain Behav. https://doi.org/10.1111/gbb.12067

Sullivan, R.M., 2003. Developing a Sense of Safety: The Neurobiology of Neonatal Attachment, in: Annals of the New York Academy of Sciences. pp. 122–131. https://doi.org/10.1196/annals.130.013

Sullivan, R.M., Hofer, M.A., Brake, S.C., 1986. Olfactory-guided orientation in neonatal rats is enhanced by a conditioned change in behavioral state. Dev. Psychobiol. 19, 615–623. https://doi.org/10.1002/dev.420190612

Sullivan, R.M., Wilson, D.A., 1993. Role of the Amygdala Complex in Early Olfactory Associative Learning. Behav. Neurosci. 107, 254–263. https://doi.org/10.1037/0735-7044.107.2.254

Upton, K.J., Sullivan, R.M., 2010. Defining age limits of the sensitive period for attachment learning in rat pups. Dev. Psychobiol. 52, 453–64. https://doi.org/10.1002/dev.20448

Wilensky, U. (1999) ‘NetLogo. http://ccl.northwestern.edu/netlogo/.’, Center for Connected Learning and ComputerBased Modeling Northwestern University Evanston IL.

Yuan, Q., Shakhawat, A. M. D. and Harley, C. W. (2014) ‘Mechanisms underlying early odor preference learning in rats’, in Progress in Brain Research. doi: 10.1016/B978-0-444-63350-7.00005-X.

ANEXO

Pôsteres apresentados em eventos acadêmicos

1. Título: "**The Operant/respondent distinction: An analysis in artificial piriform cortex**".
Evento: 2nd FALAN Congress, Buenos Aires, outubro 17-20 de 2016.
Autores:

Enver Oruro Puma (primeiro autor e apresentador)

Grace E. Pardo (Doutoranda PPG Fisiologia UFRGS)

Maria Elisa Calcagnotto (Professora associada, Dpto de Bioquímica, ICBS, UFRGS)

Marco Idiart (Professor Titular, Dpto de Física, UFRGS)

2. Título: "**O problema das assembleias celulares no modelo selecionista do córtex piriforme anterior**".
Evento: IX Oficina de Neurociências - As múltiplas dimensões da plasticidade neural. Bento Gonçalves, RS - 10 e 11 de setembro de 2016

Autores:

Enver Oruro Puma (primeiro autor e apresentador)

Grace E. Pardo (Doutoranda PPG Fisiologia UFRGS)

Maria Elisa Calcagnotto (Professora associada, Dpto de Bioquímica, ICBS, UFRGS)

Marco Idiart (Professor Titular, Dpto de Física, UFRGS)

3. Título: "**Contato materno seleciona neurônios preferentes ao odor no córtex piriforme de filhotes de rato**".
Evento: Apresentado em XXXIV Anual de Etologia, 12-15 de novembro 2016, Jaboticabal, SP, Brasil.

Autores:

Enver Oruro Puma (primeiro autor e apresentador)

Grace E. Pardo (Doutoranda PPG Fisiologia UFRGS)

Maria Elisa Calcagnotto (Professora associada, Dpto de Bioquímica, ICBS, UFRGS)

Marco Idiart (Professor Titular, Dpto de Física, UFRGS)

4. Título: "**Computational model of early odor preference learning**".
Evento: Brain, Behavior and Emotions Congress. Porto Alegre, 14-17 de junho 2017

Autores:

Enver Oruro Puma (primeiro autor e apresentador)

Grace E. Pardo (Doutoranda PPG Fisiologia UFRGS)

Maria Elisa Calcagnotto (Professora associada, Dpto de Bioquímica, ICBS, UFRGS)

Marco Idiart (Professor Titular, Dpto de Física, UFRGS)

5. Título: "**Neurocomputational Simulation of Natural Olfactory Learning in the Neonatal Rat"**

Evento: 38 th World Congress of the International Union of Physiological Sciences, 1-5 agosto 2017, Rio de Janeiro, Brasil

Primeiro autor e apresentador: Grace E. Pardo (Doutoranda PPG Fisiologia UFRGS)

Autores:

Grace E. Pardo (primeira autora e apresentadora)

Izabela Amaro Espíndula (Estudante de Iniciação Científica, Dpto Fisiologia, ICBS, UFRGS)

Enver Oruro Puma (Doutorando, PPG Neurociências UFRGS.

6. Título: "**Computational simulation of the infant maternal odor learning in the nest"**. Evento: SfN's 47th annual meeting, Neuroscience 2017, Washington, D.C, novembro 2017

Autores:

Grace E. Pardo (primeira autora e apresentadora)

Izabela Amaro Espíndula (Estudante de Iniciação Científica, Dpto Fisiologia, ICBS, UFRGS)

Enver Oruro Puma (Doutorando, PPG Neurociências UFRGS.

7. Título: "**From emitted to elicited neuronal activity in the neonatal piriform cortex**". Evento: SfN's 47th annual meeting, Neuroscience 2017, Washington, D.C, novembro 2017.

Autores:

Enver Oruro Puma (primeiro autor)

Grace E. Pardo (apresentadora, Doutoranda PPG Fisiologia UFRGS)

Izabela Amaro Espíndula (Estudante de Iniciação Científica, Dpto Fisiologia, ICBS, UFRGS)

Maria Elisa Calcagnotto (Professora associada, Dpto de Bioquímica, ICBS, UFRGS)

Marco Idiart (Professor Titular, Dpto de Física, UFRGS)

8. Título: "**Simulation of amygdala input to posterior piriform cortex: an exploration of fear conditioning from cells to cognition**".
Evento: 16th Annual MO-LECULAR AND CELLULAR COGNITION SOCIETY Symposium and Poster Session -WASHINGTON DC novembro 2017.

Autores:

Enver Oruro Puma (primeiro autor)

Grace E. Pardo (apresentadora, Doutoranda PPG Fisiologia UFRGS)

Maria Elisa Calcagnotto (Professora associada, Dpto de Bioquímica, ICBS, UFRGS)

Marco Idiart (Professor Titular, Dpto de Física, UFRGS)

Pôster SNF 2017

Computational Simulation of Maternal Odor on Neonatal Learning in the Nest

Grace Pardo *[1,2], Izabela Espíndula[1], Enver Oruro [2,3]

[1] Behavioral Neuroendocrinology Laboratory, Physiology Department, Institute of Health Sciences
[2] Neurophysiology and Neurochemistry of Neuronal Excitability and Synaptic Plasticity Laboratory, Biochemistry Department, Institute of Health Sciences,
[3] Neurocomputational and Language Processing Laboratory, Institute of Physics and Institute of Informatics, Universidade Federal do Rio Grande do Sul (UFRGS), Porto Alegre, Brazil

grace.pardo@gmail.com

NEUROSCIENCE 2017
10193

Introduction

Studies have shown that neonatal rats exhibit high ability to learn artificial odor associated with a stimulus that mimics maternal care (Sullivan, 2003). It is presumed that this association also occurs under natural circumstances within the nest (Domjan, 2005).
During the first 6 postnatal days (P), maternal care shows variation with a progressive increase in the maternal absence of the nest.

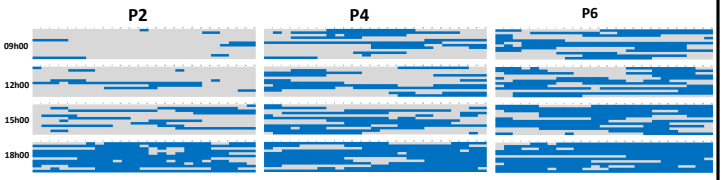

Maternal profile of the presence and absence of the nest in postpartum day 2, 4 and 6 of the rat. The graph was constructed from the work of Pardo et al. 2016 . Blue: mother outside the nest. Grey: mother in the nest. n=12

We hypothesized that the profile on P6 could shape the olfactory neural circuit to distinguish the mother odor or the nest odor than the profile of day P2.

Method

1. Network architecture of the olfactory bulb (OB) and piriform cortex (PCx)

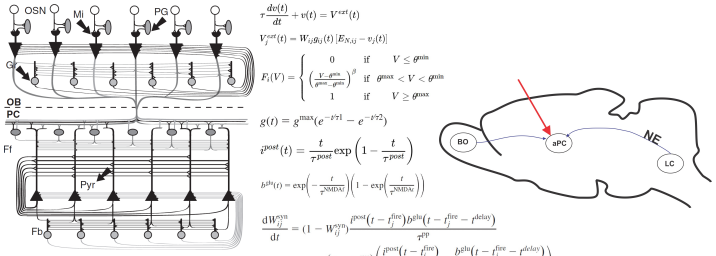

$$\tau\frac{dv(t)}{dt}+v(t)=V^{ext}(t)$$
$$V_i^{ext}(t)=W_{ij}g_{ij}(t)\,|E_{N,ij}-v_j(t)|$$
$$F_i(V)=\begin{cases}0 & \text{if} \quad V\le\theta^{min}\\ \left(\frac{V-\theta^{min}}{\theta^{max}-\theta^{min}}\right)^{\beta} & \text{if} \quad \theta^{min}<V<\theta^{max}\\ 1 & \text{if} \quad V\ge\theta^{max}\end{cases}$$
$$g(t)=g^{max}(e^{-t/\tau 1}-e^{-t/\tau 2})$$
$$i^{post}(t)=\frac{t}{\tau^{post}}\exp\left(1-\frac{t}{\tau^{post}}\right)$$
$$b^{glu}(t)=\exp\left(-\frac{t}{\tau^{NMDA}}\right)\left(1-\exp\left(\frac{t}{\tau^{NMDA}}\right)\right)$$
$$\frac{dW_{ij}^{syn}}{dt}=(1-W_{ij}^{syn})\frac{i^{post}(t-t_j^{fire})b^{glu}(t-t_j^{fire}-t^{delay})}{\tau^{pp}}+(0-W_{ij}^{syn})\left(\frac{i^{post}(t-t_j^{fire})}{\tau^{app}}+\frac{b^{glu}(t-t_j^{fire}-t^{delay})}{\tau^{pap}}\right)$$

Simplified artifical neural network of the OB and PCx(A) (from de Almeida, Idiart and Linster,) and Equations used for the artificial neural network (B) (from Almeida et al 2015).

We measured a neural activity every 1 ms and in a window of 2000 ms seconds we quantified the rate of firing every 500 ms.

2. Reduction of the data from Fig 1 to an equivalent minimal representation

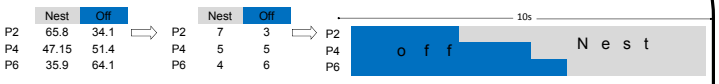

3. General protocol of natural conditioning

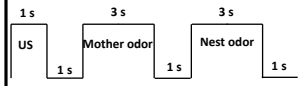

We simulated the norepinephrine release from LC as a US and odor (mother and nest) as a NS/CS and measured the neural activity of anterior piriform cortex pyramidal cell.

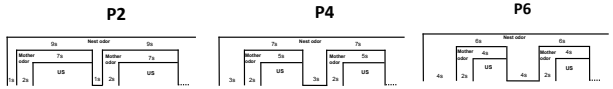

4. Criteria for data analysis

Total neural activity before, during and after conditioning

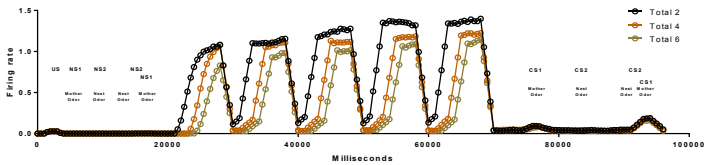

1. After the conditioning a specific test was performed to select the neurons that fire exclusively in response to the mother odor and in response to the nest odor.
2. Only data with firing rate greater than 0.0002 in response to the nest odor presentation was considered for analysis.
3. To determine if the artificial circuit discriminates the mother odor from the nest odor after conditioning, we realized a qualitative analysis based on following criteria:
   - **A)** The nest odor presentation evokes firing of set of neurons specific to nest odor but not the firing of neurons specific to mother odor
   - **B)** The mother odor presentation evokes firing of set of neurons specific to mother odor but the the firing of neurons specific to the nest odor should remain stable and not increase their firing.

Results

A higher percentage of the artificial circuit of day 6 meet the criteria for odor discrimination than that the circuit of day 2.

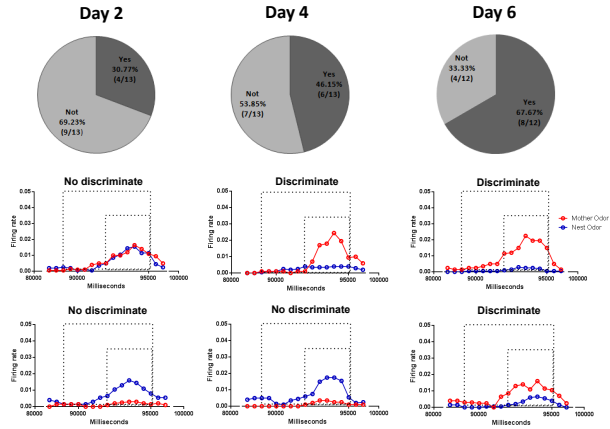

The circuit was able to learn in the three days

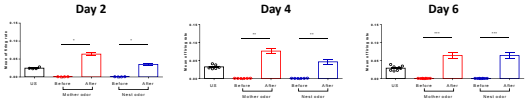

Comparision of mean of total firing rate before and after conditioning (Mann-Whitnney Test, *p<0.05, **p=0.002, ***p=0.0002)

Discussion and Conclusion

The artificial neural circuit representive for rat pup shown a progressive increase with age in discriminative capacity of mother odor from the nest odor, which is coincident with a progressive increase maternal absence from the nest during the first postpartum days.
These results suggest that the profile of maternal care at postnatal day 6, outside and inside the nest, allows a greater distinction of the mother´s odor and the nest´s odor than at postnatal day 2.

Acknowledgments

CNPq Conselho Nacional de Desenvolvimento Científico e Tecnológico
CAPES

Cartas de aceitação dos artigos e convite para submeter figura capa de jornal

not 1-4,9

Decision Letter

[Return to Queue]

To: "Enver M. Oruro" <envermiguel@gmail.com>
From: Susan Cushman <susan.j.cushman@uth.tmc.edu>
Subject: Learning and Memory -- Manuscript Accepted
Cc: macciol@cshl.edu

RE: LEARNMEM/2019/050724

Dear Dr. Oruro,

Thank you for your revised manuscript, "Maturation of pyramidal cells in anterior piriform cortex may be sufficie to explain the end of early olfactory learning in rats," which we are pleased to accept for publication in Learning Memory.

Any essential changes to the manuscript should be made in your forthcoming page proofs.

At this stage we require the LICENSE TO PUBLISH form, available in your Author Area at submit.learnmem.or be filled out, signed, and returned. Please e-mail (preferred) or fax the form to: Dana Macciola, Fax: 516-422-4094; e-mail: macciol@cshl.edu. Any delay in sending the form will cause a delay in the Production of your manuscript for publication.

IN ADDITION, DIGITAL ART FILES ARE REQUIRED for all figures (as detailed in the Author Instructions

(http://learnmem.cshlp.org/site/misc/ifora.xhtml). Please ensure that the digital art files meet the digital art guidelines at http://learnmem.cshlp.org/site/misc/ifora.xhtml. If your art files do not meet these guidelines, plea e-mail Dana Macciola, (macciol@cshl.edu), and advise her that you have revised art files to upload to the submission website. Dana will then direct you on how to upload your revised art files through the submission website.

In addition, if applicable, please check that you have acquired permission from the publisher to reproduce, mod or adapt any previously published figure or table for use both in print and online in Learning & Memory. This is essential as we can not publish an article without the permission on file. Most publishers and scientific journals list instructions for obtaining reprint permissions on their websites. All data or information obtained through personal communication also requires a letter of approval for use and any material that was obtained from ano publication requires permission for publication from the source. We remind authors that it is a condition of publication that reagents, clones, cell lines, etc., generated in the course of the work described will be made available on request to qualified members of the research community.

Information about our OPEN ACCESS option is available on our website (http://learnmem.cshlp.org/).

The editors of Learning and Memory would like to invite you to submit potential cover images to feature your recently accepted manuscript. The image does not need to be an exact duplicate of a figure from the manuscr but should represent both an artistic and informative representation of your research results. Please feel free t submit several different images for our consideration. We will select images based on artistic quality and your scientific results. Please see the instructions on our website (http://learnmem.cshlp.org/site/misc/ifora.xhtml), under "Manuscripts Accepted for Publication," for digital file requirements for artwork (note that we need only a

digital file of the image; no hard copies are necessary). We will also need a legend describing the image (including manuscript number, title and first author) and a 3-5 word caption for the cover. Please email your proposed images, legends, and cover captions to Dana Macciola (macciol@cshl.edu). Please contact us for directions for uploading if the image is too large to email.

With kind regards,

Susan Cushman, Ph.D.

Learning and Memory

PLEASE NOTE: The corresponding author for this manuscript has been designated as: Enver M. Oruro. This person to whom we will send the galleys for proofing, and at the following address. If ANY of this information is incorrect or missing, please let us know immediately.

Galleys will be sent to:

Enver M. Oruro

Enver Miguel Oruro Puma

Universidad Federal de Río Grande del Sur

Instituto de Ciências Básica e Saúde

Av Borges de Medeiros 612 ap 39

Porto alegre 90020022

Brazil

TEL: 55-51-991460204

FAX:

E-mail: envermiguel@gmail.com

LEARNING AND MEMORY

COLD SPRING HARBOR LABORATORY PRESS

Dana Macciola

500 Sunnyside Boulevard

Woodbury, NY 11797-2924

Phone (516) 422-4012

Fax (516) 422-4092

---

not 1-4,9

Decision Letter

[Return to Queue]

To: Enver Miguel Oruro <envermiguel@gmail.com>
From: Susan Cushman <susan.j.cushman@uth.tmc.edu>
Subject: Learning and Memory -- Manuscript Accepted
Cc: macciol@cshl.edu

RE: LEARNMEM/2020/052217

Dear Dr. Oruro,

Thank you for your revised manuscript, "The maturational characteristics of the GABA input in the anterior pirif cortex may also contribute to the rapid learning of the maternal odor during the sensitive period.," which we are pleased to accept for publication in Learning & Memory.

Any essential changes to the manuscript should be made in your forthcoming page proofs. Please note that th reviewer indicated figures 6 and 7 were missing from the revision and take steps to ensure these figures are included in final submission material.

At this stage we require the LICENSE TO PUBLISH form, available in your Author Area at submit.learnmem.or filled out, signed, and returned. Please e-mail (preferred) or fax the form to: Dana Macciola, Fax: 516-422-409 mail: macciol@cshl.edu. Any delay in sending the form will cause a delay in the Production of your manuscript publication.

IN ADDITION, DIGITAL ART FILES ARE REQUIRED for all figures (as detailed in the Author Instructions (http://learnmem.cshlp.org/site/misc/ifora.xhtml). Please ensure that the digital art files meet the digital art guidelines at http://learnmem.cshlp.org/site/misc/ifora.xhtml. If your art files do not meet these guidelines, plea e-mail Dana Macciola, (macciol@cshl.edu), and advise her that you have revised art files to upload to the submission website. Dana will then direct you on how to upload your revised art files through the submission website.

In addition, if applicable, please check that you have acquired permission from the publisher to reproduce, mod or adapt any previously published figure or table for use both in print and online in Learning & Memory. This is essential as we can not publish an article without the permission on file. Most publishers and scientific journals instructions for obtaining reprint permissions on their websites. All data or information obtained through person communication also requires a letter of approval for use and any material that was obtained from another publi requires permission for publication from the source. We remind authors that it is a condition of publication that reagents, clones, cell lines, etc., generated in the course of the work described will be made available on reque qualified members of the research community.

Information about our OPEN ACCESS option is available on our website (http://learnmem.cshlp.org/).

The editors of Learning and Memory would like to invite you to submit potential cover images to feature your recently accepted manuscript. The image does not need to be an exact duplicate of a figure from the manuscr but should represent both an artistic and informative representation of your research results. Please feel free t submit several different images for our consideration. We will select images based on artistic quality and your

scientific results. Please see the instructions on our website (http://learnmem.cshlp.org/site/misc/ifora.xhtml), under "Manuscripts Accepted for Publication," for digital file requirements for artwork (note that we need only a digital file of the image; no hard copies are necessary). We will also need a legend describing the image (inclu manuscript number, title and first author) and a 3-5 word caption for the cover. Please email your proposed im legends, and cover captions to Dana Macciola (macciol@cshl.edu). Please contact us for directions for uploa the image is too large to email.

With kind regards,

Susan Cushman, Ph.D.

Learning and Memory

PLEASE NOTE: The corresponding author for this manuscript has been designated as: Enver Miguel Oruro. the person to whom we will send the galleys for proofing, and at the following address. If ANY of this informati incorrect or missing, please let us know immediately.

Galleys will be sent to:

Enver Miguel Oruro

Enver Miguel Oruro Puma

Universidad Federal de Río Grande del Sur

Instituto de Ciências Básica e Saúde

Av Borges de Medeiros 612 ap 39

Porto alegre 90020022

Brazil

TEL: 55-51-991460204

FAX:

E-mail: envermiguel@gmail.com

LEARNING AND MEMORY

COLD SPRING HARBOR LABORATORY PRESS

Dana Macciola

500 Sunnyside Boulevard

Woodbury, NY 11797-2924

Phone (516) 422-4012

Fax (516) 422-4092

Gmail **Enver Miguel <envermiguel@gmail.com>**

Learning & Memory - Invitation to submit cover

Cushman, Susan J <Susan.J.Cushman@uth.tmc.edu> 5 de octubre de 2020, 13:14
Para: "envermiguel@gmail.com" <envermiguel@gmail.com>
Cc: "marco.idiart@gmail.com" <marco.idiart@gmail.com>

Dear Dr. Oruro,

The editors of Learning & Memory would like to feature your recently accepted paper (LEARNMEM/2020/052217: "The maturational characteristics of the GABA input in the anterior piriform cortex may also contribute to the rapid learning of the maternal odor during the sensitive period") as a Journal cover. Your article will appear in the December, 2020 issue and we would like to feature your cover on the same issue, so we would need your image in the near future.

The image can be either a figure from your manuscript or a creative/artistic representation of your research. We would however prefer that data charts and graphs not be used. Please feel free to submit several different images for our consideration. Images should be as large as possible (full page preferred) and submitted as either an EPS or TIFF file (TIFFs must be at least 300 dpi-resolution). In addition, please remove any panel tags from your image. When you are ready to submit your images please email them to me. If they are too large for conventional email we have used WeTransfer (https://wetransfer.com) very successfully to email large files.

We will also need a legend describing the image (including manuscript number, title and first author) and a 3-5 word caption for the cover.

Please send the caption separately; do not embed the caption in the image.

Please let me know if you would like to accept this invitation to submit cover art or if you have any questions.

Thank you in advance for your time.

Best-
Susan

Susan Cushman, PhD
Assistant Editor
Learning & Memory